



Fisheries and Oceans
Canada

Pêches et Océans
Canada

Ecosystems and
Oceans Science

Sciences des écosystèmes
et des océans

Canadian Science Advisory Secretariat (CSAS)

Research Document 2018/050

Quebec Region

Physical Oceanographic Conditions in the Gulf of St. Lawrence during 2017

P.S. Galbraith¹, J. Chassé², C. Caverhill³, P. Nicot⁴, D. Gilbert¹, D. Lefavre¹, C. Lafleur¹

(1) Fisheries and Oceans Canada, Québec Region,
Maurice Lamontagne Institute,
P.O. Box 1000, Mont-Joli, Québec, G5H 3Z4

(2) Fisheries and Oceans Canada, Gulf Region,
Gulf Fisheries Centre,
P.O. Box 5030, Moncton, New Brunswick, E1C 9B6

(3) Fisheries and Oceans Canada, Maritimes Region,
Bedford Institute of Oceanography,
P.O. Box 1006, Dartmouth, Nova Scotia, B2Y 4A2

(4) Institut des sciences de la mer de Rimouski
Université du Québec à Rimouski,
310 allée des Ursulines, Rimouski, Québec, G5L 3A1

Foreword

This series documents the scientific basis for the evaluation of aquatic resources and ecosystems in Canada. As such, it addresses the issues of the day in the time frames required and the documents it contains are not intended as definitive statements on the subjects addressed but rather as progress reports on ongoing investigations.

Published by:

Fisheries and Oceans Canada
Canadian Science Advisory Secretariat
200 Kent Street
Ottawa ON K1A 0E6

[http://www.dfo-mpo.gc.ca/csas-sccs/
csas-sccs@dfo-mpo.gc.ca](http://www.dfo-mpo.gc.ca/csas-sccs/csas-sccs@dfo-mpo.gc.ca)



© Her Majesty the Queen in Right of Canada, 2018
ISSN 1919-5044

Correct citation for this publication:

Galbraith, P.S., Chassé, J., Caverhill, C., Nicot, P., Gilbert, D., Lefaivre, D. and Lafleur, C. 2018. Physical Oceanographic Conditions in the Gulf of St. Lawrence during 2017. DFO Can. Sci. Advis. Sec. Res. Doc. 2018/050. v + 79 p.

Aussi disponible en français :

Galbraith, P.S., Chassé, J., Caverhill, C., Nicot, P., Gilbert, D., Lefaivre, D. et Lafleur, C. 2018. Conditions océanographiques physiques dans le golfe du Saint-Laurent en 2017. Secr. can. de consult. sci. du MPO. Doc. de rech. 2018/050. v + 82 p.

TABLE OF CONTENTS

ABSTRACT.....	IV
INTRODUCTION	1
AIR TEMPERATURE	2
PRECIPITATION AND FRESHWATER RUNOFF.....	2
SURFACE LAYER	3
SEA SURFACE TEMPERATURE	4
SEA ICE.....	5
WINTER WATER MASSES	6
COLD INTERMEDIATE LAYER.....	8
FORECAST FROM THE MARCH SURVEY.....	8
AUGUST–SEPTEMBER CIL.....	8
NOVEMBER CIL CONDITIONS IN THE ST. LAWRENCE ESTUARY	9
SEASONAL MEAN CIL INDEX	9
MAGDALEN SHALLOWS JUNE SURVEY	9
BOTTOM WATER TEMPERATURES ON THE MAGDALEN SHALLOWS	10
DEEP WATERS (>150 M).....	11
BOTTOM WATER TEMPERATURES IN AUGUST AND SEPTEMBER	11
TEMPERATURE AND SALINITY MONTHLY MEANS	11
SEASONAL AND REGIONAL AVERAGE TEMPERATURE STRUCTURE	12
CURRENTS AND TRANSPORTS	13
HIGH FREQUENCY SAMPLING AZMP STATIONS.....	14
OUTLOOK FOR 2018.....	14
SUMMARY	15
KEY FINDINGS.....	15
ACKNOWLEDGEMENTS	16
REFERENCES	17
FIGURES.....	20

ABSTRACT

An overview of physical oceanographic conditions in the Gulf of St. Lawrence (GSL) in 2017 is presented as part of the Atlantic Zone Monitoring Program (AZMP). AZMP data as well as data from regional monitoring programs are analysed and presented in relation to long-term means. The annual average freshwater runoff of the St. Lawrence River measured at Québec City and its combination with rivers flowing into the Estuary (RIVSUM II) were both at the highest level since 1974. Above-normal January air temperatures led to late onset of sea-ice and the sixth lowest sea ice cover maximum volume since 1969, but the winter mixed layer volume was near-normal. The August cold intermediate layer (CIL) showed warmer than normal minimum temperature (+0.8 SD) and less than normal volume of water colder than 1°C (-0.6 SD), but the seasonally average minimum temperature index was near normal. Sea-surface temperatures averaged over the Gulf were near normal or above normal from May to November 2017, leading to an above-normal May-November average (+0.6°C, +0.9 SD). The timing of summer warming onset and fall cooling were respectively slightly sooner (-0.7 weeks) and later than normal (+1.7 weeks). Deep water temperatures have been increasing overall in the Gulf, with inward advection from Cabot Strait. Gulf average temperature decreased from 2015 record highs at 150 and 200 m, remaining above-normal (2.7°C, +0.5 SD and 5.0°C, +1.4 SD), decreased slightly at 250 m (6.0°C, +2.7 SD) from the 2016 record high but increased to a new record level at 300 m (6.3°C, +5.0 SD). The bottom area covered by waters warmer than 6°C decreased in 2017 in Anticosti Channel and Esquiman Channel, but increased sharply in Central Gulf and made its first appearance in the northwest Gulf.

INTRODUCTION

This document examines the physical oceanographic conditions and related atmospheric forcing in the Gulf of St. Lawrence in 2017 (Figure 1). It complements similar reviews of the environmental conditions on the Newfoundland and Labrador Shelf and the Scotian Shelf and Gulf of Maine as part of the Department of Fisheries and Oceans' (DFO) Atlantic Zone Monitoring Program (AZMP; see Therriault et al. 1998 for background information on the program and Colbourne et al. 2016, and Hebert et al. 2016 for examples of past reviews in other AZMP regions). The last detailed report of physical oceanographic conditions in the Gulf of St. Lawrence was produced for the year 2016 (Galbraith et al. 2017). Specifically, it discusses air temperature, freshwater runoff, sea-ice volume, surface water temperature and salinity, winter water mass conditions (e.g., the near-freezing mixed layer volume, the volume of dense water that entered the Gulf through the Strait of Belle Isle), the summertime cold intermediate layer (CIL), and the temperature, salinity, and dissolved oxygen of the deeper layers. Some of the variables are spatially averaged over distinct regions of the Gulf (Figure 2). The report uses data obtained from the AZMP, other DFO surveys, and other sources. Environmental variables are usually expressed as anomalies, i.e., deviations from their long-term mean. The long-term mean or normal conditions are calculated for the standard 1981–2010 reference period when possible. Furthermore, because these series have different units ($^{\circ}\text{C}$, m^3 , m^2 , etc.), each anomaly time series is normalized by dividing by its standard deviation (SD), also calculated for the standard reference when possible. This allows a more direct comparison of the various series. Missing data are represented by grey cells in the tables, values within ± 0.5 SD of the average as white cells, and conditions corresponding to warmer than normal (higher temperatures, reduced ice volumes, reduced cold-water volumes or areas) by more than 0.5 SD as red cells, with more intense reds corresponding to increasingly warmer conditions. Similarly, blue represents colder than normal conditions. Higher than normal freshwater inflow is shown as red, but does not necessarily correspond to warmer-than-normal conditions. Higher than normal stratification values are shown in blue because they are usually caused by lower upper layer salinity.

The summertime water column in the Gulf of St. Lawrence consists of three distinct layers: the surface layer, the cold intermediate layer (CIL), and the deeper water layer (Figure 3). Surface temperatures typically reach maximum values in early to mid-August (Galbraith et al. 2012). Gradual cooling occurs thereafter, and wind forced mixing during the fall leads to a progressively deeper and cooler mixed layer, eventually encompassing the CIL. During winter, the surface layer thickens partly because of buoyancy losses (cooling and reduced runoff) and brine rejection associated with sea-ice formation, but mostly from wind-driven mixing prior to ice formation (Galbraith 2006). The surface winter layer extends to an average depth of 75 m, but may reach >150 m in places such as the Mécatina Trough where near freezing waters (-1.8 to 0°C) from the Labrador shelf entering through the Strait of Belle Isle may extend from the surface to the bottom in depths >200 m (Galbraith 2006). During spring, surface warming, sea-ice melt waters, and continental runoff produce a lower-salinity and higher-temperature surface layer. Underneath this surface layer, cold waters from the previous winter are partly isolated from the atmosphere and form the summer CIL. This layer will persist until the next winter, gradually warming up and deepening during summer (Gilbert and Pettigrew 1997; Cyr et al. 2011) and more rapidly during the fall as vertical mixing intensifies.

This report considers these three layers in turn, but first air temperature and the freshwater runoff are examined because they are significant drivers of the surface layer. The winter sea ice and winter oceanographic conditions are described; these force the summer CIL, which is

presented next. The deeper waters, mostly isolated from exchanges with the surface, are presented last along with a summary of major oceanographic surveys.

AIR TEMPERATURE

The air temperature data are the second generation of homogenized surface air temperature data, part of the Adjusted and Homogenized Canadian Climate Data (AHCCD), which accounts for shifts due to the relocation of stations, changes in observing practices and automation (Vincent et al. 2012). The monthly air temperature anomalies for several stations around the Gulf are shown in Figure 4 for 2016 and 2017, as well as the average of all station anomalies.

Figure 5 shows the annual, winter (December-March), and April-November mean air temperature anomalies averaged over all available stations shown in Figure 4 since 1873. Record-high annual and winter temperatures occurred in 2010 and record-high April-November temperatures in 2012. Galbraith et al. (2012) found the average April-November air temperature over the Gulf from Environment Canada's National Climate Data and Information Archive (NCDIA) to be a good proxy for May-November sea-surface temperature over the Gulf (but excluding the estuary) and found within the former a warming trend of 0.9°C per century between 1873 and 2011; the same trend is found here over the selected ACCHD stations between 1873 and 2017 (Figure 5). The NCDIA December-March air temperatures in the western Gulf were found to be highly correlated ($R^2=0.67$) with sea-ice properties, as well as with winter mixed layer volumes (Galbraith et al. 2010). Galbraith et al. (2013) found slightly higher correlations ($R^2=0.72$) with sea-ice using December-February ACCHD averages, possibly because March temperature are of less importance during low sea-ice cover since much of the sea-ice cover decrease has occurred much earlier in February.

Monthly records were set at four individual stations in October 2017, leading to the warmest average anomaly for that month since 1913 (+2.5°C, +2.3 SD). Overall, the winter had above-normal air temperatures in January and February but finished with below-normal temperatures in March. Later months were characterized by near-normal temperatures except for September and October, leading to near-normal seasonal averages in winter and spring and slightly above-normal in summer and fall. Averaged over all stations, the December-March air temperature average was near-normal (+0.4°C, +0.3 SD) as was the annual average (+0.4°C, +0.5 SD), while the April-November average was just above normal (+0.4°C, +0.6 SD).

PRECIPITATION AND FRESHWATER RUNOFF

Freshwater runoff data for the St. Lawrence River are updated monthly (Figure 6, lower curve) using the water level method from Bourgault and Koutitonsky (1999) and are available from the [St. Lawrence Global Observatory](#). A hydrological watershed model was used to estimate the monthly runoff since 1948 for all other major rivers flowing into the Gulf of St. Lawrence, with discharge locations as shown in Figure 7. The precipitation data (NCEP reanalysis, six hourly intervals) used as input in the model were obtained from the NOAA-CIRES Climate Diagnostics Center (Boulder, Colorado, USA; Kalnay et al. 1996). The data were interpolated to a $\frac{1}{4}^\circ$ resolution grid and the water routed to river mouths using a simple algorithm described here. When air temperatures were below freezing, the water was accumulated as snow in the watershed and later melted as a function of warming temperatures. Water regulation is modelled for three rivers that flow into the estuary (Saguenay, Manicouagan, Outardes) for which the annual runoff is redistributed following the climatology of the true regulated runoffs for 12 months thereafter. Runoffs were summed for each region shown and the climatology established for the 1981–2010 period. The waters that flow into the Estuary (region 1, Fig 7.) were added to the St. Lawrence River runoff measured at Québec City to produce the RIVSUM

II index, although no advection lags were introduced (Figure 6, upper curve). In 2017, the spring freshet occurring in April and May was the strongest since 1974 for both the St. Lawrence River and RIVSUM II index, but the latter was only caused by high St. Lawrence River runoff.

Monthly anomalies of the summed runoffs for 2016 and 2017 are shown in Figure 8. Rivers other than the St. Lawrence contribute about $5\,000\text{ m}^3\text{ s}^{-1}$ runoff to the Estuary, the equivalent of 40% of the St. Lawrence River, while the other tributaries distributed along the border of the GSL provide an additional $3\,900\text{ m}^3\text{ s}^{-1}$ in freshwater runoff to the system. River regulation has a strong impact on the relative contributions of sources. For example, in May 2015 the higher-than-average river runoff into the Estuary (an effect of the heavy precipitation in 2014 and river regulation) was almost as important as the below-normal St. Lawrence run-off (Galbraith et al. 2017). The 2017 hydrological simulation shows that rivers in regions 1 through 5 behaved similarly, with typically above normal runoff in June, but none showed the high April-May spring freshet of the St. Lawrence River. The long-term time series are shown, summed by large basins, in Figure 9. Broad long-term patterns of runoff over the large basins were similar to that of the St. Lawrence River but interannual variability is low in the Northeast basin and Magdalen Shallows basin. The average run-off into the Estuary was near-normal at -0.2 SD . The annual average runoff of the St. Lawrence River measured at Québec City and RIVSUM II both show a general downward trend from the mid-1970s until 2001, an upwards trend between 2001 and 2011 and were at their highest level since 1974 in 2017 (Figure 9) at $14\,300\text{ m}^3\text{ s}^{-1}$ ($+2.7\text{ SD}$) and $19\,200\text{ m}^3\text{ s}^{-1}$ ($+2.1\text{ SD}$). The peak monthly runoff in May was the largest since 1974 for the St. Lawrence River ($+3.8\text{ SD}$) and as well for RIVSUM II ($+3.4\text{ SD}$) in spite of a near-normal contribution from Estuary rivers, and its timing was normal (Figure 6). The fall freshet was above-normal ($+1.2\text{ SD}$). The average St. Lawrence River runoff for April-May, representing the bulk of the spring freshet, was highest of the time series ($+3.6\text{ SD}$, since 1948). This will be seen to have had a large impact on stratification.

SURFACE LAYER

The surface layer conditions of the Gulf are monitored by several complementary methods. The shipboard thermosalinograph network (Galbraith et al. 2002) consists of temperature-salinity sensors (SBE-21; Sea-Bird Electronics Inc., Bellevue, WA) that have been installed on various ships starting with the commercial ship Cicero of Oceanex Inc. in 1999 (retired in 2006) and on the Cabot from 2006 to fall 2013. The Oceanex Connaigra, was outfitted with a thermosalinograph in early 2015.

The second data source is the thermograph network (Pettigrew et al. 2016), which consists of a number of stations with moored instruments recording water temperature every 30 minutes. Most instruments are installed on Coast Guard buoys that are deployed in the ice-free season, but a few stations are monitored year-round. The data are typically only available after the instruments are recovered except for oceanographic buoys that transmit data in real-time. These data are not yet available for 2017 at this time because of the retirement of Bernard Pettigrew; products should return to the annual report by next year.

The third data source are 1 km resolution composites of Sea Surface Temperature (SST) generated using National Oceanic and Atmospheric Administration (NOAA) and European Organisation for the Exploitation of Meteorological Satellites (EUMETSAT) Advanced Very High Resolution Radiometer (AVHRR) satellite images available from the Maurice Lamontagne Institute sea surface temperature processing facility (details in Galbraith and Larouche 2011 and Galbraith et al. 2012). These data are available for the period of 1985-2013. From 2014, AVHRR composites of 1.5-km resolution provided by the Bedford Institute of Oceanography

(BIO) Operational Remote Sensing group complete the data set. Monthly climatologies for the period of 1998-2012 common to both products were compared at the 1.5-km pixel level for cross-calibration. The BIO product is adjusted to the MLI product climatology as $SST_{IML} = 0.9794 \cdot SST_{BIO} - 0.13$ (-0.13°C adjustment at 0°C; -0.54°C at 20°C). This is in part explained by the fact that the MLI product used all available SST images while the BIO product uses only daytime passes, introducing a slight diurnal bias.

SEA SURFACE TEMPERATURE

The May to November cycle of weekly averaged surface temperature over the Gulf of St. Lawrence is illustrated in Figure 10. Galbraith et al. (2012) have shown that Gulf-averaged monthly air temperature and SST climatologies match up quite well with SST lagging air temperature by half a month. Maximum sea-surface temperatures are reached on average during the second week of August but that can vary by a few weeks from year to year. The maximum surface temperature averages to 15.6°C over the Gulf during the second week of August (1985–2010), but there are spatial differences: temperatures on the Magdalen Shallows are the warmest in the Gulf, averaging 18.1°C over that area, and the coolest are at the head of the St. Lawrence Estuary (7.0°C) and upwelling areas along the lower north shore.

Figure 11 shows a mean annual cycle of water temperature at a depth of 8 m along the Montréal to St. John's shipping route based on thermosalinograph data collected from 2000 to 2017. The data were averaged for each day of the year at intervals of 0.1 degree of longitude to create a climatological composite along the ship track. The most striking feature is the area at the head of the Laurentian Trough (69.5°W), where strong vertical mixing leads to cold summer water temperatures (around 5°C to 6°C and sometimes lower) and winter temperatures that are always above freezing (see also Figure 10). The climatological cycle shows the progression to winter conditions, first reaching near-freezing temperatures in the Estuary and then progressing eastward with time, usually reaching Cabot Strait by the end of the winter (but no further).

Thermosalinograph data show that near-freezing surface layer conditions first appeared later than normal in winter (Figure 11), consistent with the above normal January air temperatures over the Gulf (Figure 4).

Monthly mean sea-surface temperatures from AVHRR imagery are presented as maps (Figure 12), temperature anomaly maps (Figure 13), spatial averages expressed as anomalies (Figure 14) or as mean temperatures for the last two years (Figure 15) as well as since 1985 (Figs. 16 and 17). Near-surface water temperatures averaged over the Gulf were near normal or above normal from May to November 2017, leading to an above-normal May-November average (+0.6°C, +0.9 SD). A record low was reached in June in Mécatina Trough (3.5°C, below normal by 2.2°C at -2.1 SD). Note the absence of any negative monthly anomalies from May to November in the regions of Centre Gulf, Cabot Strait and the Magdalen Shallows. The thermosalinograph data show above-normal surface layer conditions in September as well (Figure 11).

Sea-surface temperature monthly climatologies and time series were also extracted for more specific regions of the Gulf. The Magdalen Shallows, excluding Northumberland Strait, is divided into western and eastern areas as shown in Figure 18. The monthly average SST for the Magdalen Shallows as a whole (region 8) is repeated in Figure 19 along with averages for the western and eastern areas. Climatologies differ by roughly 0.5°C to 1°C between the western and eastern regions. Temperatures were normal to above normal from May to November and always above normal in the Eastern portion from June to November.

The number of weeks in the year that the mean weekly temperature is above 10°C for each pixel (Figure 20) integrates summer surface temperature conditions into a single map

displaying the length of the warm season. The average number of weeks with mean weekly temperature above 10°C are shown for each region as time series in Figure 21. All regions except the Estuary had a longer than normal warm season. On average over the Gulf, it was 1.8 weeks longer than normal (+1.1 SD).

Seasonal trends in relation to air temperature are examined by first displaying weekly averaged AVHRR SST in the GSL for all years between 1985 and 2017 (Figure 22) with years on the x-axis and weeks of the year on the y-axis (See Galbraith and Larouche 2013 for a full description). Isotherms show the first and last occurrences of temperature averages of 12°C over the years. These temperatures are chosen to be representative of spring (and fall) transitions to (and from) typical summer temperatures. Although the selected temperature is arbitrary, the results that follow are not particularly sensitive to the exact temperature chosen because the surface mixed layer tends to warm and cool linearly in spring and fall (e.g. Figure 10). A 10°C threshold is also used to demonstrate this. The Gulf has experienced earlier summer onset and later fall cooling between 1985 and 2017, with trends of -0.5 and +0.6 weeks per decade respectively (confidence intervals of ± 0.4 weeks per decade, therefore significantly different from zero). In 2017, the timing of 12°C summer onset was near-normal but the onset of fall cooling was later than normal by 1.6 weeks. The interannual variability in the time of year when the 12°C threshold is crossed is correlated with June-July average air temperature for the summer onset (1.1 week sooner per 1°C increase; $R^2=0.60$) and with September average air temperature for the fall (0.8 week later per 1°C increase; $R^2=0.48$). These air temperature averages, shown in Figure 22, can be used as proxies prior to 1985. The implication is that the Gulf of Lawrence warm season will be longer by about 2 weeks for each 1°C of warming associated with climate change.

SEA ICE

Ice volume is estimated from three ice cover products obtained from the Canadian Ice Service (CIS), further processed into regular grid that are used in analyses. These are weekly Geographic Information System (GIS) charts covering the period 1969-2017 and daily charts covering the period 2009-2017. Both were gridded on a 0.01° latitude by 0.015° longitude grid (approximately 1 km resolution). The third CIS product consists of 5-km resolution gridded daily files covering the period 1998-2008. Some of the analyses described below were done using the weekly data exclusively, for long-term consistency, while for others daily data were used when available with results filtered using a 3-day running mean in order to make them more comparable to results calculated from weekly data.

Several products were computed to describe the sea-ice cover interannual variability: day of first and last occurrence and duration maps (Figure 23) and regional averages (Figure 24); distribution of ice thickness during the week of maximum volume (Figure 25, upper panels) and maximum thickness reached at any time during the season (Figure 25, lower panels); daily evolution of the estimated sea-ice volume in relation to the climatology and historical extremes (Figure 26); estimated seasonal maximum ice volumes within the Gulf as well as on the Scotian Shelf (Figure 27); time series of seasonal maximum ice volume and area (excluding thin new ice), ice season duration and December-to-March air temperature anomaly (Figure 28).

There has been a declining trend in ice cover severity since 1990 with rebounds in 2003 and 2014 (Figure 28). The correlation between annual maximum ice volume (including the cover present on the Scotian Shelf) and the December-February air temperature averaged over five Western Gulf stations (Sept-Îles, Mont-Joli, Gaspé, Charlottetown and Îles-de-la-Madeleine) accounted for 72% of the variance using the 1969–2012 time series (Galbraith et al. 2013). Figure 28 shows a similar comparison using ice volume and the ACCHD December-to-March

air temperature anomaly from Figure 5 also yielding $R^2 = 0.72$. The correlation between air temperature and the ice parameters season duration and area are also very high ($R^2 = 0.77$ - 0.78). Correlation coefficients are slightly higher when using January to February air temperatures, perhaps because March air temperatures have no effect on ice cover that has almost disappeared by then during very mild winters. Sensitivity of the ice cover to climate change can be estimated using past co-variations between winter air temperature and sea-ice parameters, which indicate losses of 17 km^3 , $31,000 \text{ km}^2$ and 14 days of sea-ice season for each 1°C increase in winter air temperature

Ice typically forms first in December in the St. Lawrence estuary and in shallow waters along New Brunswick, Prince Edward Island and the lower north shore and melts last in the northeast Gulf where the ice season duration tends to be longest apart from shallow bays elsewhere (Figure 23a). Offshore sea ice is typically produced in the northern parts of the Gulf and drifts towards Îles-de-la-Madeleine and Cabot Strait during the ice season.

In 2017, the sea-ice cover formed later than normal (Figure 23, Figure 24) and its volume was close to historical minimums until early February (Figure 26). The seasonal maximum ice volume of only 23 km^3 occurred the week of March 13th was (Figure 25). While the peak sea-ice volume is typically reached early during low sea-ice year (Figure 26), the low seasonal maximum was reached at a near-normal time of year in mid-March, probably due to below-normal air temperatures in March (-1.5°C , -0.7 SD). The seasonal maximum ice volume was well below-normal (-1.5 SD) and sixth lowest of the time series that began in 1969 (Figure 27). The duration was below-normal (-0.9 SD) as was the area (-1.2 SD) (Figure 28). The short duration was mostly associated with delayed first occurrence of sea-ice (Figure 24). These are weaker sea-ice conditions that might have been expected from near-normal winter air temperatures ($+0.4^\circ\text{C}$, $+0.3 \text{ SD}$). Six of the eight lowest maximum ice volumes of the time series have occurred in the previous eight years (Figure 28). Almost no ice was exported from the Gulf of St. Lawrence onto the Scotian Shelf in 2017 (Figure 25, Figure 27). The ice cover decreased to almost zero after mid-May before late advection from the Strait of Belle Isle led to a rare second maximum and around June 1st the estimated volume exceeded historical observations (Figure 26). The inflow consisted of very thick ($>120 \text{ cm}$) first year ice and traces of second-year ice. While unusual, the June presence of sea-ice in the area has occurred as recently as 2014 and was fairly common during the heavy ice conditions of the 1990s, although not usually as plentiful; sea-ice was present in the area into July in 1991.

First occurrence of sea-ice was late and last occurrence was typically near-normal except for the previously discussed late presence in Mécatina Trough spilling into Esquiman Channel. This led to a mix of durations ranging from much below normal in the Northwest Gulf and Cabot Strait to above normal in Mécatina Trough by more than 5 weeks (Figure 23, Figure 24).

WINTER WATER MASSES

A wintertime survey of the Gulf of St. Lawrence waters (typically 0–200 m) has been undertaken in early March since 1996, typically using a Canadian Coast Guard helicopter but from Canadian Coast Guard ships in 2016 and 2017. The survey, sampling methods, and results of the cold-water volume analysis in the Gulf and the estimate of the water volume advected into the Gulf via the Strait of Belle Isle over the winter are described in Galbraith (2006) and in Galbraith et al. (2006). Figure 29 and Figure 30 show gridded interpolations of near-surface temperature, temperature difference above freezing, salinity, cold layer thickness and bottom contacts, and thickness of the Labrador Shelf water intrusion for 2017 as well as climatological means.

The March surface mixed layer is usually very close (within 0.1°C) to the freezing point in most regions of the Gulf but thickness of the surface layer varies, leaving variability in the cold-water volume between mild and severe winters rather than in temperature. One exception was 2010 when, for the first time since the inception of the winter survey, the mixed layer was on average 1°C above freezing. During typical winters, surface waters in the temperature range of $\sim 0^{\circ}\text{C}$ to -1°C are only found from the northeast side of Cabot Strait and into the Gulf. Some of these warm waters have presumably entered the Gulf during winter and flowed northward along the west coast of Newfoundland, however it is also possible that local waters could have simply not cooled close to freezing. Conditions in March 2017 were warm in the triangle formed roughly by Gros Morne (NL), offshore of Heath Point on Anticosti and Port aux Basques (NL) (Figure 29), consistent with the lack of sea-ice in that part of the Gulf in the observed maximum ice cover field (Figure 25).

Near-freezing waters with salinities of around 32 are responsible for the (local) formation of the CIL since that is roughly the salinity at the temperature minimum during summer. These are coded in green-blue in the salinity panel of Figure 29 and are typically found to the north and east of Anticosti Island. Surface salinities were a bit lower than the climatology in this part of the Gulf during the winter of 2017.

Near-freezing waters with salinity >32.35 (colour-coded in violet) are considered to be too saline to have been formed from waters originating within the Gulf (Galbraith 2006) and are presumed to have been advected from the Labrador Shelf through the Strait of Belle Isle. These waters were present at the surface only at the northeast end of Mécatina Trough in March 2017 (Figure 29). A T-S water mass criterion from Galbraith (2006) was used to identify intruding Labrador Shelf waters that have exhibited no evidence of mixing with warm and saline deep Gulf water. These waters occupied a thick sub-surface layer throughout Mécatina Trough in March 2017, (top-right panel of Figure 30). The recent history of Labrador Shelf water intrusions is shown in Figure 31, where its volume is shown as well as the fraction it represents of all the cold-water volume in the Gulf. This volume was near-normal in March 2017, at 1500 km^3 ($+0.1\text{ SD}$) representing 12% (-0.1 SD) of the cold water ($T < -1^{\circ}\text{C}$) in the Gulf.

The cold mixed layer depth typically reaches about 75 m in the Gulf and is usually delimited by the -1°C isotherm because the mixed layer is typically near-freezing and deeper waters are much warmer (Galbraith 2006). In March 2010 and 2011 much of the mixed layer was warmer than -1°C such that the criterion of $T < 0^{\circ}\text{C}$ was also introduced (see middle panels of Figure 30). The cold surface layer is the product of local formation as well as cold waters advected from the Labrador Shelf, and can consist either of a single water mass or of layers of increasing salinity with depth. This layer reaches the bottom in many regions of the Gulf, with interannual variability in whether the deepest parts of the Magdalen Shallow or of Mécatina Trough are reached (see bottom panels of Figure 30). The interannual variability of winter volumes of water colder than 0 and 1°C are shown in Figure 32.

Integrating the cold layer depth over the area of the Gulf (excluding the Estuary and the Strait of Belle Isle) yields a cold-water ($< -1^{\circ}\text{C}$) volume of $12\,200\text{ km}^3$ in 2017, 0.2 SD above the 1996–2017 average. The time series of winter cold-water ($< -1^{\circ}\text{C}$) volume observed in the Gulf is shown in Figure 33. The mixed layer volume increases to $15\,300\text{ km}^3$ when water temperatures $< 0^{\circ}\text{C}$ are considered which is 0.5 SD above the 1996–2017 average. This last volume of cold water corresponds to 46% of the total water volume of the Gulf ($33\,500\text{ km}^3$, excluding the Estuary).

COLD INTERMEDIATE LAYER

FORECAST FROM THE MARCH SURVEY

The summer CIL minimum temperature index (Gilbert and Pettigrew 1997) has been found to be highly correlated with the Gulf (excluding the estuary) volume of cold water ($<-1^{\circ}\text{C}$) measured the previous March when much of the mixed layer is near-freezing (Galbraith 2006; updated relation in right panel of the present document Figure 32). This is expected because the CIL is the remnant of the winter cold surface layer. A measurement of the volume of cold water present in March is therefore a valuable tool for forecasting the coming summer CIL conditions. The winter mixed layer in 2017 was not near-freezing throughout the Gulf. The overall thickness and volume of the layer colder than -1°C was near normal at $+0.2$ SD. The Cold Intermediate Layer for summer 2017 was therefore forecasted to be colder than in 2016, with a Gilbert and Pettigrew (1997) index of around -0.2°C compared to -0.1°C in 2016 (Galbraith et al. 2017).

AUGUST–SEPTEMBER CIL

The CIL minimum temperature, thickness and volume for $T<0^{\circ}\text{C}$ and $<1^{\circ}\text{C}$ were estimated using temperature profiles from all sources for August and September. Most data are from the multi-species surveys in September for the Magdalen Shallows and August for the rest of the Gulf. Using all available temperature profiles, spatial temperature interpolations of the Gulf were done for each 1-m depth increment, with the interpolated field bound between the minimum and maximum values observed within each of the different regions of the Gulf (Figure 2) to avoid spurious extrapolations. The CIL thickness at each grid point is simply the sum of depth bins below the threshold temperature, and the CIL minimum temperature is only defined at grid points where temperature rises by at least 0.5°C at depths greater than that of the minimum, or if the grid point minimum temperature is below the CIL spatial average of the Gulf.

Figure 33 shows the gridded interpolation of the CIL thickness $<1^{\circ}\text{C}$ and $<0^{\circ}\text{C}$ and the CIL minimum temperature for August–September 2017 as well their 1985-2010 climatology (1994-2010 for Mécatina Trough). The CIL thickness for $T<0^{\circ}\text{C}$ and $T<1^{\circ}\text{C}$ increased compared to 2016, with conditions similar to 2009 (not shown). Similar maps were produced for all years back to 1971 (although some years have no data in some regions), allowing the calculation of volumes for each region for each year as well as the climatologies shown on the left side of Figure 33. The 2017 CIL water mass was thinner and warmer than the 1985-2010 climatologies, except for the northeast Gulf.

The time series of the regional August–September CIL volumes are shown in Figure 34 (for $<0^{\circ}\text{C}$ and $<1^{\circ}\text{C}$). Most regions show increased CIL volumes in 2017 compared to 2016. Figure 35 shows the total volume of CIL water ($<0^{\circ}\text{C}$ and $<1^{\circ}\text{C}$) and the average CIL core temperature from the August–September interpolated grids (e.g., Figure 33). The CIL areal minimum temperature average and volume shown in Figure 35 exclude data from Mécatina Trough which has very different water masses from the rest of the Gulf; it is influenced by inflow through the Strait of Belle Isle and is therefore not indicative of the climate in the rest of the Gulf. The CIL volume as defined by $T<1^{\circ}\text{C}$ increased significantly (to -0.6 SD) compared to 2016 conditions

(-1.9 SD) while remaining less (warmer) than average. The volume delimited by 0°C also increased, from -1.2 to -0.6 SD from climatology means.

The time series of the CIL regional average minimum core temperatures are shown in Figure 36. All regions, again except for the northeast Gulf, show a decrease in core temperature compared to 2016. The 2017 average temperature minimum (excluding Mécatina Trough, the

Strait of Belle Isle and the Magdalen Shallows) was 0.1°C ($+0.8$ SD), a decrease of 0.2°C from 2016, and is shown in Figure 35 (bottom panel, green line). The average difference between this CIL index and the Gilbert and Pettigrew (1997) index (described below) is 0.27°C because of the warming between mid-June and the August survey. This index corresponds to a Gilbert and Pettigrew (1997) index of -0.2°C after rounding to the nearest decimal. The overall 2017 CIL water mass properties are similar to observations of 2009.

NOVEMBER CIL CONDITIONS IN THE ST. LAWRENCE ESTUARY

The AZMP November survey provides a high-resolution conductivity-temperature-depth (CTD) sampling grid in the St. Lawrence estuary since 2006 although measurements are sparser in some years. This allows a higher resolution display of the CIL minimum temperature in the Estuary (Figure 37). The data also show the temporal warming (Figure 34) and thinning (Figure 36) of the CIL since the August survey. The CIL was colder in November 2017 than in 2016, but again none of it was below 0°C . Figure 36 shows that the fairly rapid increase of the CIL minimum temperature occurring between August and November is fairly constant inter-annually in spite of the differences in August temperature.

SEASONAL MEAN CIL INDEX

The Gilbert and Pettigrew (1997) CIL index is defined as the mean of the CIL minimum core temperatures observed between 1 May and 30 September of each year, adjusted to 15 July with a region-dependant warming rate. It was updated using all available temperature profiles measured within the Gulf between May and September inclusively since 1947 (black line of the bottom panel of Figure 35). As expected, the CIL core temperature interpolated to 15 July is almost always colder than the estimate based on August and September data for which no temporal corrections were made. This is because the CIL is eroded over the summer and therefore its core warms over time.

This CIL index for summer 2017 was -0.30°C , near-normal at $+0.3$ SD. The 0.20°C decrease from the summer 2016 CIL index is consistent with the decrease in CIL volume between August 2016 and 2017 discussed above and the decrease of 0.2°C in the areal average of the minimum temperature in August. The warm winter conditions from 2010 to 2012 led to CIL indices that were still far below the record high observed in the 1960s and 1980s. The earlier CIL temperature minimums will need to be re-examined to confirm that they were calculated using data with sufficient vertical resolution to correctly resolve the core minimum temperature. It is also becoming increasingly clear that the winter mixed layer is not the only factor explaining summertime CIL conditions and that mechanisms having a multi-year cumulative effect are required to explain the interannual autocorrelations observed. For example, this may be linked to temperatures below the CIL, which in warm years may create a higher temperature gradient that leads to higher heat fluxes and faster summertime CIL warming rates.

As a summary, Figure 38 shows selected time series of winter and summertime CIL conditions (June and September bottom temperatures also related to the CIL are outlined below) and highlights the strong correlations between these various time series. Conditions related to the CIL were near-normal to warmer-than-normal in 2017.

MAGDALEN SHALLOWS JUNE SURVEY

A long-standing assessment survey covering the Magdalen Shallows has taken place in June for mackerel assessments and was since merged with the June AZMP survey. This survey provides good coverage of the temperature conditions that are greatly influenced by the cold

intermediate layer that reaches the bottom at roughly half of the surface area at this time of the year.

Near-surface waters warm quickly in June, mid-way between the winter minimum and the annual maximum in early August. This can introduce a bias if the survey dates are not the same each year. To account for this, the seasonal warming observed at the Shediac Valley AZMP monitoring station was evaluated. A linear regression was performed of temperature versus time for each meter of the water column for each year with monitoring data at Shediac Valley between May and July. Visual inspection showed that the depth-dependent warming rate was fairly constant for all years and an average was computed for every depth. Warming is maximal at the surface at 18°C per 100 days and, in spite of some uncertainties between 30 and 55 m, decreases almost proportionally with depth to reach 2°C per 100 days at 40 m, followed by a further linear decrease to reach 1°C per 100 days at 82 m (Galbraith and Grégoire 2015).

All available temperature profiles taken in June from a given year are binned at 1 m depth intervals (or interpolated if the resolution is too coarse) and then adjusted according to the sampling date to offset them to June 15th according to the depth-dependent warming rate extracted from Shediac Valley monitoring data. An interpolation scheme is used to estimate temperature at each 1 m depth layer on a 2 km resolution grid. Figure 39 shows temperatures and anomalies at depths of 20, 30 and 50 m. Figure 40 shows averages over the grids at 0, 10, 20, 30, 50 and 75 m for all years when interpolation was possible, as well as SST June averages since 1985, for both western and eastern regions of the Magdalen Shallows (Figure 18). Temperatures were on average near normal to above normal except at 10 m in the western portion (Figure 39 and Figure 40).

BOTTOM WATER TEMPERATURES ON THE MAGDALEN SHALLOWS

Bottom temperature is also estimated at each point of the grids constructed from the June survey by looking up the interpolated temperature at the depth level corresponding to a bathymetry grid provided by the Canadian Hydrographic Service with some corrections applied (Dutil et al. 2012). The method is fully described in Tamdrari et al. (2012). A climatology was constructed by averaging all available temperature grids between 1981 and 2010 and anomaly grids were computed for each year. The June bottom temperature climatology as well as the 2017 reconstructed temperature and anomaly fields are shown in Figure 41. The same method was applied using the available CTD data from August and September, thus including the multispecies surveys for the northern Gulf in August and for the Magdalen Shallows in September. These results are also shown in Figure 41. While much of the deeper bottom water temperatures are climatologically still below 0°C in June, a remnant from the winter near-freezing mixed layer that reached the bottom, most of the area usually warms to below 1°C by August-September. Temperature anomalies in coastal shallow waters range from <-2.5°C to >+2.5°C, but anomalies tend to be of smaller magnitude in deeper waters.

Time series of the bottom area covered by water in various temperature intervals were estimated from the gridded data for the June surveys as well as for the September multispecies survey on the Magdalen Shallows (Figure 42). The time series of areas of the Magdalen Shallows covered by water colder than 0, 1, 2, and 3°C in June and September are also shown in Figure 38 as part of the CIL summary. Some of the bottom of the Magdalen Shallows was covered by water with temperatures <-1°C in June 2017, in contrast to warmer conditions in June 2016, and by water with temperatures <0°C by August-September; these are near normal conditions that are nevertheless colder than during the recent 2010-2013 period. The area covered by water temperatures <1°C in September had reached a low (warm conditions) not seen since 1982 in 2012, but rebounded to near-normal in 2014 and 2015, and again in 2017.

At higher threshold temperatures, areas with $T < 2^{\circ}\text{C}$ and $< 3^{\circ}\text{C}$ were below normal in June but above normal in September 2017 (Figure 38).

DEEP WATERS (>150 M)

The deeper water layer (>150 m) below the CIL originates at the entrance of the Laurentian Channel at the continental shelf and circulates towards the heads of the Laurentian, Anticosti, and Esquiman channels without much exchange with the upper layers. The layer from 150 to 540 m is characterized by temperatures between 1 and $>7^{\circ}\text{C}$ and salinities between 32.5 and 35 (except for Mécatina Trough where near-freezing waters may fill the basin to 235 m in winter and usually persist throughout the summer). Interdecadal changes in temperature, salinity, and dissolved oxygen of the deep waters entering the Gulf at the continental shelf are related to the varying proportion of the source cold–fresh and high dissolved oxygen Labrador Current water and warm–salty and low dissolved oxygen slope water (McLellan 1957; Lauzier and Trites 1958; Gilbert et al. 2005). These waters travel from the mouth of the Laurentian Channel to the Estuary in roughly three to four years (Gilbert 2004), decreasing in dissolved oxygen from in situ respiration and oxidation of organic material as they progress to the channel heads. The lowest levels of dissolved oxygen (around 20 percent saturation in recent years) are therefore found in the deep waters at the head of the Laurentian Channel in the Estuary.

BOTTOM WATER TEMPERATURES IN AUGUST AND SEPTEMBER

The same method used to calculate bottom water temperature on the Magdalen Shallows was applied to the entire Gulf by combining all available CTD data from August and September, thus including the multispecies surveys for the northern Gulf in August and for the Magdalen Shallows in September into a single map (Figure 43). All of the Gulf deep bottom water temperatures were above normal, with large areas of Anticosti and Esquiman Channels above 6°C , spreading into the northwest Gulf on the flanks of the Laurentian Channel.

Time series of the bottom area covered by water in various temperature intervals were also estimated for the other regions of the Gulf based on August–September temperature profile data (Figs. 44 and 45). Many areas had bottom waters colder than 0°C , and Mécatina Trough had bottom waters colder than -1°C . The figures also show compression of the bottom habitat area in the temperature range of $5\text{--}6^{\circ}\text{C}$ in 1992, offset by larger colder $4\text{--}5^{\circ}\text{C}$ habitat. In 2012, a return of $>6^{\circ}\text{C}$ temperatures to the sea floor began. By 2015, it had caused a large decrease of the $5\text{--}6^{\circ}\text{C}$ habitat in Anticosti and Esquiman Channels, this time replace by warmer $6\text{--}7^{\circ}\text{C}$ habitat. The $6\text{--}7^{\circ}\text{C}$ area decreased a bit in these Channels in 2017, but increased sharply in Central and northwest Gulf.

The warm waters found at the bottom of the Laurentian Channel and elsewhere are associated with the deep temperature maximum evident in the temperature profiles in these areas (e.g. Figure 3). The recent inter-annual progression to current conditions of the deep temperature maximum is shown on Figure 46. Temperatures above 7°C have been recorded since 2012 in the Gulf near Cabot Strait. The Gulf-wide average and regional areal averages are shown in Figure 47 for temperature and in Figure 48 for salinity. The deep maximum temperature Gulf-wide average was at a series record high in 2017, at 6.28°C , however the regional average for Anticosti Channel decreased from a record high set in 2015.

TEMPERATURE AND SALINITY MONTHLY MEANS

Monthly temperature and salinity averages were constructed for various depths using a method used by Petrie et al. (1996) but using the geographical regions shown in Figure 2. In this

method, all available data obtained during the same month within a region and close to each depth bin are first averaged together for each year. Monthly averages from all available years and their standard deviations are then computed for climatologies. This two-fold averaging process reduces the bias that occurs when the numbers of profiles in any given year are different. These monthly averages were further averaged into regional yearly time series that are presented in Figs. 47 (temperature) and 48 (salinity) for 200 and 300 m. The 300 m observations in particular suggest that temperature anomalies are advected up-channel from Cabot Strait to the northwestern Gulf in two to three years, consistent with the findings of Gilbert (2004). The regional averages are weighted into a Gulf-wide average in accordance to the surface area of each region at the specified depth. These Gulf-wide averages are shown for 150, 200 and 300 m in Figs. 48-50. Linear trends in temperature and salinity at 300 m of 2.2°C and 0.3 per century, respectively are shown on Figure 49 (See also Galbraith et al. 2013 for other long term trends).

In 2017, the gulf-wide average salinities decreased at all depths shallower than 300 m shown in Figs. 48 and 49 from 2016 levels to below normal at 150 and 200 m and near-normal at 250 m. Temperature decreased from 2015 record highs at 150 and 200 m, remaining above-normal (2.7°C, +0.5 SD and 5.0°C, +1.4 SD), decreased slightly at 250 m (6.0°C, +2.7 SD) from the 2016 record high but increased to a new record level at 300 m (6.3°C, +5.0 SD). At 300 m, temperature increased to regional record highs in all deep regions of the Gulf: Estuary (5.5°C, +2.5 SD), Northwest Gulf (5.9°C, +3.7 SD), Central Gulf (6.4°C, +4.6 SD) and Cabot Strait (6.7°C, +4.4 SD).

The warm anomalies present since 2010 at Cabot Strait have been progressing up the channel towards the Estuary since then, but waters that have followed into the gulf have also remained very warm and even increased in temperature such that the average overall temperature may continue to increase (Figure 46). The potential for still warmer waters entering the Gulf exists, as evidenced by an average temperature of 9.2°C observed at the Laurentian Mouth at 200 m in 2016 (Figure 47), a record since the series began in 1914, and a 2015 record high of 7.6°C at 300 m.

SEASONAL AND REGIONAL AVERAGE TEMPERATURE STRUCTURE

In order to show the seasonal progression of the vertical temperature structure, regional averages are shown in Figs. 50 to 53 based on the profiles collected during the March helicopter survey, the June AZMP and mackerel surveys, the August multi-species survey (September survey for the Magdalen Shallows), and the October-November AZMP survey. All additional archived CTD data for those months were also used. The temperature scale was adjusted to highlight the CIL and deep-water features; the display of surface temperature variability is best suited to other tools such as remote sensing and thermographs. Average discrete depth layer conditions are summarized for the months of the 2016 and 2017 AZMP surveys in Figure 54 for temperature and in Figure 55 for salinity and 0-50 m stratification. For each survey the anomalies were computed relative to monthly temperature and salinity 1981-2010 climatologies calculated for each region, shown in grey as the mean value \pm 0.5 SD in Figs. 50 to 53.

Caution is needed in interpreting the March profiles. Indeed, regional averaging of winter profiles does not work very well in the northeast Gulf (regions 3 and 4) because very different water masses are present in the area such as the cold Labrador Shelf intrusion with saltier and warmer deeper waters of Anticosti Channel or Esquiman Channel. For example, the sudden temperature changes near the bottom of Mécatina Trough in 2016 resulted from the deepest cast used which contained colder deep waters. The highlights of March water temperatures

shown in Figure 50 include the previously discussed winter mixed layer, with near-normal thicknesses for $T < -1^{\circ}\text{C}$ and above-normal for $T < 0^{\circ}\text{C}$. The thermocline was much shallower than usual in Esquiman Channel and in particular in the Estuary. Waters in the deepest parts of Mécatina Trough were near-freezing, indicating renewal from a Labrador Shelf intrusion. Deep water masses in Mécatina Trough remained cold through to November.

Temperatures in June and August 2017 were characterized by CIL conditions that were typically close to normal in thickness. Deep-water temperatures were above normal in all regions along the Laurentian Channel, with most regions showing increases compared with 2016 conditions in waters deeper than 250 m depth. Temperatures at the depth of the temperature maximum (200 to >250 m) remained above normal in Esquiman Channel and central Gulf, exceeding 6°C at depth, presumably advected in from the Cabot Strait recent record-high conditions. Temperatures exceeded 7°C around 250 m in Cabot Strait in the Fall.

CURRENTS AND TRANSPORTS

Currents and transports are derived from a numerical model of the Gulf of St. Lawrence, Scotian Shelf, and Gulf of Maine. The model is prognostic, i.e., it allows for evolving temperature and salinity fields. It has a spatial resolution of $1/12^{\circ}$ with 46 depth-levels in the vertical. The atmospheric forcing is taken from the Global Environmental Multiscale (GEM) model running at the Canadian Meteorological Center (CMC). Freshwater runoff is obtained from observed data and the hydrological model, as discussed in the freshwater runoff section. A simulation was run for 2006–2017 from which transports were calculated. The reader is reminded that the results outlined below are not measurements but simulations and improvements in the model may lead to changes in the transport values.

Figs. 56–58 show seasonal depth-averaged currents for 0–20 m, 20–100 m, and 100 m to the bottom for 2017. Currents are strongest in the surface mixed layer, generally 0–20 m, except in winter months when the 20–100 m and the 100 m to bottom averages are almost as high (note the different scale for this depth). Currents are also strongest along the slopes of the deep channels. The Anticosti Gyre is always evident but strongest during winter months, when it even extends strongly into the bottom-average currents.

Monthly averaged transports across seven sections of the Gulf of St. Lawrence are shown in Figure 59 for sections with some estuarine circulation, and in Figure 60 for sections where only net transports are relevant. In Figure 59, the net transport integrates both up and downstream circulation and, for example, corresponds to freshwater runoff at the Pointe-des-Monts section. The outflow transport integrates all currents heading toward the ocean, while the estuarine ratio corresponds to the outflow divided by the net transports. Note that the only section where estuarine circulation is dominant is at Pointe-des-Monts. The net transport at Honguedo is on average 15 times higher, consisting mostly of circulation around Anticosti Island first observed at the Jacques-Cartier section. Similarly, the net transport at Cabot Strait is mostly balanced by inflow from Belle Isle Strait such perhaps an estuarine ratio is perhaps a misleading description. Transports through sections under the direct estuarine influence of the St. Lawrence River (e.g., Pointe-des-Monts) have a more direct response to change in freshwater runoff while others (e.g., Cabot Strait, Bradelle Bank) have a different response, presumably due to redistribution of circulation in the GSL under varying runoff. The estuarine circulation ratio is determined by the mixing intensities within the estuary and is greatly influenced by stratification. It is on average greatest during winter months and weakest during the spring freshet. In fact, it is sufficiently reduced in spring that the climatological outward transport at Pointe-des-Monts reaches its minimum value in June even though this month corresponds to the third highest net transport of the year, i.e. the estuary becomes sufficiently stratified that fresh water runoff tends to slip on

top of the denser salty waters underneath. In 2017, the exceptionally April freshet led to decreased modeled estuarine circulation and decreased outward transport by entrainment.

HIGH FREQUENCY SAMPLING AZMP STATIONS

Sampling by the Maurice Lamontagne Institute began in 1991 at a station offshore of Rimouski (48° 40' N 68° 35' W, 320 m depth; Plourde et al. 2009), typically once a week during summer and less often during spring and fall and almost never in winter (Figure 61). In 2013, following several analyses that identified good correlations and correspondences between the prior AZMP Anticosti Gyre and Gaspé Current stations with the Rimouski station, it was decided to drop sampling efforts at these logistically difficult stations and integrate the Rimouski station officially in the AZMP program and begin winter sampling there when opportunities arose. The AZMP station in the Shediac Valley (47° 46.8' N, 64° 01.8' W, 84 m depth) is sampled on a regular basis by the Bedford Institute of Oceanography as well as occasionally by DFO Gulf Region and by the Maurice Lamontagne Institute during their Gulf-wide surveys (Figure 61). This station has been sampled irregularly since 1947, nearly every year since 1957, and more regularly during the summer months since 1999 when the AZMP program began. However, observations were mostly limited to temperature and salinity prior to 1999.

In 2017, oceanographic buoys equipped with an automatic temperature and salinity profiler carried out 866 full-depth casts at Shediac Valley station between June 16 and October 27, and 1208 casts to typically 200 m depth at Rimouski station between April 25 and November 13.

Isotherms and isohalines as well as monthly averages of layer temperature and salinity, stratification, and CIL core temperature and thickness at <1°C are shown for 2013-2017 for the Rimouski station in Figure 62 and for the Shediac Valley station in Figure 63. The scorecard climatologies are calculated from 1991-2010 data for Rimouski station, and for 1981-2016 for Shediac Valley (The time span of the climatology is extended at Shediac Valley because of the sparseness of data prior to 1999). Buoy data are used for scorecard metrics down to 200 m for Rimouski station but not for the display of isotherms and isohalines.

At the Rimouski station, the gradual shift of cold-fresh 200-300 waters present in 2010 to warmer-saltier waters advected from Cabot Strait lead to a shift to warm anomalies by May 2013 and series records in temperature (5.64°C) observed in December 2017. Below-normal near-surface salinities were recorded between March and June, including the second lowest monthly average in May 2017 (after May 1996), creating the second highest monthly average stratification, coinciding with the record high spring freshet.

Below normal near-surface salinities were recorded between June and August at Shediac Valley station (Figure 63), including a series record in June 2017 for both low salinity and high stratification.

Figure 64 shows the interannual variability of some bulk layer averages from May to October for the two stations. Stratification was above normal at both stations, but not record breaking. Near-bottom temperature was not record-breaking at Rimouski station in spite of the year holding the individual monthly record.

OUTLOOK FOR 2018

Air temperatures were near normal over the Gulf from November 2017 through February 2018. This was the setting for the March 2018 survey, which provides an outlook for CIL conditions expected for the remainder of 2018. Figure 65 shows the surface mixed layer temperature, salinity, and thickness (at $T < -1^{\circ}\text{C}$ and $T < 0^{\circ}\text{C}$), as well as the thickness and extent of the cold

and saline layer that has intruded into the Gulf from the Labrador shelf. A much smaller portion of the winter mixed layer was warm (above -1°C) than in March 2017. In spite of this, perhaps partially offset by a very small inflow of high-salinity Labrador Shelf water into the Gulf, the volume of the surface mixed layer colder than -1°C was only slightly larger than in 2017. The Cold Intermediate Layer for summer 2018 is therefore forecasted to be slightly colder than in 2017, with a Gilbert and Pettigrew (1997) index of around -0.28°C compared to -0.2°C in 2017.

Concerning deep waters, recall that record high temperatures have been recorded in Cabot Strait since 2012, and that overall the Gulf waters at 300m were in 2017 at a 100+ year record high. Although the March helicopter survey only rarely samples deeper than 230 m, temperatures higher than 7°C were measured at three stations in the area of Cabot Strait, reached 7.6°C inside the Gulf. This signifies the continuation of warmer than normal conditions at depth.

SUMMARY

Figure 66 summarizes SST, summertime CIL and deep-water average temperatures. For May-November SST, a proxy is used prior to 1985 using the April-November air temperature anomaly averaged over all stations of Figure 4 except the two from the Estuary, similar to the index developed in Galbraith et al. (2012). For August SST, the proxy is based on July and August air temperatures. While May-November SST and August SST are well correlated ($R^2 = 0.57$ for the 1985-2017 AVHRR record), the August SST reached in 2012 and 2014 were very high anomalies compared the May-November averages, while in 2006 the reverse was found to be the case. The SST summer and fall timing are from Figure 22 (12°C threshold) with air temperature proxies used prior to 1985.

Figure 66 shows no change from 2016 for May-November average SST (10.2°C and $+0.9$ SD), a small decrease in CIL temperature minimum and deep temperature at 200 m, a larger decrease in temperature at 150 m, but an increase to a new series record high temperature at 300 m (6.3°C , $+5.0$ SD). The CIL temperature minimum was near-normal ($+0.3$ SD), consistent with normal winter air temperatures ($+0.4^{\circ}\text{C}$, $+0.3$ SD).

Another summary of the temperature state of the Gulf of St. Lawrence over a shorter time span (since 1971) allows the inclusion of more data sets, and three sets of four time series are chosen to represent surface, intermediate and deep conditions (Figure 67). Here, sea-ice is grouped as an intermediate feature since all are associated with winter formation. Figure 67 shows the sums of these three sets of anomalies representing the state of different parts of the system and is reproduced on Figure 68 with each time series contribution shown as stacked bars (Petrie et al. 2007). These composite indices measure the overall state of the climate system with positive values representing warm conditions and negative representing cold conditions. The plot also indicates the degree of correlation between the various measures of the environment. In 2017, the surface index was above-normal at $+1.0$ SD, the intermediate index was near-normal at $+0.3$ SD and the deep index decreased slightly to its third highest value record after the 2015 record high and 2016 value.

KEY FINDINGS

- The annual average runoff from the St. Lawrence River measured at Québec City and RIVSUM II were the highest recorded since 1974 in 2017 ($14\,300\text{ m}^3\text{s}^{-1}$, $+2.7$ SD and $19\,200\text{ m}^3\text{s}^{-1}$, $+2.1$ SD, respectively). The St. Lawrence River spring freshet in April-May was highest of the time series ($+3.6$ SD, since 1948).

-
- The winter surface mixed cold layer (< -1°C) volume of 12 200 km³ was near normal (+0.2 SD against 1996–2017 climatology). The Labrador Shelf water intrusion volume into Mécatina Trough was near normal in March 2017 (+0.1 SD), representing 12% (-0.1 SD) of the cold water in the Gulf.
 - Sea ice maximum volume was sixth lowest since 1969 at 23 km³ (-1.5 SD). Six of the eight lowest maximum ice volumes of the time series have occurred in the previous eight years.
 - The August cold intermediate layer (CIL) showed warmer (+0.8 SD) and slightly thinner (-0.6 SD for volume colder than 1°C) than normal. The Gilbert and Pettigrew minimum temperature index, which includes data over a longer season, was near normal (-0.3°C, +0.3 SD). This slightly different result in terms of anomaly is caused by the different years included in the climatology; the temperatures are consistent with each other when adjusted for warming between mid-July and mid-August.
 - The timing of summer onset and post-season cooling were respectively slightly sooner (-0.6 SD, -0.7 weeks) and later than normal (+1.4 SD, +1.7 weeks).
 - Near-surface water temperatures were near normal or above normal from May to November 2017, leading to an above-normal May–November average (+0.6°C, +0.9 SD).
 - Deep water temperatures have been increasing overall in the Gulf, with inward advection from Cabot Strait. Temperature decreased from 2015 record highs at 150 and 200 m, remaining above-normal (2.7°C, +0.5 SD and 5.0°C, +1.4 SD), decreased slightly at 250 m (6.0°C, +2.7 SD) from the 2016 record high but increased to a new record level at 300 m (6.3°C, +5.0 SD). At 300 m, temperature increased to regional record highs in all deep regions of the Gulf: Estuary (5.5°C, +2.5 SD), Northwest Gulf (5.9°C, +3.7 SD), Central Gulf (6.4°C, +4.6 SD) and Cabot Strait (6.7°C, +4.4 SD).
 - Bottom area covered by waters warmer than 6°C decreased in 2017 in Anticosti Channel and Esquiman Channel, remaining quite large, but increased sharply in Central Gulf and the northwest Gulf.

ACKNOWLEDGEMENTS

We are grateful to the people responsible for CTD data acquisition during the surveys used in this report:

- Rimouski station monitoring: Roger Pigeon, Félix St-Pierre, Michel Rousseau, Rémi Desmarais, Anthony Ouellet, Steve Desrosiers, Jean-Denis Thibeault, Hubert Lapointe-Lavoie
- Shediac Valley monitoring station: Roger Pigeon, Félix St-Pierre, Kevin Pauley, Tom Hurlbut
- March survey: Peter Galbraith, Rémi Desmarais, Caroline Lafleur, Yves Gagnon, Félix St-Pierre, David Leblanc; the officers and crew of the CCGS Earl Grey.
- June AZMP transects: Félix St-Pierre, Yves Gagnon, Michel Rousseau, Marie-Lyne Dubé, François Villeneuve, Isabelle St-Pierre, Rémi Desmarais, Marie-Noëlle Bourassa, Jean-Denis Thibeault, Steve Desrosiers, Roger Pigeon, Anthony Ouellet; the officers and crew of the CCGS Teleost.

- August Multi-species survey: Caroline Lafleur, Jean-Denis Thibeault, Félix St-Pierre, Anthony Ouellet, Roger Pigeon, Michel Rousseau, Rémi Desmarais; the officers and crew of the CCGS Teleost.
- October-November AZMP survey: Félix St-Pierre, Michel Rousseau, François Villeneuve, David Leblanc, Roger Pigeon, Rémi Desmarais, Anthony Ouellet, Isabelle St-Pierre, Brian Boivin, Marie-Noëlle Bourassa; the officers and crew of the Coriolis II.
- September Multi-species survey: Luc Savoie for providing the CTD data.
- Northumberland Strait survey: Chief scientists Mark Hanson and Joël Chassé.
- Data management: Laure Devine, Caroline Lafleur, Isabelle St-Pierre, Brian Boivin.
- CTD maintenance: Roger Pigeon, Félix St-Pierre, Michel Rousseau, Sylvain Chartrand.

Data from the following sources are also gratefully acknowledged:

- Air temperature: Environment Canada.
- Sea-ice: Canadian Ice Service, Environment Canada. Processing of GIS files by Paul Nicot.
- Runoff at Québec City: Denis Lefavre.
- Runoff from hydrological modelling: Joël Chassé and Diane Lavoie.
- Historical AVHRR SST remote sensing (IML): Pierre Larouche, Bernard Pettigrew.
- AVHRR SST remote sensing (BIO): Carla Caverhill.

All figures were made using the free software Gri (Kelley and Galbraith 2000).

We are grateful to David Hebert and Frédéric Cyr for reviewing the manuscript and providing insightful comments.

REFERENCES

- Benoît, H.P., Savenkoff, C., Ouellet, P., Galbraith, P.S., Chassé, J. and Fréchet, A. 2012. Impacts of fishing and climate-driven changes in exploited marine populations and communities with implications for management, in State-of-the-Ocean Report for the Gulf of St. Lawrence Integrated Management (GOSLIM) Area, H. P. Benoît, J. A. Gagné, C. Savenkoff, P. Ouellet and M.-N. Bourassa, Eds. Can. Manuscr. Rep. Fish. Aquat. Sci. 2986: viii + 73 pp.
- Bourgault, D. and Koutitonsky, V.G. 1999. Real-time monitoring of the freshwater discharge at the head of the St. Lawrence Estuary. *Atmos. Ocean*, 37 (2): 203–220.
- Colbourne, E., Holden, J., Senciall, D., Bailey, W., Snook, S. and Higdon, J. 2016. [Physical Oceanographic Conditions on the Newfoundland and Labrador Shelf during 2015](#). DFO Can. Sci. Advis. Sec. Res. Doc. 2016/079. v +40 p.
- Cyr, F., Bourgault, D. and Galbraith, P.S. 2011. Interior versus boundary mixing of a cold intermediate layer. *J. Geophys. Res. (Oceans)*, 116, C12029, doi:10.1029/2011JC007359.
- Dutil, J.-D., Proulx, S., Galbraith, P.S., Chassé, J., Lambert, N. and Laurian, C. 2012. Coastal and epipelagic habitats of the estuary and Gulf of St. Lawrence. *Can. Tech. Rep. Fish. Aquat. Sci.* 3009: ix + 87 p.
- Galbraith, P.S. 2006. Winter water masses in the Gulf of St. Lawrence. *J. Geophys. Res.*, 111, C06022, doi:10.1029/2005JC003159.
- Galbraith, P.S. et Grégoire, F. 2015. [Habitat thermique du maquereau bleu; profondeur de l'isotherme de 8 °C dans le sud du golfe du Saint-Laurent entre 1960 et 2014](#). Secr. can. de consult. sci. du MPO. Doc. de rech. 2014/116. v + 13 p.

-
- Galbraith, P.S. and Larouche, P. 2011. Sea-surface temperature in Hudson Bay and Hudson Strait in relation to air temperature and ice cover breakup, 1985-2009. *J. Mar. Systems*, 87, 66-78.
- Galbraith, P.S. and Larouche, P. 2013. Trends and variability in eastern Canada sea-surface temperatures. Ch. 1 (p. 1-18) In: *Aspects of climate change in the Northwest Atlantic off Canada* [Loder, J.W., G. Han, P.S. Galbraith, J. Chassé and A. van der Baaren (Eds.)]. *Can. Tech. Rep. Fish. Aquat. Sci.* 3045: x + 190 p.
- Galbraith, P.S., Saucier, F.J., Michaud, N., Lefavre, D., Corriveau, R., Roy, F., Pigeon, R. and Cantin, S. 2002. Shipborne monitoring of near-surface temperature and salinity in the Estuary and Gulf of St. Lawrence. *Atlantic Zone Monitoring Program Bulletin*, Dept. of Fisheries and Oceans Canada. No. 2: 26–30.
- Galbraith, P.S., Desmarais, R., Pigeon, R. and Cantin, S. 2006. Ten years of monitoring winter water masses in the Gulf of St. Lawrence by helicopter. *Atlantic Zone Monitoring Program Bulletin*, Dept. of Fisheries and Oceans Canada. No. 5: 32–35.
- Galbraith, P.S., Larouche, P., Gilbert, D., Chassé, J. and Petrie, B. 2010. Trends in sea-surface and CIL temperatures in the Gulf of St. Lawrence in relation to air temperature. *Atlantic Zone Monitoring Program Bulletin*, 9: 20-23.
- Galbraith P.S., Larouche, P., Chassé, J. and Petrie, B. 2012. Sea-surface temperature in relation to air temperature in the Gulf of St. Lawrence: interdecadal variability and long term trends. *Deep Sea Res. II*, V77–80, 10–20.
- Galbraith, P.S., Hebert, D., Colbourne, E. and Pettipas, R. 2013. Trends and variability in eastern Canada sub-surface ocean temperatures and implications for sea ice. Ch.5 In: *Aspects of climate change in the Northwest Atlantic off Canada* [Loder, J.W., G. Han, P.S. Galbraith, J. Chassé and A. van der Baaren (Eds.)]. *Can. Tech. Rep. Fish. Aquat. Sci.* 3045: x + 192 p.
- Galbraith, P.S., Chassé, J., Caverhill, C., Nicot, P., Gilbert, D., Pettigrew, B., Lefavre, D., Brickman, D., Devine, L., and Lafleur, C. 2017. [Physical Oceanographic Conditions in the Gulf of St. Lawrence in 2016](#). DFO Can. Sci. Advis. Sec. Res. Doc. 2017/044. vi + 91 p.
- Gilbert, D. 2004. Propagation of temperature signals from the northwest Atlantic continental shelf edge into the Laurentian Channel. *ICES CM*, 2004/N:7, 12 pp.
- Gilbert, D. and Pettigrew, B. 1997. Interannual variability (1948-1994) of the CIL core temperature in the Gulf of St. Lawrence. *Can. J. Fish. Aquat. Sci.*, 54 (Suppl. 1): 57–67.
- Gilbert, D., Sundby, B., Gobeil, C., Mucci, A. and Tremblay, G.-H. 2005. A seventy-two-year record of diminishing deep-water oxygen in the St. Lawrence estuary: The northwest Atlantic connection. *Limnol. Oceanogr.*, 50(5): 1654–1666.
- Hammill, M.O. and Galbraith, P.S. 2012. Changes in seasonal sea-ice cover and its effect on marine mammals, in *State-of-the-Ocean Report for the Gulf of St. Lawrence Integrated Management (GOSLIM) Area*, H. P. Benoît, J. A. Gagné, C. Savenkoff, P. Ouellet and M.-N. Bourassa, Eds. *Can. Manuscr. Rep. Fish. Aquat. Sci.* 2986: viii + 73 pp.
- Hebert, D., Pettipas, R., Brickman, D., and Dever, M. 2016. [Meteorological, sea ice and physical oceanographic conditions on the Scotian Shelf and in the Gulf of Maine during 2015](#). DFO Can. Sci. Advis. Sec. Res. Doc. 2016/083. v + 49 p.
-

-
- Kalnay, E., Kanamitsu, M., Kistler, R., Collins, W., Deaven, D., Gandin, L., Iredell, M., Saha, S., White, G., Woollen, J., Zhu, Y., Chelliah, M., Ebisuzaki, W., Higgins, W., Janowiak, J., Mo, K., Ropelewski, C., Wang, J., Leetmaa, A., Reynolds, R., Jenne, R. and Josephé, D. 1996. The NCEP/NCAR 40-year reanalysis project. *Bull. Am. Meteorol. Soc.* 77, 437–470.
- Kelley, D.E. and Galbraith, P.S. 2000. Gri: A language for scientific illustration, *Linux J.*, 75, 92–101.
- Lauzier, L.M. and Trites, R.W. 1958. The deep waters of the Laurentian Channel. *J. Fish. Res. Board Can.* 15: 1247–1257.
- McLellan, H.J. 1957. On the distinctness and origin of the slope water off the Scotian Shelf and its easterly flow south of the Grand Banks. *J. Fish. Res. Board. Can.* 14: 213–239.
- Petrie, B., Drinkwater, K., Sandström, A., Pettipas, R., Gregory, D., Gilbert, D. and Sekhon, P. 1996. Temperature, salinity and sigma-t atlas for the Gulf of St. Lawrence. *Can. Tech. Rep. Hydrogr. Ocean Sci.*, 178: v + 256 pp.
- Petrie, B., Pettipas, R.G. and Petrie, W.M. 2007. [An overview of meteorological, sea ice and sea surface temperature conditions off eastern Canada during 2006](#). DFO Can. Sci. Advis. Sec. Res. Doc. 2007/022.
- Pettigrew, B., Gilbert, D. and Desmarais R. 2016. Thermograph network in the Gulf of St. Lawrence. *Can. Tech. Rep. Hydrogr. Ocean Sci.* 311: vi + 77 p.
- Plourde, S., Joly, P., St-Amand, L. and Starr, M. 2009. La station de monitoring de Rimouski : plus de 400 visites et 18 ans de monitoring et de recherche. *Atlantic Zone Monitoring Program Bulletin*, Dept. of Fisheries and Oceans Canada. No. 8: 51-55.
- Tamdrari, H., Castonguay, M., Brêthes, J.-C., Galbraith, P.S. and Duplisa, D.E. 2012. The dispersal pattern and behaviour of cod in the northern Gulf of St. Lawrence: results from tagging experiments, *Can. J. Fish. Aquat. Sci.* 69: 112-121.
- Therriault, J.-C., Petrie, B., Pépin, P., Gagnon, J., Gregory, D., Helbig, J., Herman, A., Lefavre, D., Mitchell, M., Pelchat, B., Runge, J. and Sameoto, D. 1998. Proposal for a Northwest Atlantic zonal monitoring program. *Can. Tech. Rep. Hydrogr. Ocean Sci.*, 194: vii + 57 pp.
- Vincent, L. A., Wang, X. L., Milewska, E. J., Wan, H., Yang, F. and Swail, V. 2012. A second generation of homogenized Canadian monthly surface air temperature for climate trend analysis. *J. Geophys. Res.* 117, D18110, doi:10.1029/2012JD017859.

FIGURES

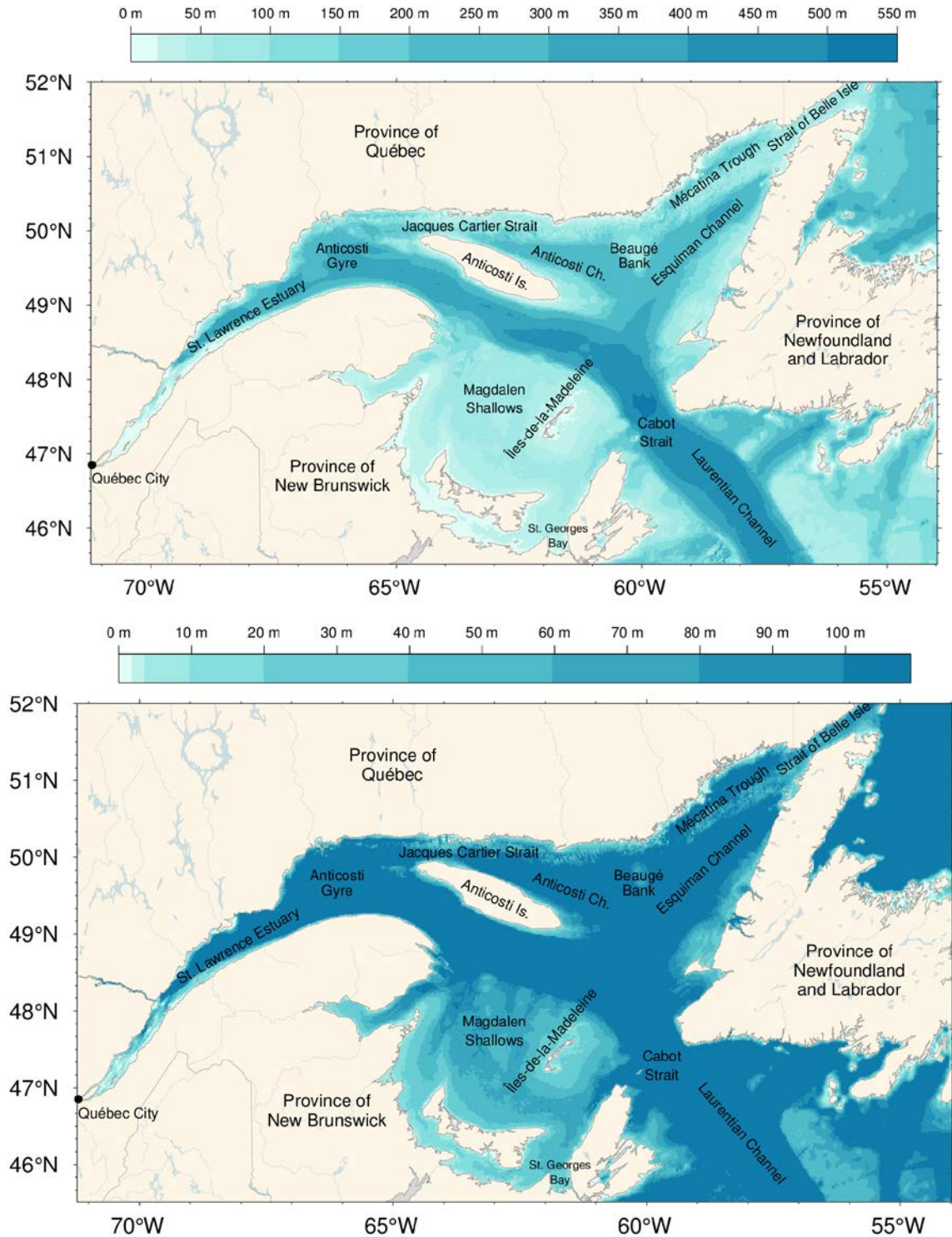


Figure 1. The Gulf of St. Lawrence. Locations discussed in the text are indicated. Bathymetry datasets used are from the Canadian Hydrographic Service to the west of $56^{\circ}47' W$ (with some corrections applied to the baie des Chaleurs and Magdalen Shallows) and TOPEX data to the east. Bottom panel shows detail for 0-100 m bathymetry.

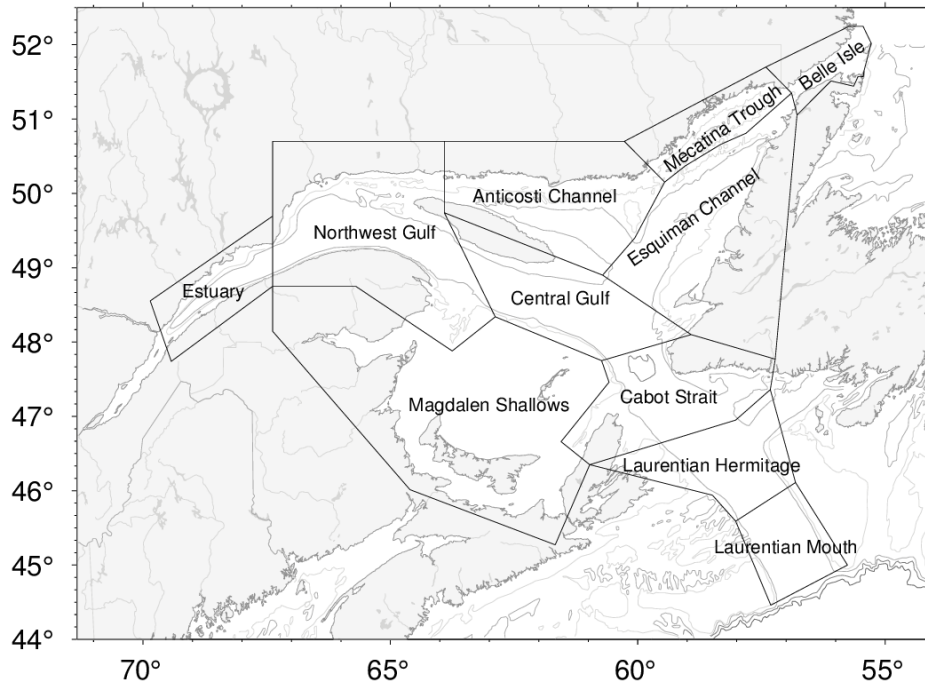


Figure 2. Gulf of St. Lawrence divided into oceanographic regions.

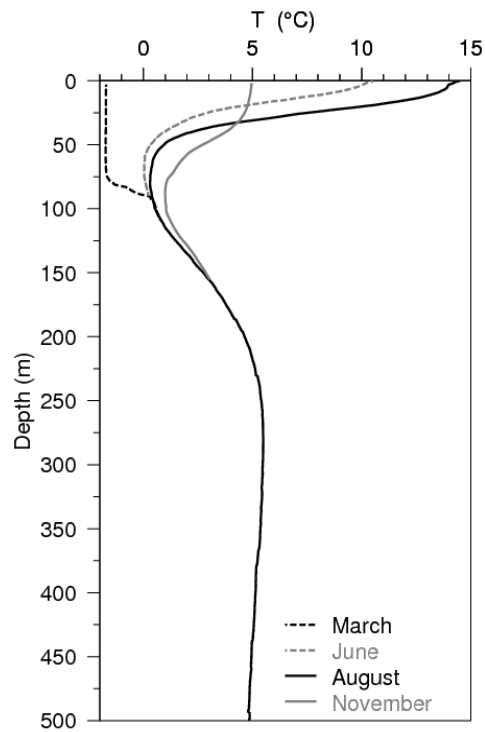


Figure 3. Typical seasonal progression of the depth profile of temperature observed in the Gulf of St. Lawrence. Profiles are averages of observations in August, June and November 2007 in the northern Gulf. The dashed line at left shows a single winter temperature profile (March 2008), with near freezing temperatures in the top 75 m. The cold intermediate layer (CIL) is defined as the part of the water column that is colder than 1°C, although some authors use a different temperature threshold. Figure from Galbraith et al. (2012).

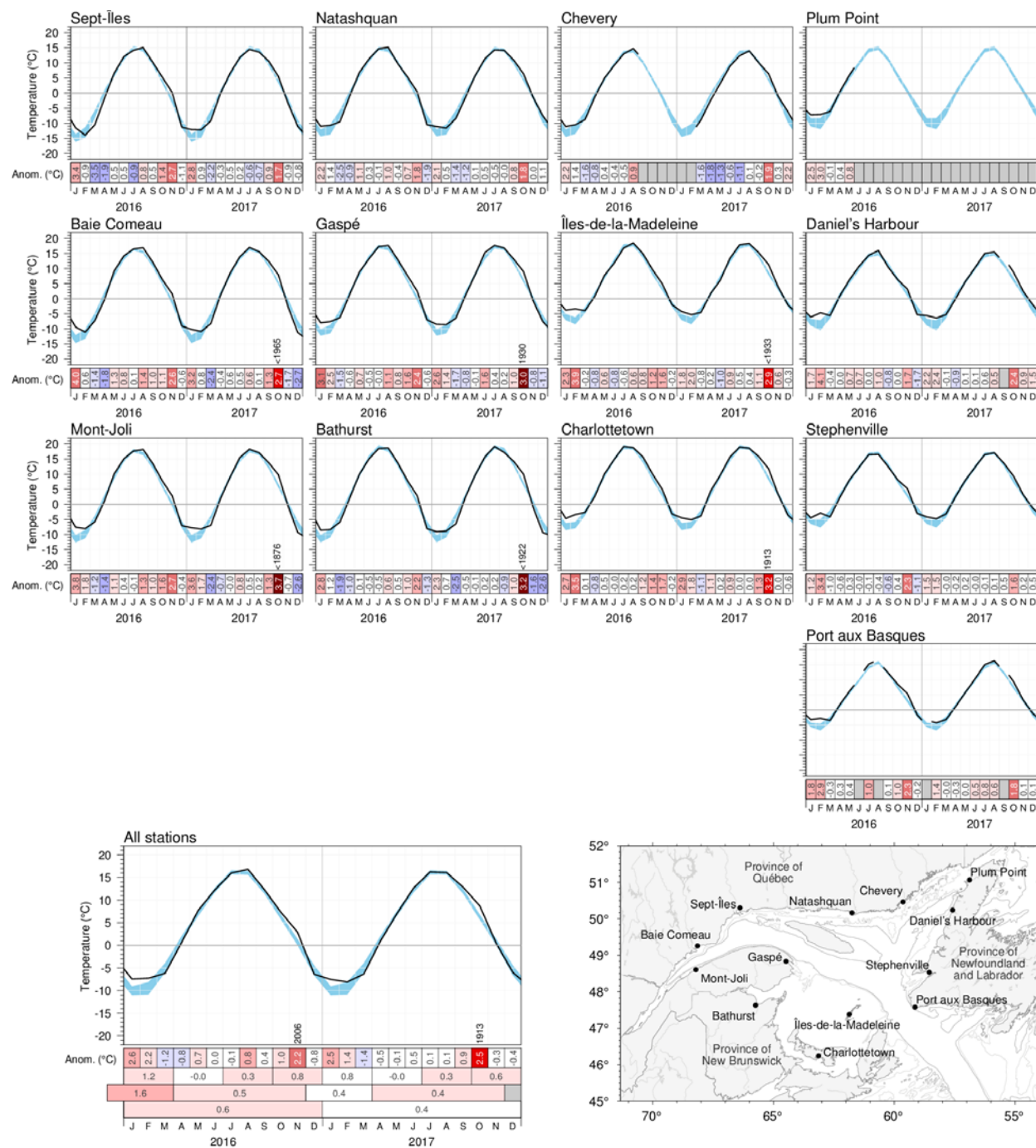


Figure 4. Monthly air temperatures and anomalies for 2016 and 2017 at selected stations around the Gulf as well as the average for all stations. The blue area represents the 1981–2010 climatological monthly mean ± 0.5 SD. Months with 4 or more days of missing data are omitted. The bottom scorecards are colour-coded according to the monthly normalized anomalies based on the 1981–2010 climatologies for each month, but the numbers are the monthly anomalies in $^{\circ}\text{C}$. For anomalies greater than 2 SD from normal, the prior year with a greater anomaly is indicated. Seasonal, December-March, April-November and annual anomalies are included for the all-station average.

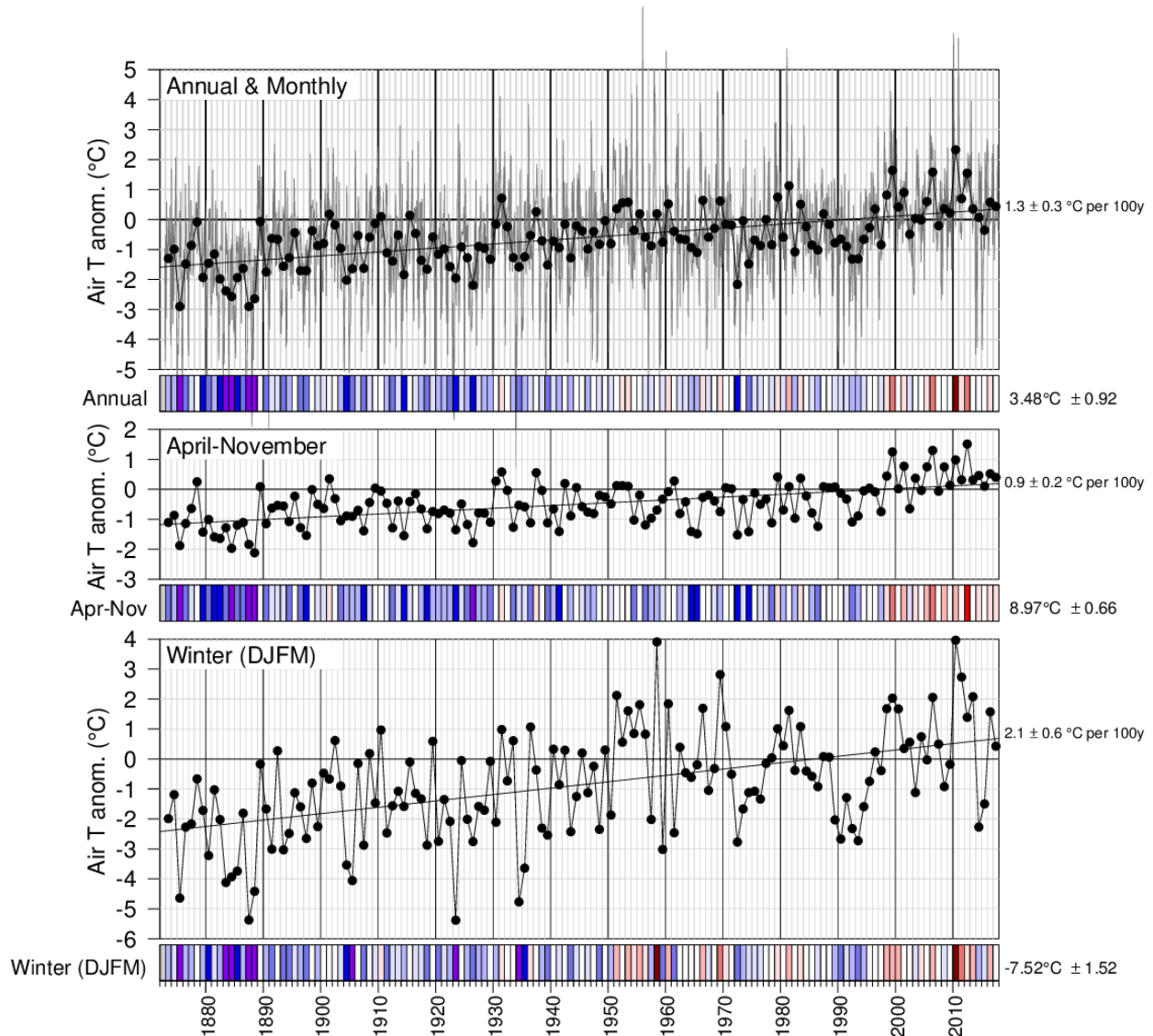


Figure 5. Annual, April-November December-March mean air temperature anomalies averaged for the selected stations around the Gulf from Figure 4. The bottom scorecards are colour-coded according to the normalized anomalies based on the 1981–2010 climatology. Trends plus and minus their 95% confidence intervals are shown. April-November air temperature anomalies tend to be highly-correlated with May–November sea-surface temperature anomalies (Galbraith et al. 2012; Galbraith and Larouche 2013) whereas winter air temperature anomalies correlate highly with sea-ice cover parameters and winter mixed-layer volume (Galbraith et al. 2010; Galbraith et al. 2013)

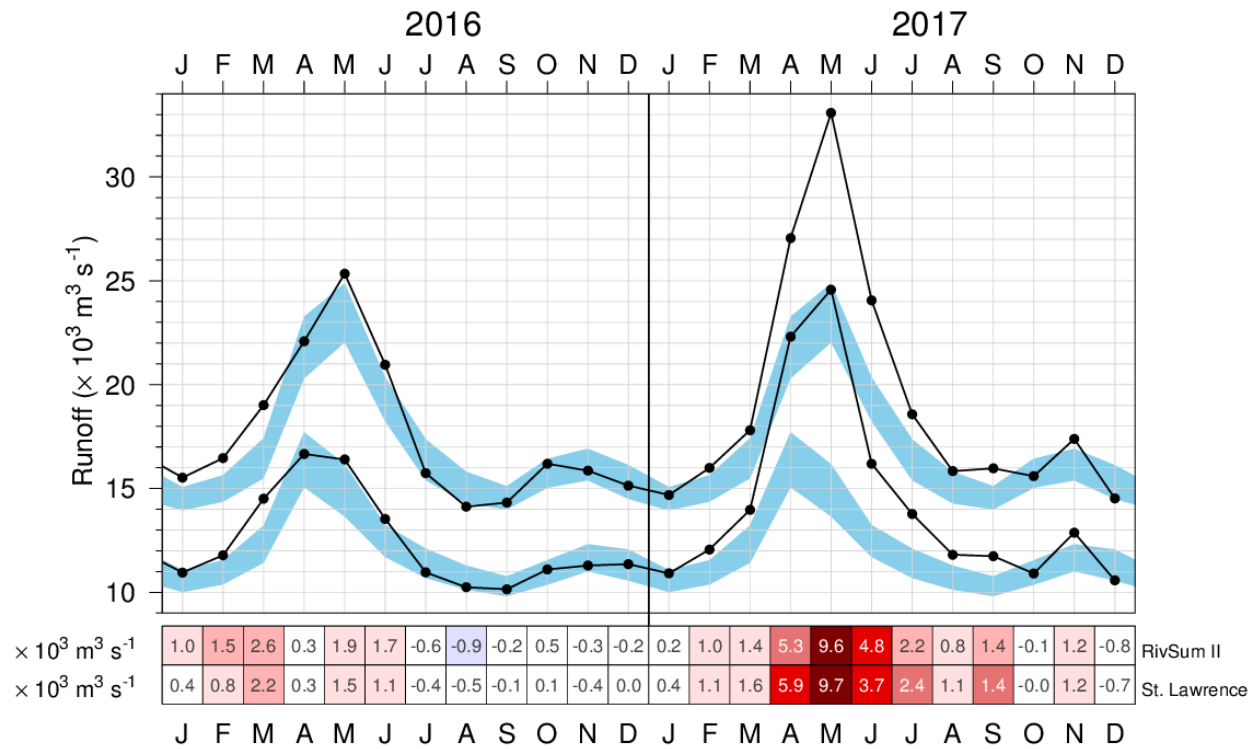


Figure 6. Monthly mean freshwater flow of the St. Lawrence River at Québec City (lower curve) and its sum with rivers flowing into the St. Lawrence Estuary (RIVSUM II, upper curve). The 1981–2010 climatological mean (± 0.5 SD) is shown (blue shading). The scorecards are colour-coded according to the monthly anomalies normalized for each month of the year, but the numbers are the actual monthly anomalies in $10^3 \text{ m}^3 \text{ s}^{-1}$.

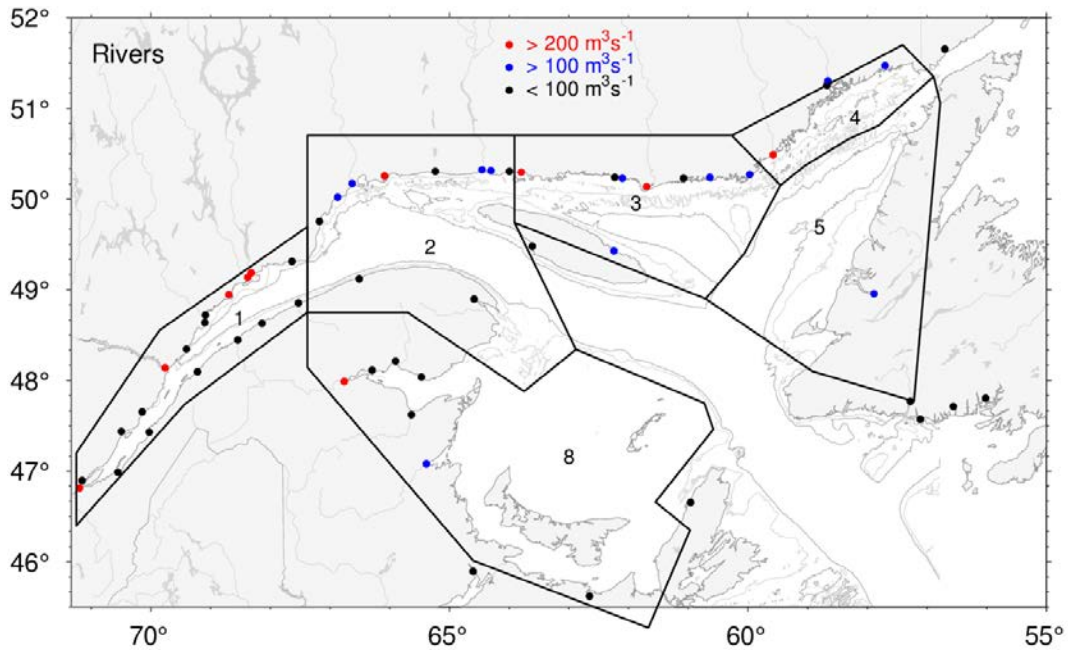


Figure 7. River discharge locations for the regional sums of runoffs listed in Figure 8. Red and blue dots indicate rivers that have climatological mean runoff greater than $200 \text{ m}^3 \text{ s}^{-1}$ and between 100 and $200 \text{ m}^3 \text{ s}^{-1}$, respectively.

St. Lawrence River	10955	11785	14505	16662	16393	13536	10959	10244	10149	11100	11290	11359	10912	12065	13970	22310	24574	16193	13774	11812	11740	10908	12874	10573	11994 $\text{m}^3 \text{ s}^{-1}$
1 - Estuary	4569	4675	4508	5425	8950	7421	4780	3876	4173	5091	4568	3780	3777	3925	3837	4741	8511	7863	4802	4021	4228	4684	4510	3946	4978 $\text{m}^3 \text{ s}^{-1}$
2 - Northwest Gulf	76	116	112	674	2295	3550	1491	651	817	1103	825	191	35	95	104	455	2297	4505	1869	1084	1114	956	864	262	1129 $\text{m}^3 \text{ s}^{-1}$
3 - Anticosti Channel	206	355	268	859	2489	4155	1642	743	640	967	886	308	125	144	188	618	2615	4937	2359	1245	978	891	1381	675	1234 $\text{m}^3 \text{ s}^{-1}$
4 - Mécatina Trough	62	147	135	435	1361	2518	964	337	207	464	379	93	32	62	84	206	1096	2671	1621	670	517	476	774	357	738 $\text{m}^3 \text{ s}^{-1}$
5 - Esquiman Channel	101	176	142	294	467	213	13	26	107	216	179	155	131	75	72	181	388	570	210	77	35	46	202	213	162 $\text{m}^3 \text{ s}^{-1}$
8 - Magdalen Shallows	505	549	494	1258	1841	484	21	35	133	420	434	364	322	282	364	1286	2472	1188	194	104	265	393	987	687	617 $\text{m}^3 \text{ s}^{-1}$
	J	F	M	A	M	J	J	A	S	O	N	D	J	F	M	A	M	J	J	A	S	O	N	D	
	2016												2017												

Figure 8. Monthly anomalies of the St. Lawrence River runoff and sums of all other major rivers draining into separate Gulf regions for 2016 and 2017. The scorecards are colour-coded according to the monthly normalized anomalies based on the 1981–2010 climatologies for each month, but the numbers are the monthly average runoffs in $\text{m}^3 \text{ s}^{-1}$. Numbers on the right side are annual climatological means. Runoff regulation is simulated for three rivers that flow into the Estuary (Saguenay, Manicouagan, Outardes).

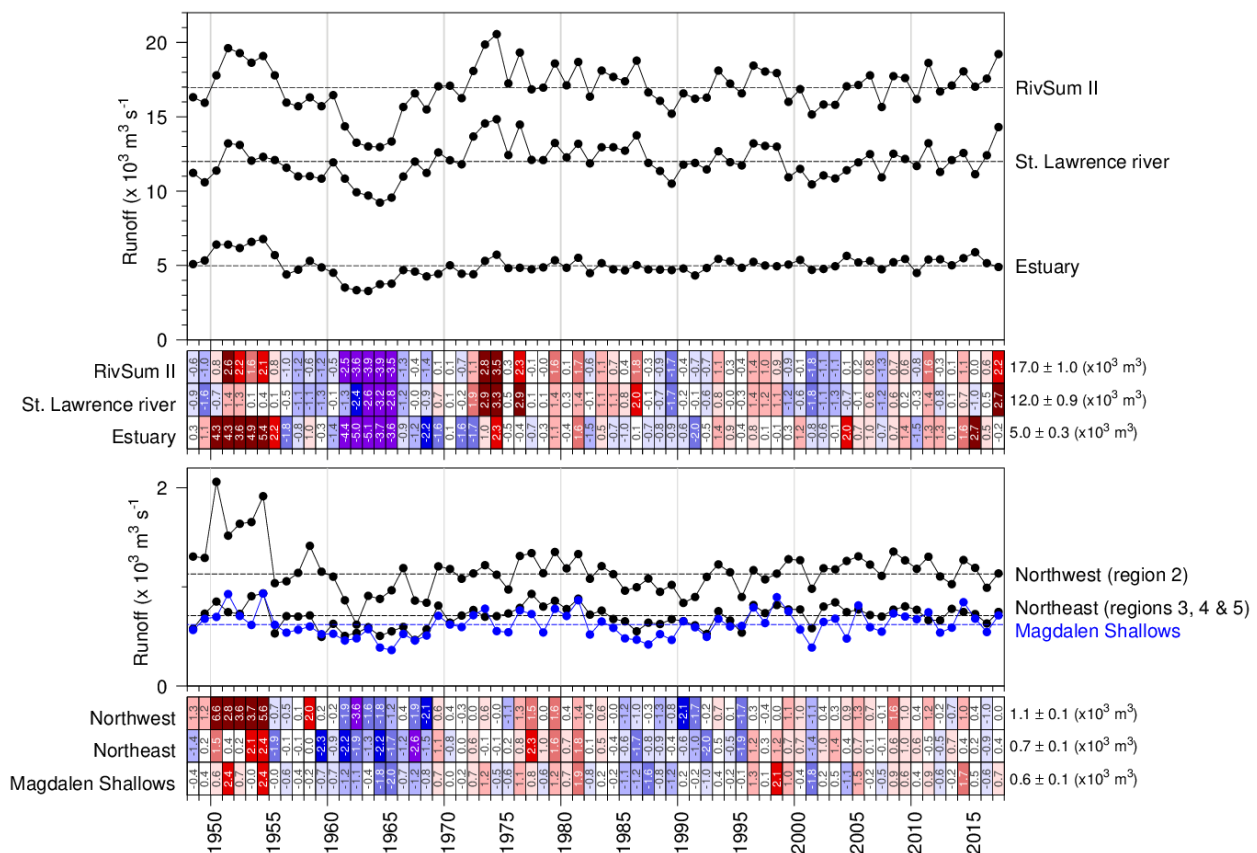


Figure 9. Annual mean freshwater flow of the St. Lawrence River at Québec City and of the sum of all rivers flowing into regions of the Estuary and Gulf (RivSum II). The 1981–2010 climatological mean is shown as horizontal lines and indicated on the right side of the scorecards. Numbers in scorecards are normalized anomalies.

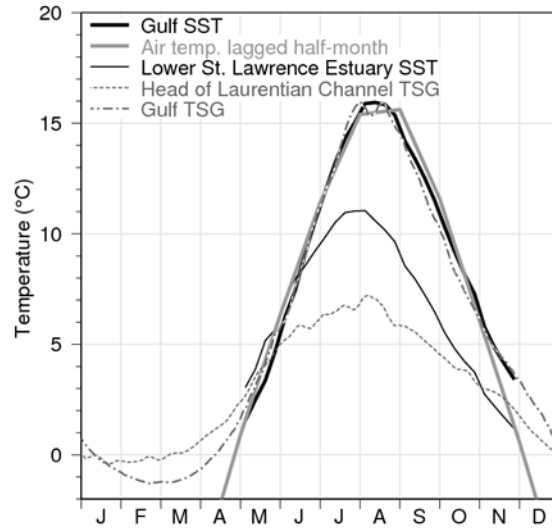


Figure 10. Sea-surface temperature climatological seasonal cycle in the Gulf of St. Lawrence. AVHRR temperature weekly averages for 1985 to 2010 are shown from May to November (ice-free months) for the Gulf (thick black line) and the cooler Lower St. Lawrence Estuary (thin black line), defined as the area west of the Pointe-des-Monts section and east of approx 69°30'W. Thermosalinograph data averages for 2000 to 2010 are shown for the head of the Laurentian Channel (at 69°30'W, grey dashed line) and for the average over the Gulf waters along the main shipping route between the Pointe-des-Monts and Cabot Strait sections (gray dash-dotted line). Monthly air temperature averaged over eight stations in the Gulf of St. Lawrence are shown offset by 2 weeks into the future (thick grey line; winter months not shown). Figure from Galbraith et al. (2012).

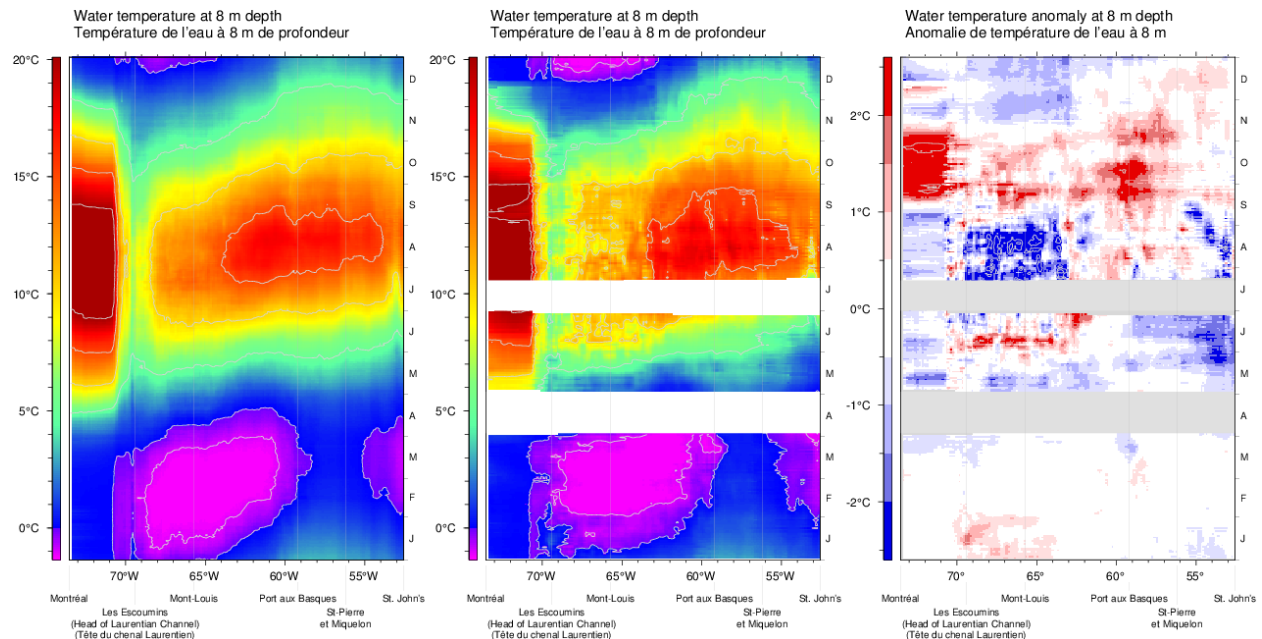


Figure 11. Thermosalinograph data at 8 m depth along the Montréal to St. John's shipping route: composite mean annual cycle of the water temperature for the 2000–2017 period (left panel), composite annual cycle of the water temperature for 2017 (middle panel), and water temperature anomaly for 2017 relative to the 2000–2017 composite (right panel).

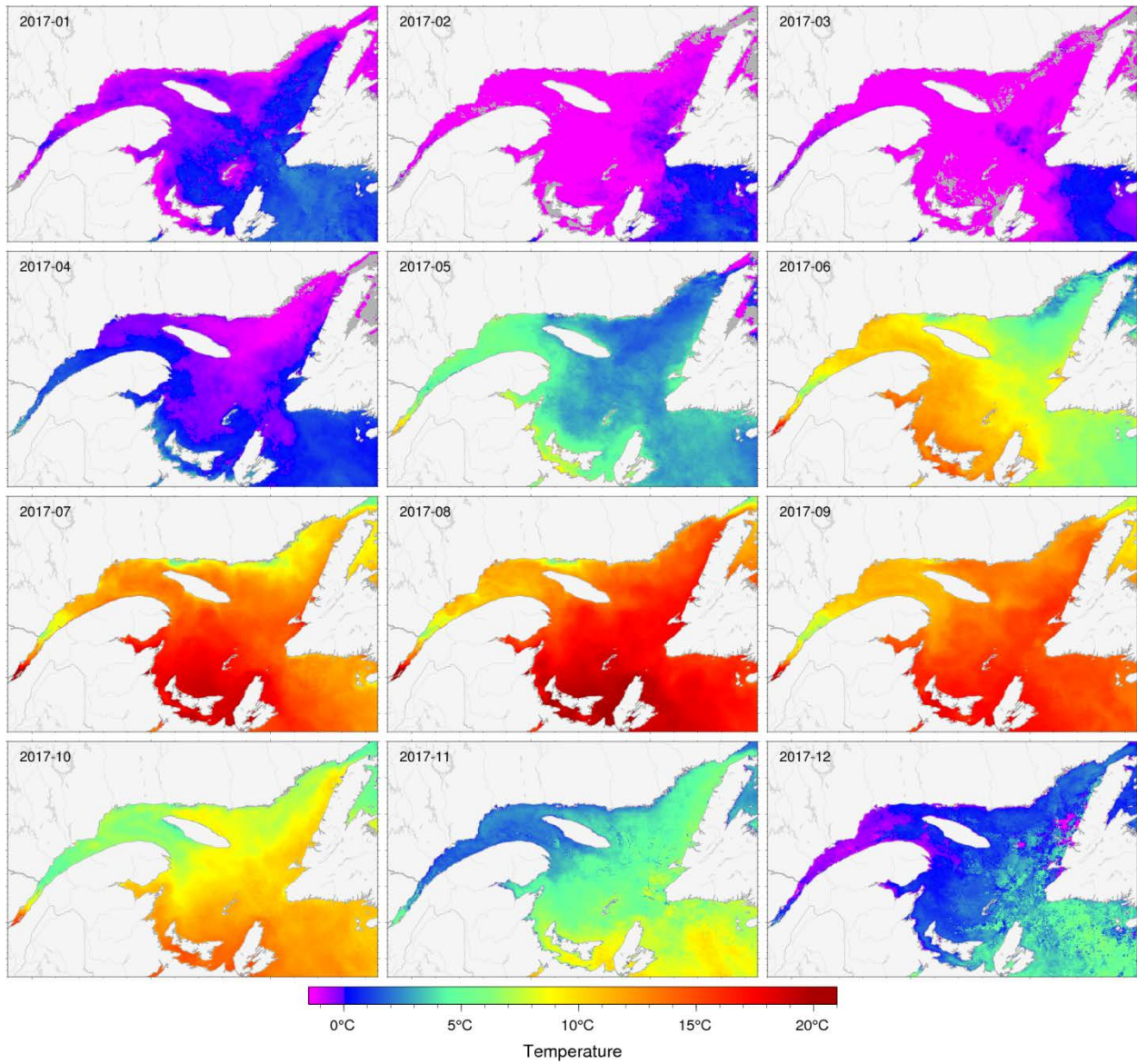


Figure 12. Sea-surface temperature monthly averages for 2017 as observed with AVHRR remote sensing. Grey areas have no data for the period due to ice cover or clouds.

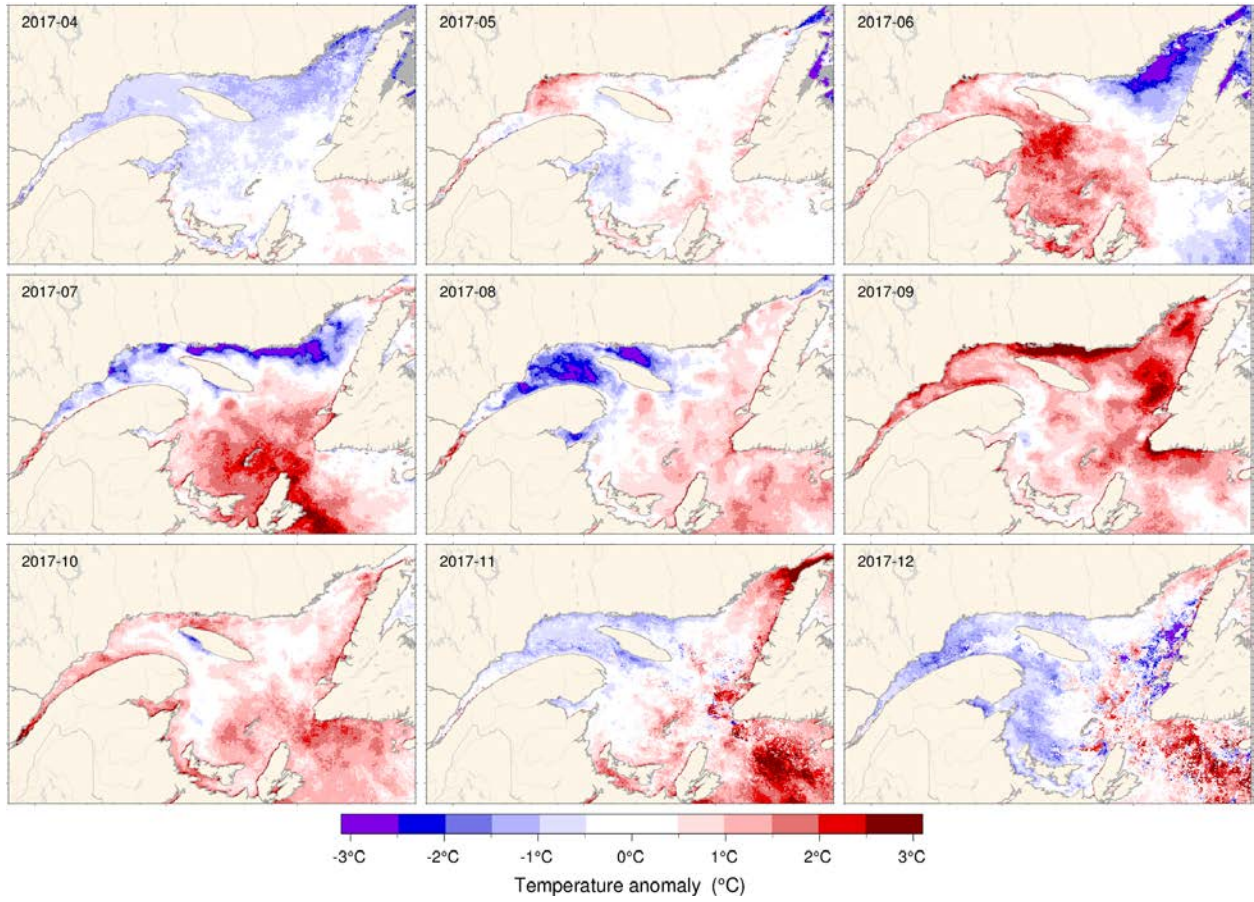


Figure 13. Sea-surface temperature monthly anomalies for April-December 2017 based on monthly climatologies calculated for the 1985–2010 period observed with AVHRR remote sensing.

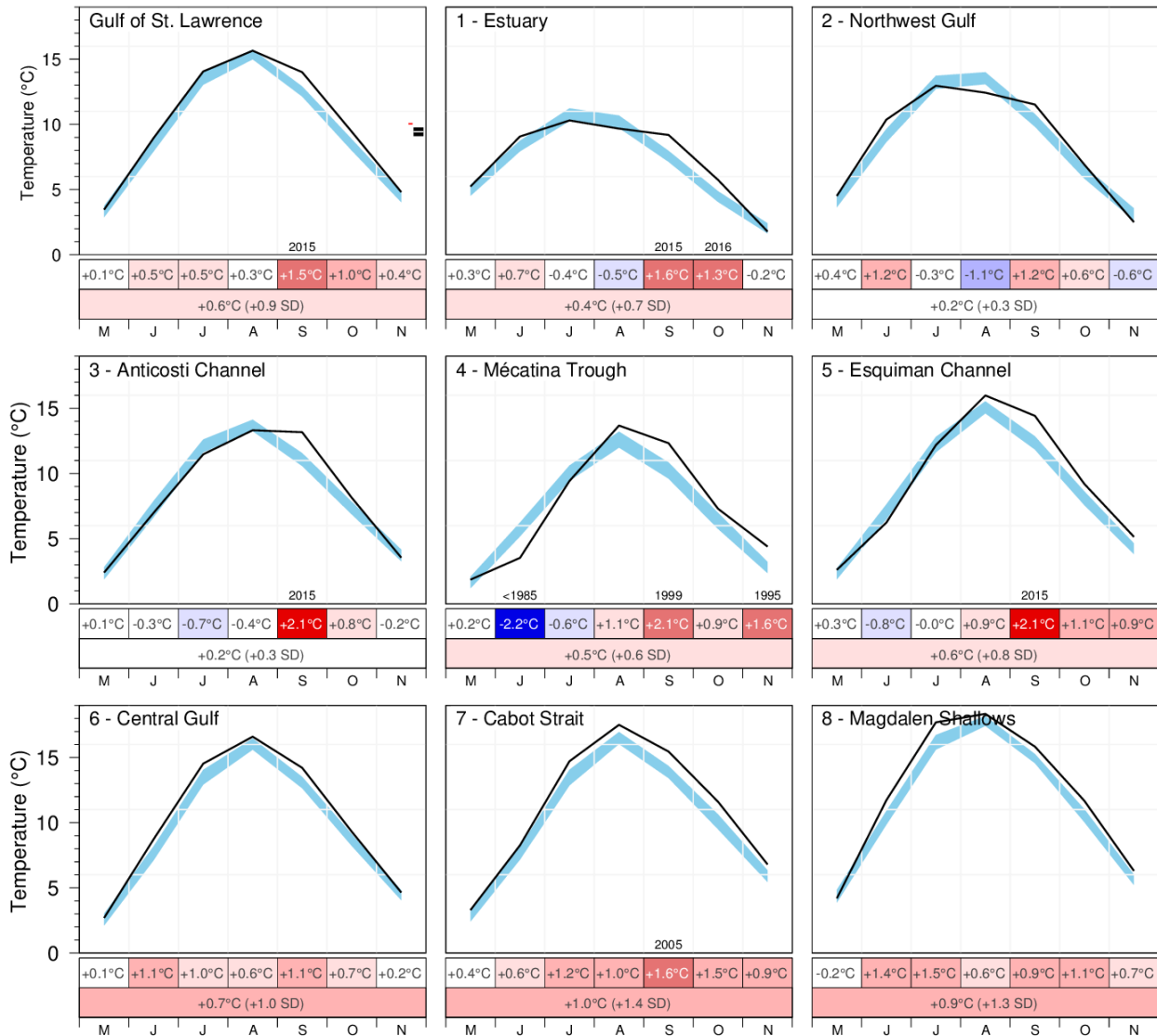


Figure 14. AVHRR SST May to November monthly averages over the Gulf and over the eight regions of the Gulf. The blue area represents the 1981–2010 climatological monthly mean \pm 0.5 SD. The scorecards are colour-coded according to the normalized anomalies based on the 1985–2010 climatologies for each month or for the May–November period (bottom row), but the numbers are the monthly average temperature anomalies.

GSL		4.1	8.2	13.7	16.2	12.9	9.2	6.1						3.5	9.0	14.1	15.7	14.0	9.4	4.8	
1 - Estuary		6.1	9.9	11.5	11.5	8.9	6.4	3.8						5.2	9.1	10.3	9.7	9.2	5.7	1.8	
2 - Northwest Gulf	0.2	5.2	9.0	13.6	13.9	11.1	8.3	5.0				0.1	4.5	10.4	13.0	12.4	11.5	6.9	2.5		
3 - Anticosti Channel		3.8	7.1	12.4	14.3	11.1	8.0	4.5					2.4	7.0	11.5	13.3	13.2	8.2	3.5		
4 - Mécatina Trough		2.8	5.2	10.2	14.5	10.6	5.7	3.7					1.9	3.5	9.4	13.7	12.3	7.3	4.4		
5 - Esquiman Channel		3.0	7.0	12.3	16.6	12.0	8.1	6.0					2.6	6.2	12.2	16.0	14.4	9.2	5.2		
6 - Central Gulf		3.2	7.3	13.1	16.8	12.8	9.1	5.8					2.7	8.7	14.5	16.6	14.2	9.3	4.7		
7 - Cabot Strait		3.2	7.8	13.9	17.6	13.6	10.2	8.1					3.3	8.3	14.7	17.5	15.5	11.6	6.8		
8 - Magdalen Shallows		4.8	9.7	16.2	18.4	15.8	11.4	7.6					4.2	11.7	17.7	18.4	15.8	11.7	6.3		
		A	M	J	J	A	S	O	N	D	J	F	M	A	M	J	J	A	S	O	N
		2016										2017									

Figure 15. AVHRR SST May to November monthly anomalies averaged over the Gulf and the eight regions of the Gulf for 2016 and 2017 (April results are also shown for the Northwest Gulf). The scorecards are colour-coded according to the monthly normalized anomalies based on the 1985–2010 climatologies for each month, but the numbers are the monthly average temperatures.

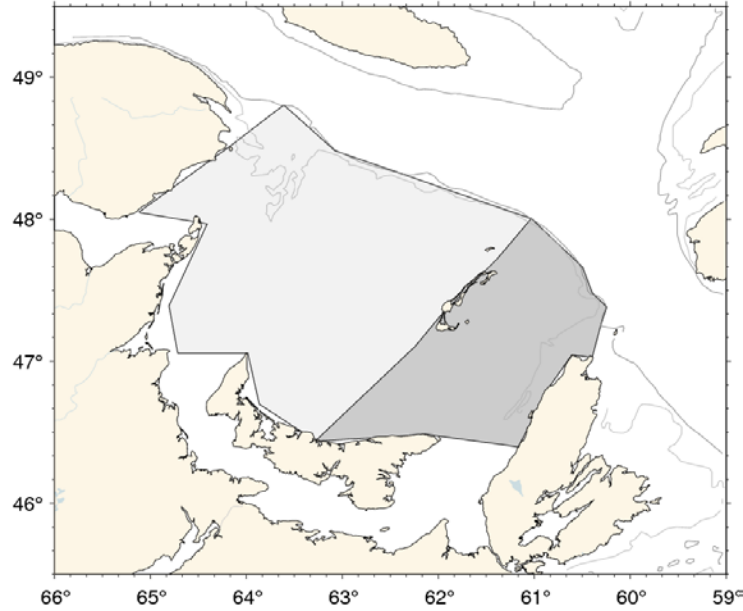


Figure 18. Areas defined as the western and eastern Magdalen Shallows.

																						Mean ± S.D.													
Magdalen Shallows	M	3.6	4.4	3.8	3.9	3.9	2.7	3.6	3.5	3.0	4.4	4.7	4.1	3.7	6.2	5.2	4.4	5.3	4.3	3.7	3.7	4.1	7.0	4.6	5.3	5.3	5.2	4.9	6.0	4.2	4.3	4.0	4.8	4.2	4.36°C ± 0.97
	J	8.2	9.2	10.6	8.6	10.6	9.7	10.5	9.5	9.3	11.1	11.3	11.6	9.3	10.9	12.1	10.5	11.9	10.0	10.4	9.4	10.0	12.6	10.4	10.7	10.7	10.5	9.7	11.3	10.6	11.4	9.8	9.7	11.7	10.37°C ± 1.05
	J	14.5	14.2	16.1	15.9	15.9	14.7	15.5	14.2	14.7	18.1	17.6	15.9	15.9	16.6	18.0	16.5	17.1	15.8	16.6	16.0	16.5	17.6	16.6	17.4	15.4	17.0	15.3	17.2	17.1	17.2	15.7	16.2	17.7	16.17°C ± 1.12
	A	17.4	15.9	17.2	17.7	17.2	17.8	16.8	16.4	18.1	18.5	18.5	18.8	17.7	17.9	18.1	18.2	18.9	18.1	17.3	18.6	18.2	17.9	17.1	17.1	18.5	18.7	17.4	19.6	17.9	18.5	18.9	18.4	18.4	17.80°C ± 0.75
	S	14.6	13.4	14.1	14.3	14.0	15.1	14.2	15.0	15.5	15.3	14.5	16.0	15.1	15.2	15.9	15.4	16.1	14.8	15.2	14.2	16.2	15.4	14.3	14.9	14.8	14.8	14.8	16.0	14.5	15.1	16.3	15.8	15.8	14.92°C ± 0.70
	O	10.0	9.3	10.2	8.8	7.8	11.3	11.3	9.5	10.9	10.2	11.1	11.1	10.4	9.6	10.1	10.5	12.0	11.2	11.9	11.0	11.7	11.5	11.0	10.6	9.9	10.9	10.8	11.1	11.5	11.1	11.0	11.4	11.7	10.54°C ± 0.99
	N	5.3	4.4	4.3	4.6	5.4	4.5	6.0	4.4	5.4	6.4	6.5	6.7	6.1	5.5	5.7	6.0	5.8	4.8	5.2	4.9	6.2	6.3	6.8	6.5	6.2	6.3	7.4	6.6	6.7	5.3	6.2	7.6	6.3	5.62°C ± 0.79
Eastern Magdalen Shelf	M	2.4	3.5	2.6	3.0	2.8	1.7	2.2	2.3	2.1	3.7	3.5	3.2	2.6	5.2	3.9	3.6	4.2	3.2	2.9	2.6	3.5	6.2	3.3	4.0	4.2	4.2	4.5	5.1	3.5	3.5	2.7	3.6	3.8	3.33°C ± 0.99
	J	7.1	8.3	9.8	7.3	9.2	8.1	8.6	8.1	7.7	9.8	10.0	10.5	8.0	10.2	11.1	9.3	10.8	9.0	9.0	8.2	8.9	11.5	9.5	9.7	9.6	9.2	8.4	10.7	9.6	10.1	8.1	8.7	10.5	9.17°C ± 1.13
	J	13.5	13.6	15.7	15.1	15.3	14.1	14.7	13.4	13.4	17.6	16.7	15.1	15.3	16.2	18.1	16.1	16.7	15.4	15.8	15.4	15.6	17.7	15.7	17.2	14.7	16.4	14.0	17.1	16.8	16.5	14.7	15.5	17.5	15.56°C ± 1.32
	A	17.7	16.1	17.6	17.4	17.4	17.4	16.6	16.4	17.6	19.2	18.6	19.2	17.6	18.3	18.6	18.5	19.2	18.4	17.6	19.0	18.2	18.0	16.9	17.2	18.7	19.2	17.5	19.8	18.4	19.2	18.4	18.9	18.9	17.95°C ± 0.90
	S	14.6	13.7	14.9	14.6	14.2	15.0	14.2	15.5	15.9	16.0	14.4	16.1	15.3	14.9	16.3	16.0	16.5	15.0	15.4	14.1	16.7	15.5	14.2	15.2	15.0	14.8	15.3	16.3	14.6	14.8	16.2	15.9	16.4	15.14°C ± 0.79
	O	10.2	9.8	10.7	9.7	8.2	11.2	12.1	9.9	12.4	10.5	11.2	11.7	10.8	9.6	10.4	10.7	12.5	11.1	12.3	11.5	12.3	11.7	11.1	11.2	10.0	11.6	10.8	11.3	11.7	11.0	11.1	11.3	12.1	10.94°C ± 1.04
	N	6.2	4.9	4.4	5.3	5.9	4.3	6.1	4.6	6.0	6.3	6.8	7.4	6.8	5.9	5.9	6.9	6.0	5.2	5.5	5.1	6.2	6.3	7.2	7.1	6.4	6.9	8.0	7.2	6.9	5.3	6.0	8.1	6.7	5.99°C ± 0.86
Western Magdalen Shelf	M	3.2	4.0	3.6	3.1	3.4	2.2	3.0	2.9	2.8	3.5	4.3	3.3	3.3	5.8	4.6	3.8	4.7	3.8	3.1	3.3	3.6	6.5	4.0	5.1	4.6	4.5	3.8	5.5	3.6	3.7	3.5	4.4	3.5	3.85°C ± 0.96
	J	8.0	8.6	10.6	8.0	10.5	9.1	10.0	9.4	8.8	10.4	11.1	11.2	9.0	10.6	11.6	9.8	11.7	9.6	9.8	8.8	9.6	11.9	9.8	10.1	10.2	9.8	9.4	10.8	9.8	10.9	9.6	8.9	11.4	9.92°C ± 1.06
	J	14.4	13.9	15.8	15.6	15.7	13.8	14.5	13.8	14.1	17.4	17.6	15.4	15.5	16.3	17.5	16.3	16.7	15.3	16.0	15.8	16.3	17.2	16.3	16.9	15.0	16.4	15.0	16.9	16.2	16.9	15.1	15.5	17.1	15.75°C ± 1.15
	A	17.1	15.4	16.5	17.6	16.7	16.9	16.0	15.6	17.9	17.7	18.1	18.2	17.3	17.3	17.4	18.0	18.3	17.4	16.7	17.9	17.9	17.6	16.4	16.9	18.0	18.3	17.1	19.3	17.1	17.8	18.5	17.8	17.5	17.27°C ± 0.82
	S	13.9	12.7	13.3	13.7	12.8	14.4	13.4	13.9	14.7	14.4	13.8	15.5	14.8	14.8	15.0	14.6	15.3	13.7	14.3	13.2	15.6	14.7	13.1	14.3	14.0	14.2	14.0	15.6	13.5	14.2	15.3	14.7	14.8	14.16°C ± 0.79
	O	9.3	8.4	9.4	7.8	6.8	10.5	10.2	8.6	9.7	9.3	10.3	10.4	9.8	9.0	9.3	9.8	10.9	10.4	11.2	10.2	10.6	10.6	9.8	9.7	9.2	10.1	10.0	10.3	10.5	10.0	10.0	10.4	10.3	9.66°C ± 0.99
	N	4.8	3.9	3.6	3.7	4.5	4.1	5.4	3.9	4.7	6.0	5.8	6.2	5.5	5.0	5.0	5.3	5.0	4.4	4.4	4.6	5.8	5.8	6.1	5.9	5.8	5.6	6.8	5.9	6.1	4.4	5.6	6.7	5.3	5.03°C ± 0.81
		1985	1986	1987	1988	1989	1990	1991	1992	1993	1994	1995	1996	1997	1998	1999	2000	2001	2002	2003	2004	2005	2006	2007	2008	2009	2010	2011	2012	2013	2014	2015	2016	2017	

Figure 19. AVHRR SST May to November monthly anomalies averaged over the Magdalen Shallows (region 8 of the Gulf) and the eastern and western subregions of the Magdalen Shallows (Figure 18). The scorecards are colour-coded according to the monthly normalized anomalies based on the 1985–2010 climatologies for each month, but the numbers are the monthly average temperatures in °C. The 1985–2010 mean and standard deviation are indicated for each month on the right side of the table.

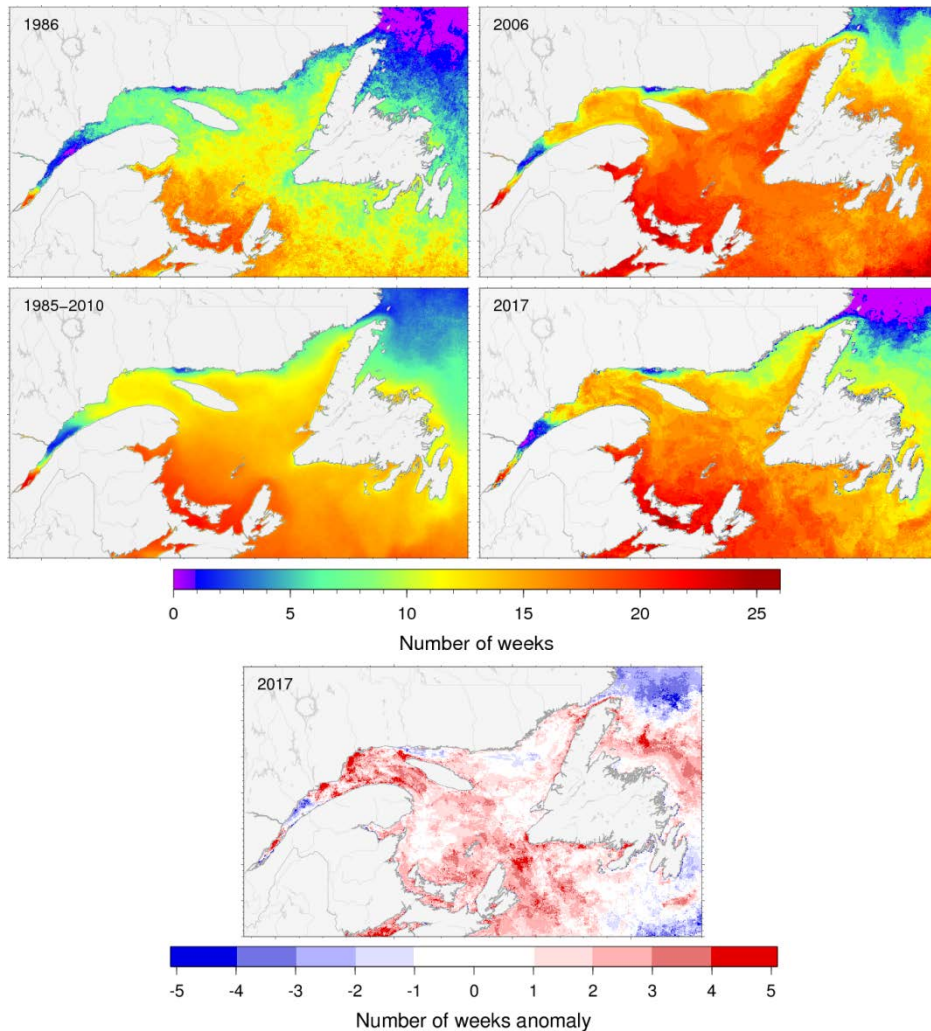


Figure 20. Yearly number of weeks with mean weekly surface temperature >10°C. (Top) Years with the minimum (1986, top left) and maximum (2006, top right) number of weeks are shown along with the 1985–2010 climatological average (lower left) and the chart for 2017. (Bottom) Anomaly for 2017 relative to 1985–2010 climatology, expressed in numbers of weeks.

	1985	1986	1987	1988	1989	1990	1991	1992	1993	1994	1995	1996	1997	1998	1999	2000	2001	2002	2003	2004	2005	2006	2007	2008	2009	2010	2011	2012	2013	2014	2015	2016	2017	
Gulf of St. Lawrence	11.4	10.4	13.0	11.0	12.1	12.0	11.8	10.8	12.4	14.0	14.9	14.8	13.7	14.4	16.2	14.1	15.6	12.7	14.8	13.1	14.2	16.3	13.8	14.4	14.2	14.2	13.7	15.9	14.0	15.0	14.3	13.9	15.3	13.5 w ± 1.6
1 - Estuary	4.9	3.5	5.1	6.6	5.4	5.5	5.0	5.2	10.1	6.9	7.4	8.1	7.6	7.9	8.2	8.0	7.8	8.1	6.9	5.8	6.7	9.1	6.6	8.7	6.3	8.8	9.1	10.3	4.4	10.0	9.3	9.6	7.2	6.9 w ± 1.6
2 - Northwest Gulf	11.0	8.0	9.0	9.2	10.7	10.0	9.6	9.4	13.0	12.6	13.6	15.0	12.6	14.6	15.1	12.3	13.1	11.1	12.6	10.5	12.7	13.8	11.6	13.0	11.9	13.9	13.0	14.6	11.5	13.9	14.1	12.3	14.2	11.9 w ± 1.9
3 - Anticosti Channel	9.5	8.8	11.5	8.9	11.4	7.3	7.7	8.9	9.4	11.4	12.6	13.4	12.0	13.0	15.2	11.3	12.9	11.3	11.9	10.8	13.0	14.6	10.7	11.9	12.7	12.5	10.9	13.2	12.9	12.2	13.0	11.8	12.4	11.3 w ± 2.0
4 - Mécatina Trough	4.6	5.4	9.0	6.7	5.9	7.7	2.9	2.8	4.2	8.3	7.8	7.8	8.8	8.4	12.5	11.6	10.7	8.0	11.8	9.5	9.7	11.7	8.6	10.2	9.9	9.1	8.3	12.0	10.9	8.7	10.2	9.0	9.9	8.2 w ± 2.7
5 - Esquiman Channel	9.9	9.4	13.0	10.8	10.9	10.9	8.9	8.2	9.2	12.9	13.1	11.9	12.4	12.6	15.6	13.6	14.5	10.1	15.3	11.8	12.6	16.8	13.1	13.3	13.3	12.6	11.7	15.2	12.7	13.7	12.8	12.4	13.4	12.2 w ± 2.1
6 - Central Gulf	12.3	10.9	14.2	11.3	12.4	12.2	12.6	11.8	12.8	14.6	15.5	15.4	13.9	14.2	16.7	14.2	16.1	12.4	15.3	13.3	13.8	17.2	13.1	13.9	14.9	13.9	13.5	16.2	14.3	14.9	13.4	13.9	15.5	13.8 w ± 1.6
7 - Cabot Strait	11.6	11.1	15.0	11.8	12.6	14.4	13.6	11.3	14.1	16.1	16.9	16.1	14.6	15.6	17.3	15.4	18.1	12.5	16.2	14.0	15.6	17.4	15.4	15.4	15.8	15.0	14.6	17.4	15.0	16.8	14.5	15.2	17.1	14.7 w ± 1.9
8 - Magdalen Shallows	14.8	14.5	16.6	14.1	15.5	16.3	17.6	15.1	16.1	17.5	18.8	18.2	16.6	17.4	18.6	17.6	19.8	17.4	18.1	17.8	17.9	19.5	18.7	18.2	17.7	17.6	17.7	19.0	17.9	18.4	17.3	17.3	19.3	17.2 w ± 1.5

Figure 21. Yearly number of weeks with mean weekly surface temperature >10°C, averaged for the entire Gulf and each region of the Gulf. The scorecards are colour-coded according to the normalized anomalies based on the 1985–2010 time series, but the numbers are the average number of weeks above 10°C for each year.

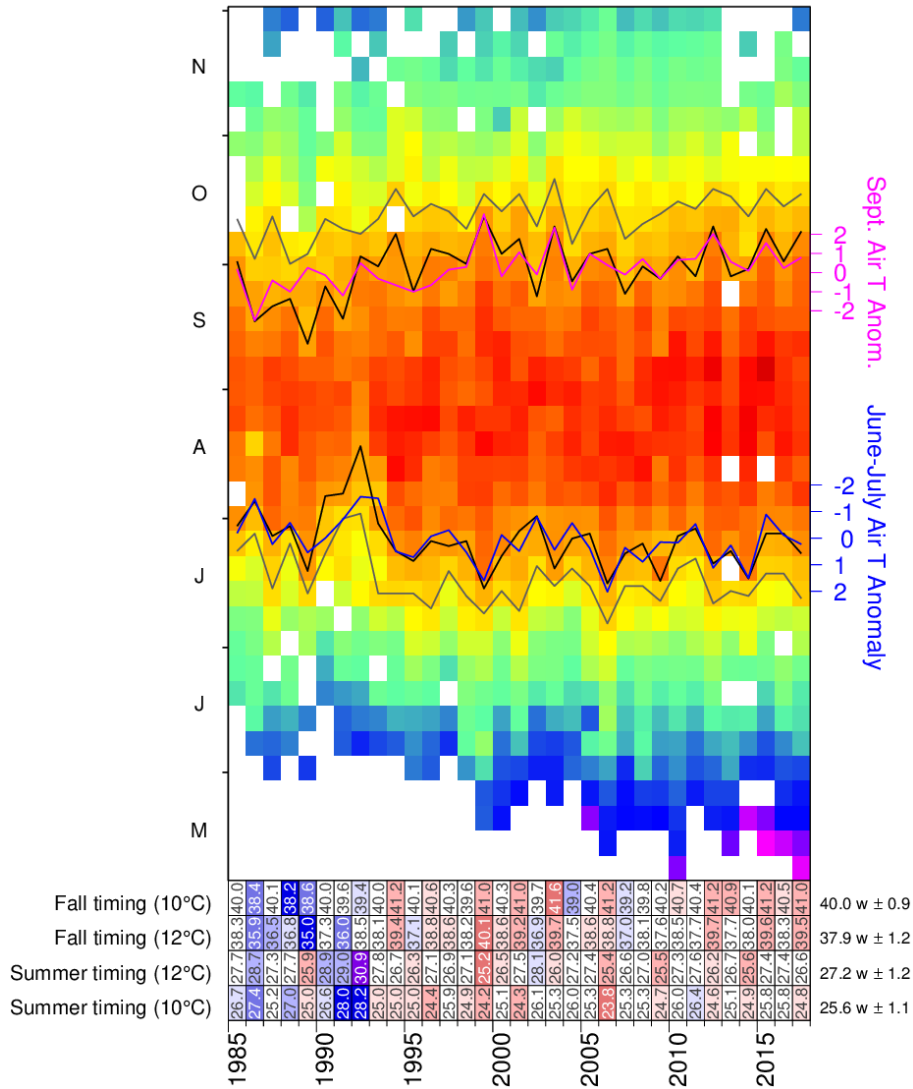


Figure 22. Weekly average SST (1985-2017) matrix for the Gulf of St. Lawrence. Black lines show first and last occurrence of the 12°C isotherm and proxies based on June-July (blue line) and September (magenta) average air temperature are also shown (axes on right). Gray lines show first and last occurrence of the 10°C isotherm. The scorecards are colour-coded according to the normalized anomalies based on the 1985–2010 time series, but the numbers are week numbers when the threshold was crossed. Updated from Galbraith and Larouche 2013.

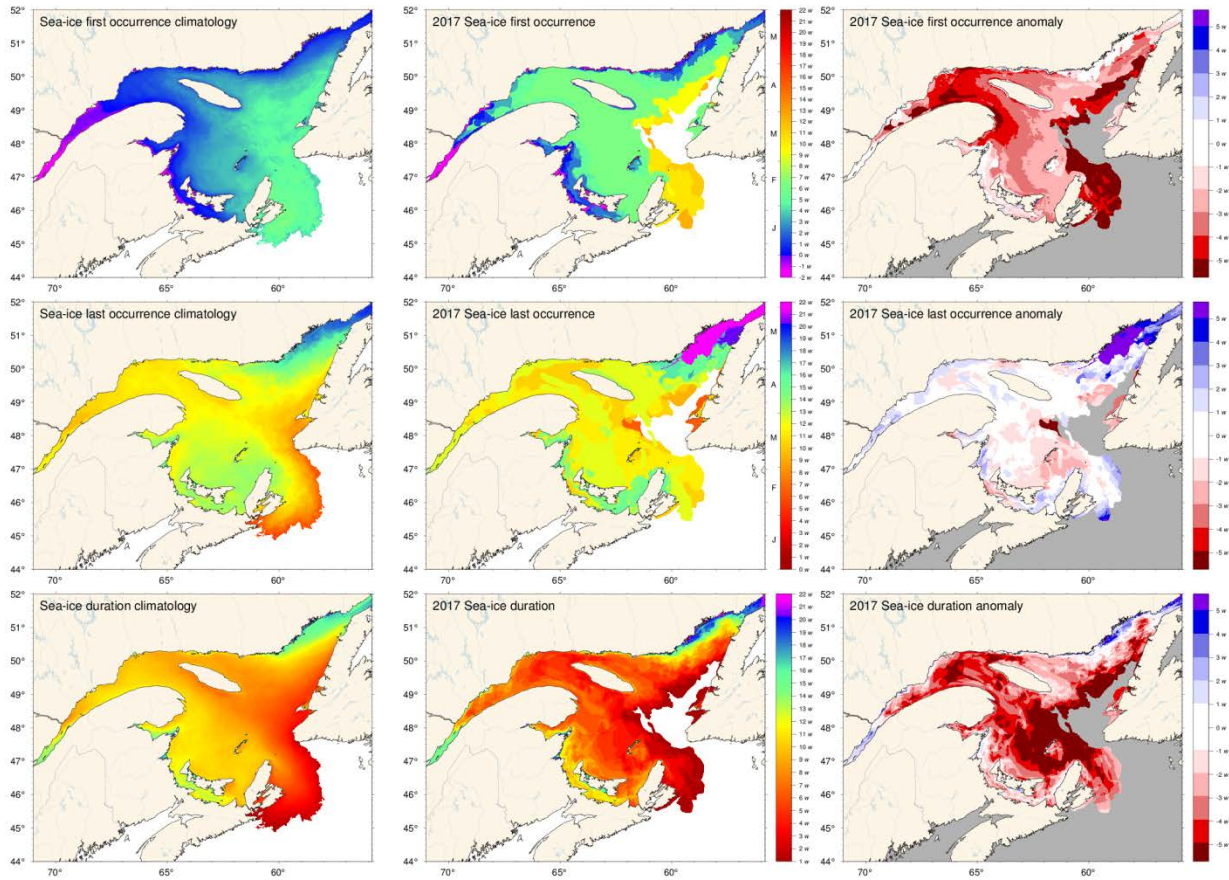


Figure 23. First and last occurrence of ice and ice season duration based on weekly data. The 1981-2010 climatologies are shown (left) as well as the 2017 values (middle) and anomalies (right). First and last occurrence is defined here as the first and last weekly chart in which any amount of ice is recorded for each pixel and are illustrated as day-of-year. Ice duration sums the number of weeks with ice cover for each pixel. Climatologies are shown for pixels that had at least 15 years out of the 30 with occurrence of sea-ice, and therefore also show the area with 50% likelihood of having some sea-ice at any time during any given year.

		Mean ± S.D.											
First occurrence of ice	1 - Estuary	17	56	77	43	17	17	84	137	66	84	84	85 ± 12
	2 - Northwest Gulf	12	31	29	52	12	12	124	129	102	81	88	93 ± 13
	3 - Anticosti Channel	-5	25	13	12	11	9	9	104	100	90	93	120 ± 24
	4 - Mécatina Trough	-12	10	0	-6	-12	-10	-12	140	130	114	104	140 ± 19
	5 - Esquiman Channel	4	19	13	8	5	3	-3	113	113	120	168	118 ± 25
	6 - Central Gulf	5	27	23	26	3	7	1	127	131	117	140	101 ± 15
	7 - Cabot Strait	4	31	12	32	-5	-5	-5	103	106	127	144	109 ± 16
	8 - Magdalen Shallows	3	26	19	32	3	2	1	112	120	99	130	112 ± 15
Last occurrence of ice	1 - Estuary	21	37	12	11	-28	-26	-23	81	69	75	68	93 ± 14
	2 - Northwest Gulf	5	30	30	27	0	-10	5	103	104	74	124	90 ± 19
	3 - Anticosti Channel	8	48	21	40	-11	-9	-2	120	104	79	89	107 ± 29
	4 - Mécatina Trough	-5	27	11	12	-2	-3	-2	113	111	112	133	138 ± 26
	5 - Esquiman Channel	9	16	9	4	-15	-7	-9	108	106	97	109	107 ± 31
	6 - Central Gulf	2	25	20	13	1	-1	-8	109	118	110	125	74 ± 31
	7 - Cabot Strait	9	24	11	4	-7	-6	-9	130	114	127	169	76 ± 28
	8 - Magdalen Shallows	20	2	0	3	-21	-20	-21	123	105	111	123	109 ± 22
Duration of ice season	1 - Estuary	93	104	74	124	129	102	81	88	103	104	136	93 ± 14
	2 - Northwest Gulf	104	100	90	90	93	77	83	70	136	136	145	90 ± 19
	3 - Anticosti Channel	142	140	136	135	128	139	114	104	149	118	121	107 ± 29
	4 - Mécatina Trough	127	130	103	124	140	133	91	77	140	121	104	138 ± 26
	5 - Esquiman Channel	113	113	120	168	179	160	96	78	110	95	103	95 ± 36
	6 - Central Gulf	127	131	117	140	165	126	91	77	123	105	95	74 ± 31
	7 - Cabot Strait	103	103	106	127	144	124	104	93	102	73	95	76 ± 28
	8 - Magdalen Shallows	112	112	108	136	142	132	96	104	139	68	80	109 ± 22
Maximum ice volume (km ³)	1 - Estuary	117	104	101	83	137	111	96	84	107	83	57	6.2 km ³ ± 3.2
	2 - Northwest Gulf	81	69	75	68	95	82	65	53	89	61	70	5.5 km ³ ± 2.1
	3 - Anticosti Channel	107	111	104	123	156	144	83	83	113	43	59	12.0 km ³ ± 7.9
	4 - Mécatina Trough	120	104	79	89	117	103	93	106	108	97	86	7.1 km ³ ± 4.7
	5 - Esquiman Channel	141	91	105	132	147	132	103	101	123	96	104	6.4 km ³ ± 4.1
	6 - Central Gulf	106	113	112	133	147	144	90	77	123	96	111	25.8 km ³ ± 11.0
	7 - Cabot Strait	113	128	94	124	122	122	116	86	113	106	97	62 km ³ ± 25
	8 - Magdalen Shallows	113	106	97	109	135	135	85	79	118	95	100	8 km ³ ± 7
GSL	1 - Estuary	109	118	110	125	134	110	90	91	109	110	124	68 km ³ ± 30
	2 - Northwest Gulf	123	123	120	127	184	139	92	103	136	133	124	
	3 - Anticosti Channel	136	133	124	139	129	132	105	95	120	133	139	
	4 - Mécatina Trough	120	113	121	146	163	161	133	94	120	113	124	
	5 - Esquiman Channel	126	123	116	138	151	146	121	105	122	96	91	
	6 - Central Gulf	115	101	98	102	125	109	97	77	127	82	88	
	7 - Cabot Strait	127	135	119	131	150	137	97	89	110	42	51	
	8 - Magdalen Shallows	108	93	105	103	137	100	94	88	109	93	48	
GSL + Scotian Shelf	91	73	81	83	118	86	85	84	80	41	41	31	
	96	95	98	93	111	94	87	83	84	59	62	70	
	116	115	98	120	130	102	95	88	109	93	48	71	
	114	114	92	92	98	93	87	81	52	26	0	71	
	89	85	111	118	118	80	78	71	53	41	99	136	
	112	114	97	117	150	104	97	90	103	71	174	101	
	109	104	98	116	129	114	87	81	106	83	81	88	
	82	80	100	107	82	79	85	63	22	0	0	10	
78	75	73	107	77	75	73	61	87	24	27	22		
110	110	58	107	123	97	61	82	97	72	5	58		
115	111	109	154	160	158	95	89	123	92	102	135		
130	130	123	132	137	88	88	77	123	97	74	95		
96	91	86	84	94	89	89	81	96	91	34	18		
106	107	89	84	89	119	90	91	93	28	41	82		

Figure 24. First and last day of ice occurrence, ice duration and maximum seasonal ice volume by region. The time when ice was first and last seen in days from the beginning of each year is indicated for each region, and the colour code expresses the anomaly based on the 1981–2010 climatology, with blue representing earlier first occurrence and later last occurrence. The threshold is 5% of the largest ice volume ever recorded in the region. Numbers in the table are the actual day of the year or volume, but the colour coding is according to normalized anomalies based on the climatology of each region. Duration is the numbers of days that the threshold was exceeded. All results based on weekly data.

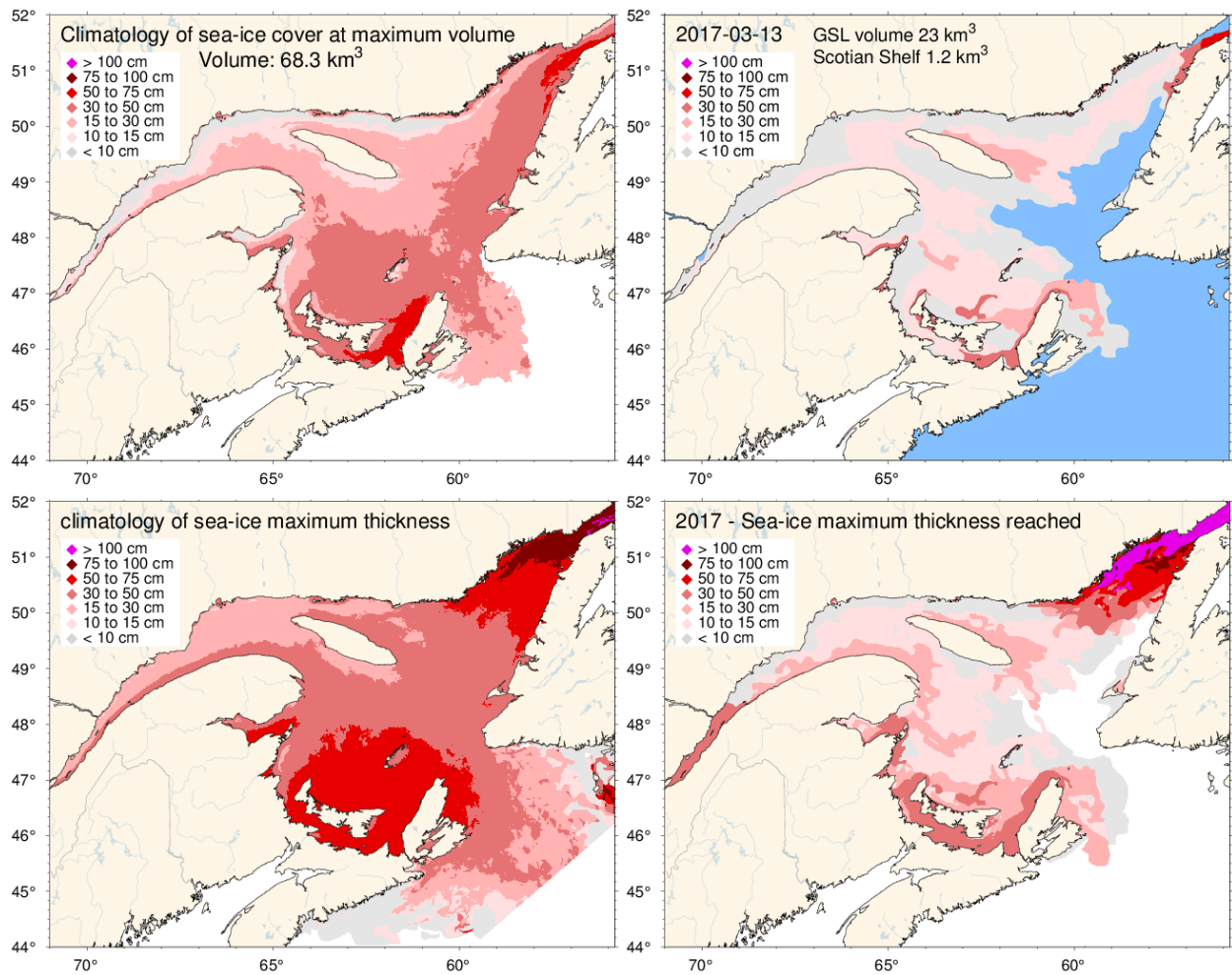


Figure 25. Ice thickness map for 2017 for the week of the year with the maximum annual volume including the portion covering the Scotian Shelf (upper right panel) and similarly for the 1981-2010 climatology of the weekly maximum (upper left panel). Note that these maps reflect the ice thickness distribution on that week, and not the maximum observed at any given location during the year. That information is shown by the lower panels, showing the 1981-2010 climatology and 2017 distribution of the thickest ice recorded during the season at any location.

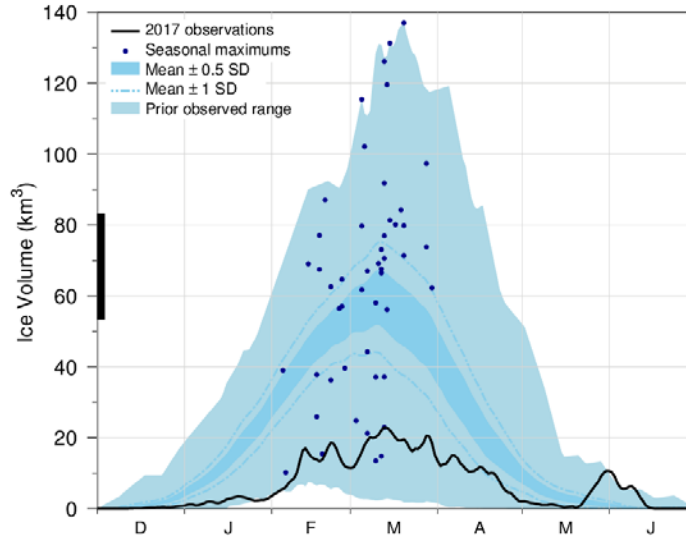


Figure 26. Time series of the 2016-2017 daily mean ice volume for the Gulf of St. Lawrence and Scotian Shelf (black line), the 1981-2010 climatological mean volume plus and minus 0.5 and 1 SD (dark blue area and dashed line), the minimum and maximum span of 1969-2017 observations (light blue) and the date and volumes of 1969-2017 seasonal maximums (blue dots). The black thick line on the left indicates the mean volume plus and minus 0.5 SD of the annual maximum ice volume, which is higher than the peak of the mean daily ice volume distribution.

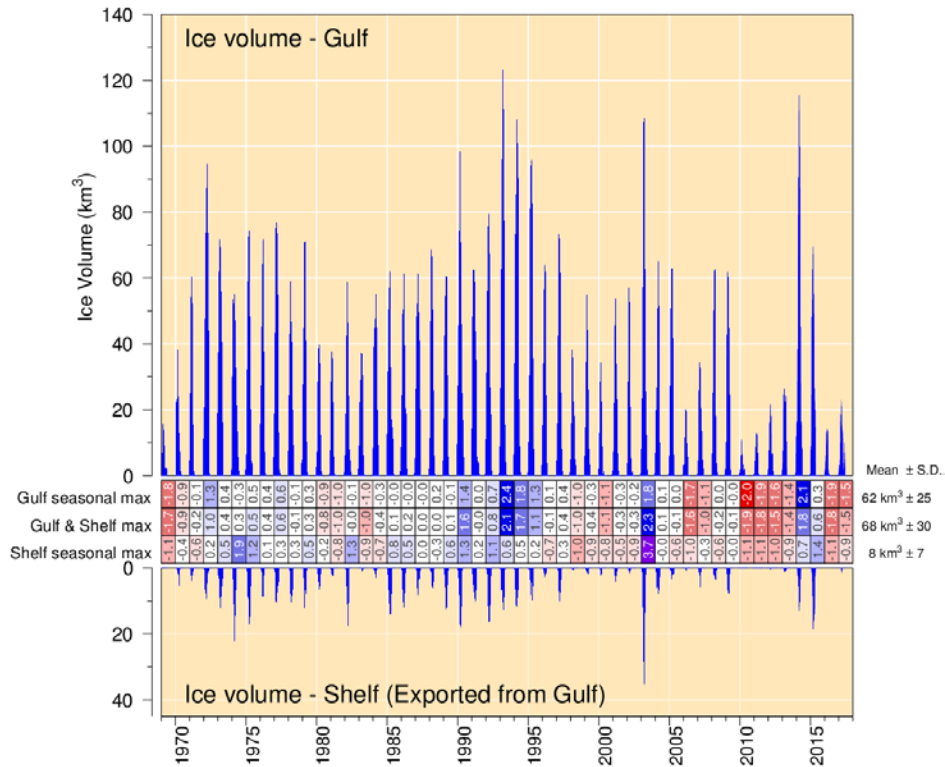


Figure 27. Estimated weekly maximum ice volume in the Gulf of St. Lawrence (upper panel) and on the Scotian Shelf seaward of Cabot Strait defined by its narrowest crossing (lower panel). Scorecards show numbered normalized anomalies for the Gulf, combined Gulf and Shelf and Shelf-only annual maximum volumes from weekly ice data. The mean and standard deviation are indicated on the right side using the 1981–2010 climatology.

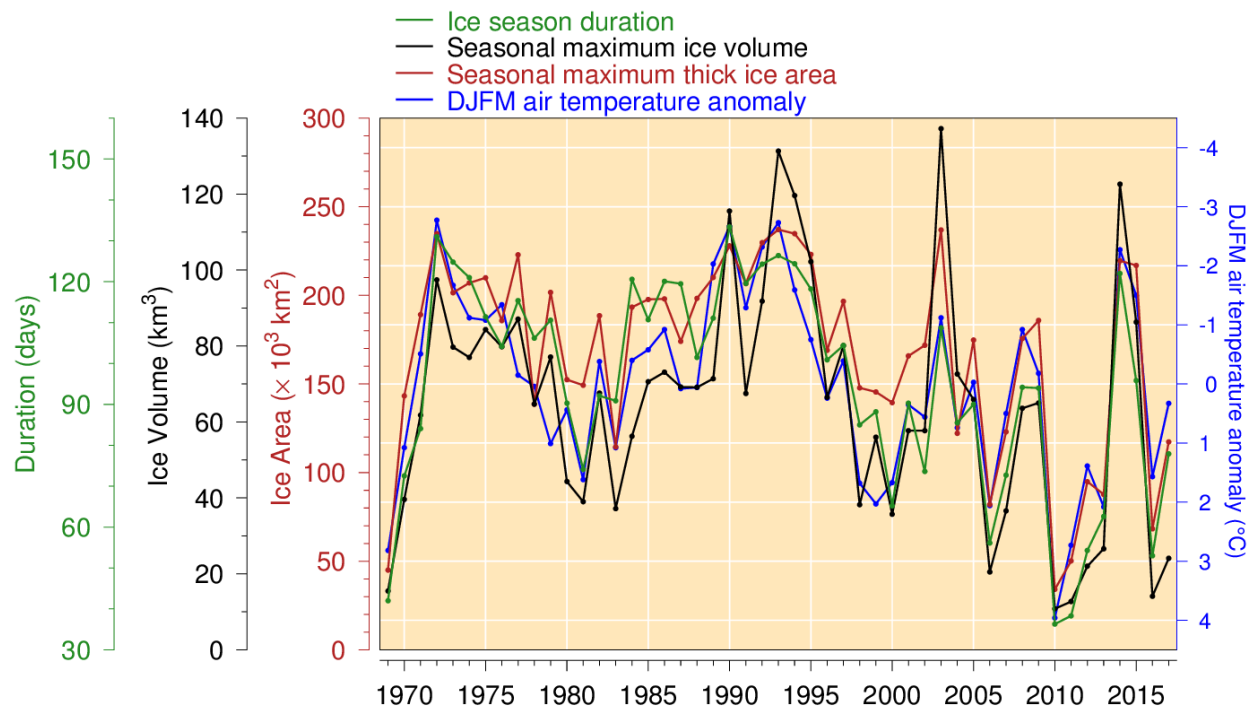


Figure 28. Seasonal maximum ice volume and area including the portion on the Scotian Shelf (excluding ice less than 15 cm thick), ice season duration and December-to-March air temperature anomaly (Figure adapted from Hammill and Galbraith 2012, but here not excluding small floes and adding February and March data to the air temperature anomalies). All sea-ice products are based on weekly data. Linear relations indicate losses of 17 km³, 31,000 km² and 14 days of sea-ice season for each 1°C increase in winter air temperature (R^2 of 0.72, 0.78 and 0.77 respectively).

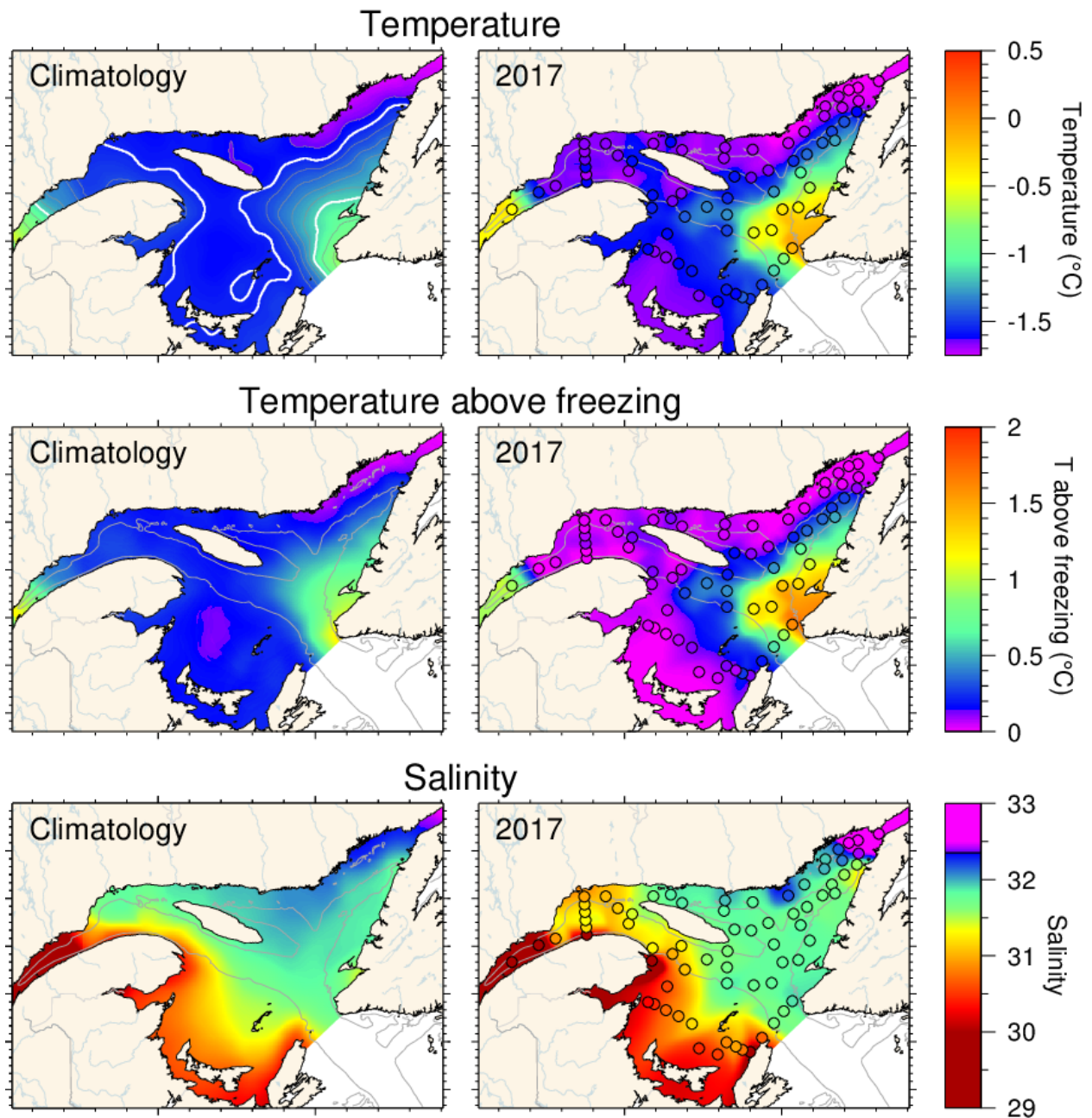


Figure 29. Winter surface layer characteristics from the March 2017 survey compared with climatological means: surface water temperature (upper panel), temperature difference between surface water temperature and the freezing point (middle panel), and salinity (lower panel). Symbols are coloured according to the value observed at the station, using the same colour palette as the interpolated image. A good match is seen between the interpolation and the station observations where the station colours blend into the background. Black symbols indicate missing or bad data. The climatologies are based on 1996-2017 for salinity but exclude 2010 as an outlier for temperature and temperature above freezing.

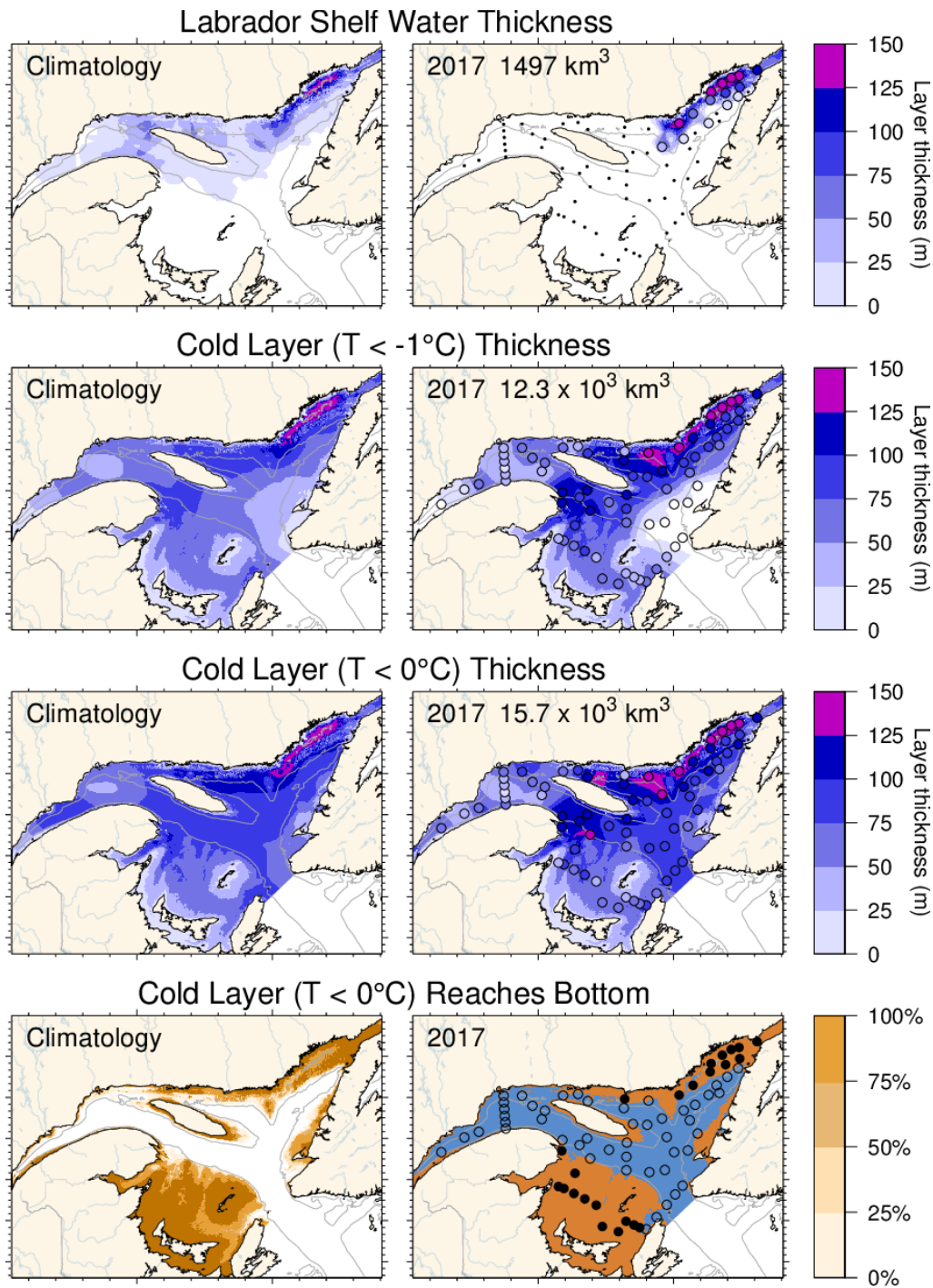


Figure 30. Winter surface layer characteristics from the March 2017 survey compared with climatological means: estimates of the thickness of the Labrador Shelf water intrusion (upper panels), cold layer ($T < -1^{\circ}\text{C}$, $T < 0^{\circ}\text{C}$) thickness (middle panels), and maps indicating where the cold layer ($T < 0^{\circ}\text{C}$) reaches the bottom (in brown; lower panels). Station symbols are coloured according to the observed values as in Figure 29. For the lower panels, the stations where the cold layer reached the bottom are indicated with filled circles while open circles represent stations where the layer did not reach the bottom. Integrated volumes are indicated for the first six panels (including an approximation for the Estuary but excluding the Strait of Belle Isle). The climatologies are based on 1997-2017 for the Labrador Shelf water intrusion, 1996-2017 for the cold layer ($T < 0^{\circ}\text{C}$) but excludes 2010 for $T < -1^{\circ}\text{C}$.

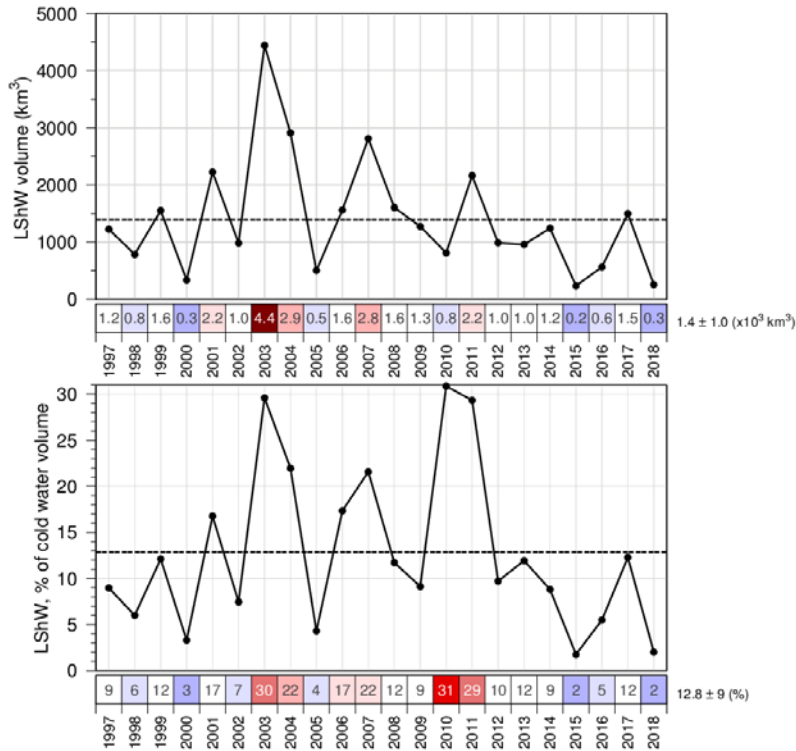


Figure 31. Estimated volume of cold and saline Labrador Shelf water that flowed into the Gulf over the winter through the Strait of Belle Isle. The bottom panel shows the volume as a percentage of total cold-water volume ($<-1^{\circ}\text{C}$). The numbers in the boxes are actual values colour-coded according to their 1997-2017 climatology anomaly. Coverage of Mecatina Trough was insufficient in 1996 to provide an estimated volume.

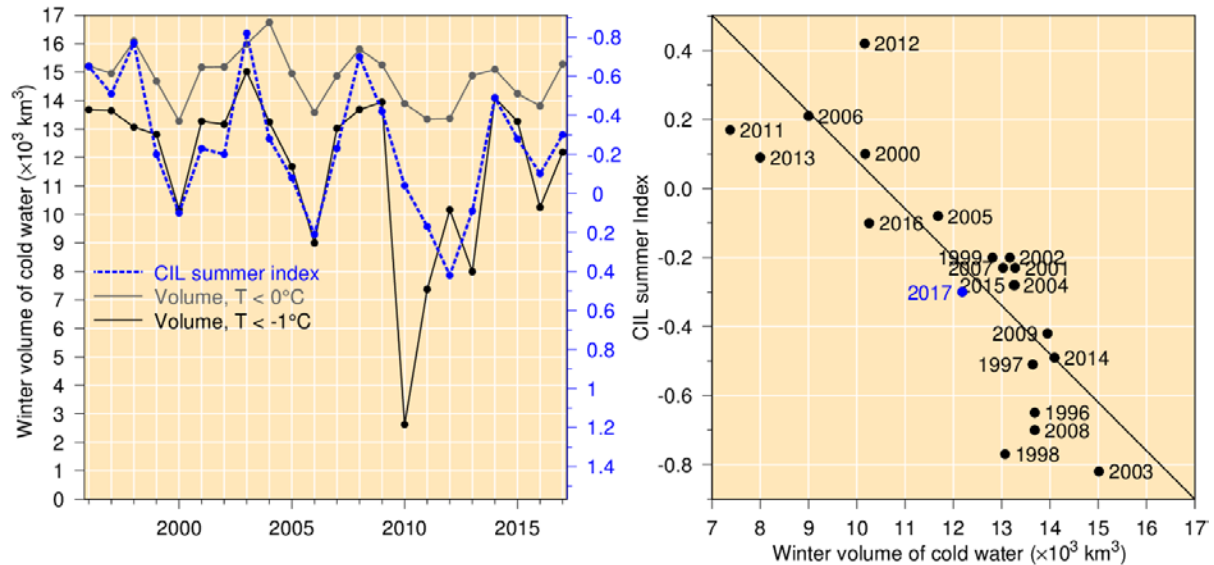


Figure 32. Left panel: winter surface cold ($T < -1^{\circ}\text{C}$ and $T < 0^{\circ}\text{C}$) layer volume (excluding the Estuary and the Strait of Belle Isle) time series (black and grey lines) and summer CIL index (blue dashed line). Right panel: Relation between summer CIL index and winter cold-water volume with $T < -1^{\circ}\text{C}$ (regression for 1996-2017 data pairs, excluding 1998 [see Galbraith 2006] as well as the 2010 and 2011 mild winters). Note that the CIL scale in the left panel is reversed.

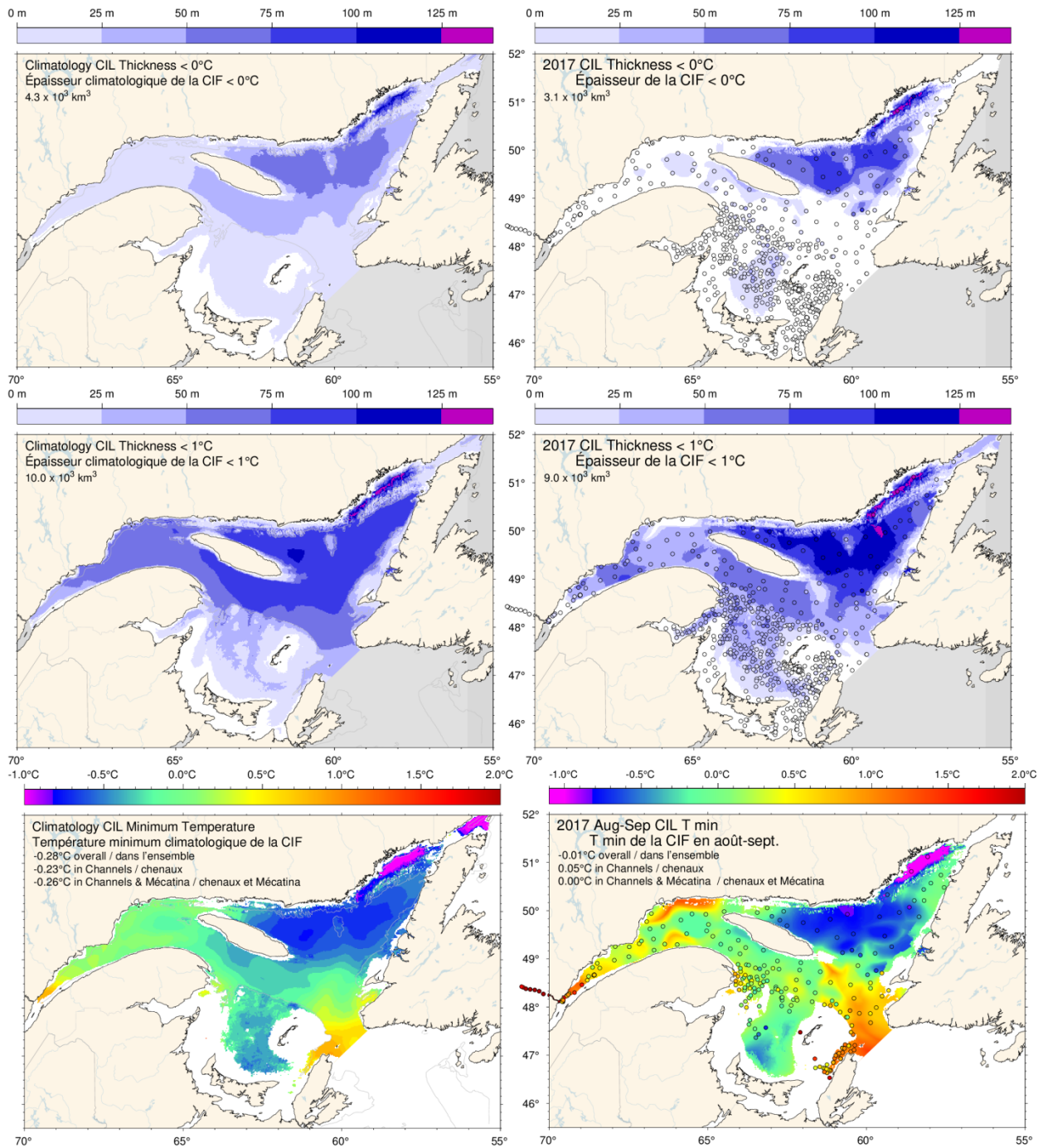


Figure 33. Cold intermediate layer thickness ($T < 0^\circ\text{C}$, top panels; $T < 1^\circ\text{C}$, middle panels) and minimum temperature (bottom panels) in August and September 2017 (right) and 1985-2010 climatology (left). Station symbols are colour-coded according to their CIL thickness and minimum temperature. Numbers in the upper and middle panels are integrated CIL volumes and in the lower panels are monthly average temperatures.

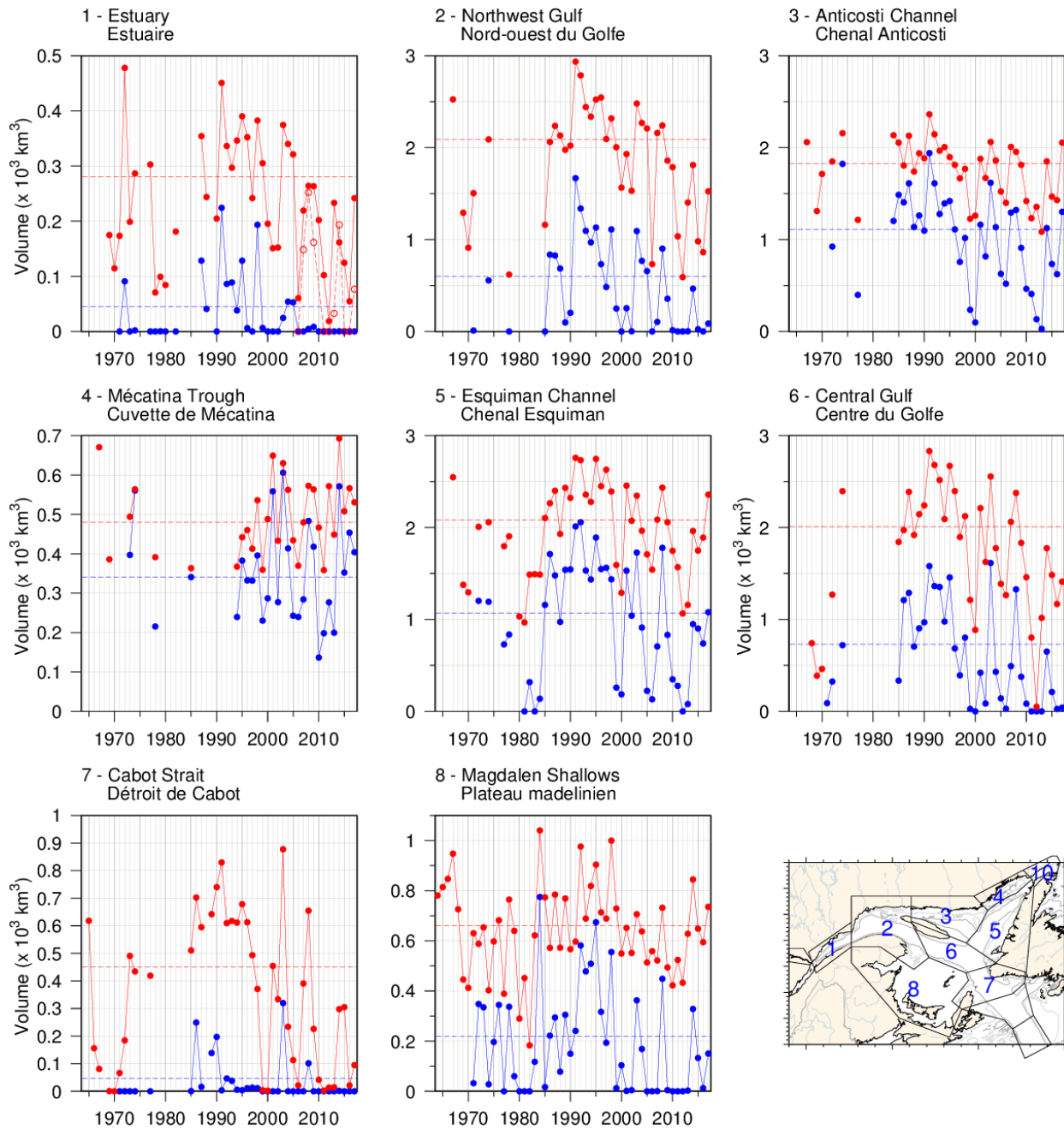


Figure 34. Volume of the CIL colder than 0°C (blue) and colder than 1°C (red) in August and September (primarily region 8 in September). The volume of the CIL colder than 1°C in November for available years since 2006 is also shown for the St. Lawrence Estuary (dashed line).

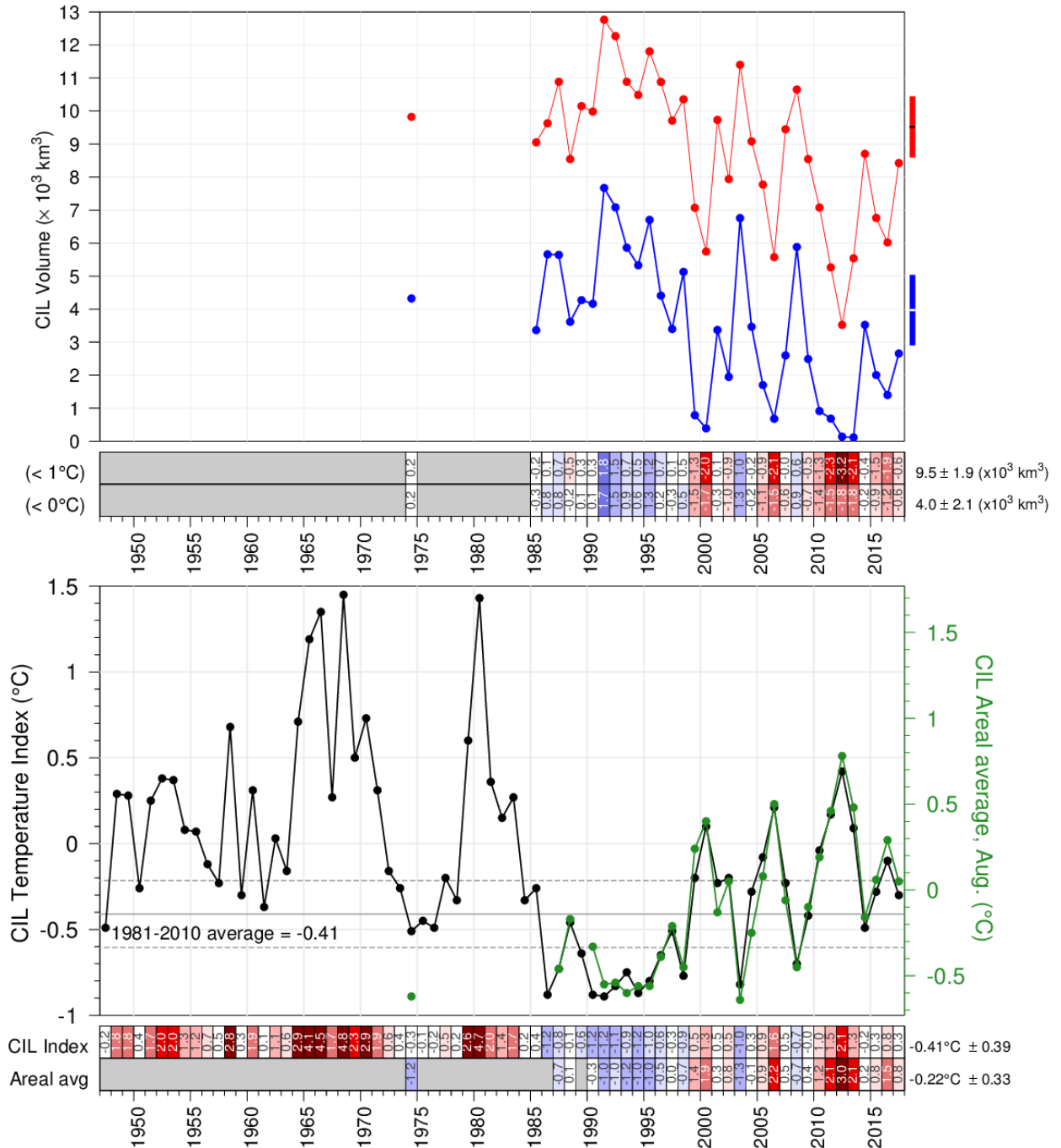


Figure 35. CIL volume (top panel) delimited by 0°C (in blue) and 1°C (in red), and minimum temperature index (bottom panel) in the Gulf of St. Lawrence. The volumes are integrals of each of the annual interpolated thickness grids such as those shown in the top panels of Figure 33 excluding Mécatina Trough and the Strait of Belle Isle. Rectangles on right side show mean ± 0.5 SD. In the lower panel, the black line is the updated Gilbert and Pettigrew (1997) index interpolated to 15 July (with dashed lines showing mean ± 0.5 SD) and the green line is the spatial average of each of the annual interpolated grid such as those shown in the two bottom panels of Figure 33, excluding Mécatina Trough, the Strait of Belle Isle and the Magdalen Shallows. The numbers in the boxes are normalized anomalies relative to 1980-2010 climatologies constructed using all available years.

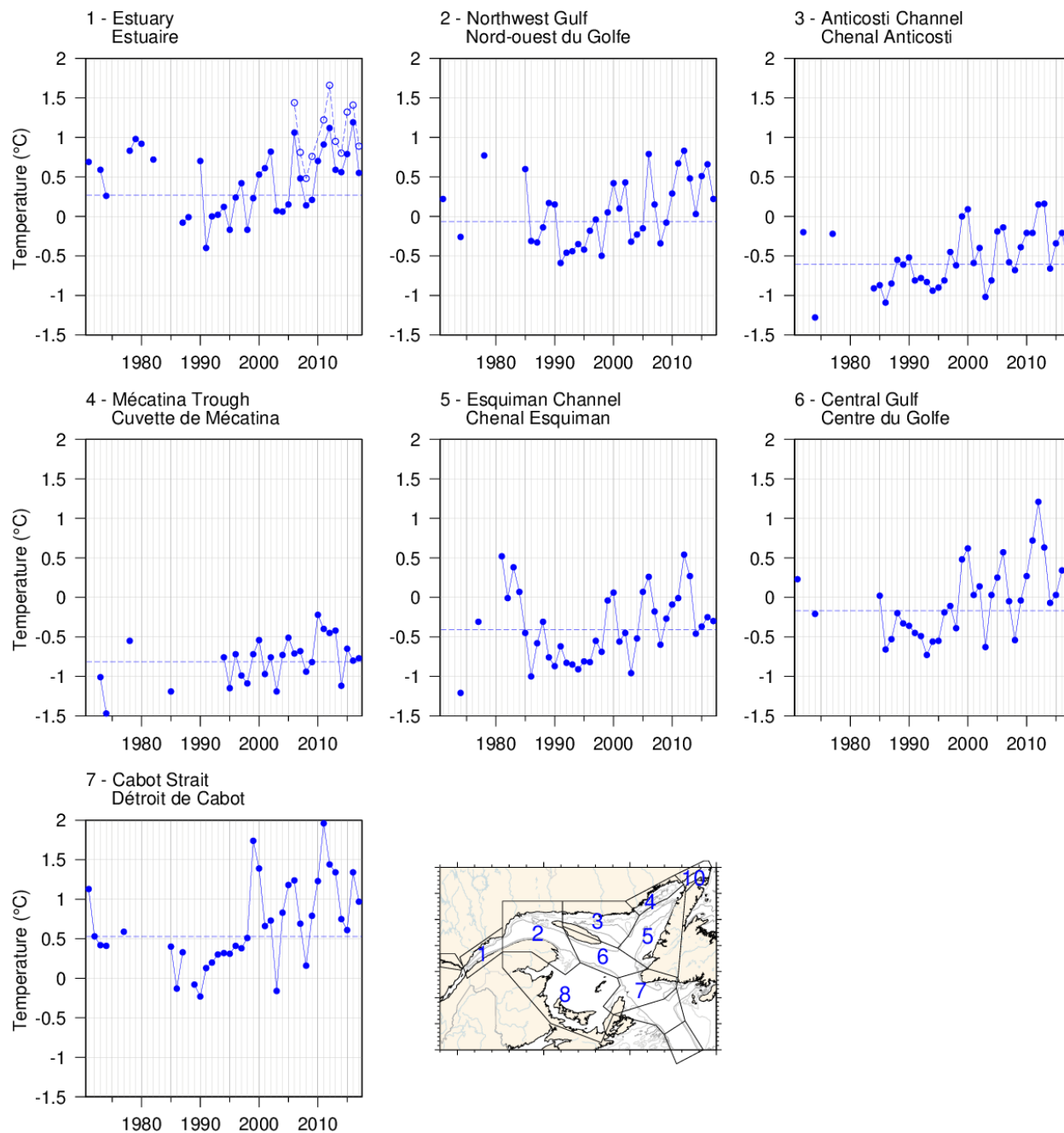


Figure 36. Temperature minimum of the CIL spatially averaged for the seven areas where the CIL minimum temperature can be clearly identified. The spatial average of the November CIL temperature minimum for available years since 2006 is also shown for the St. Lawrence Estuary (dashed line).

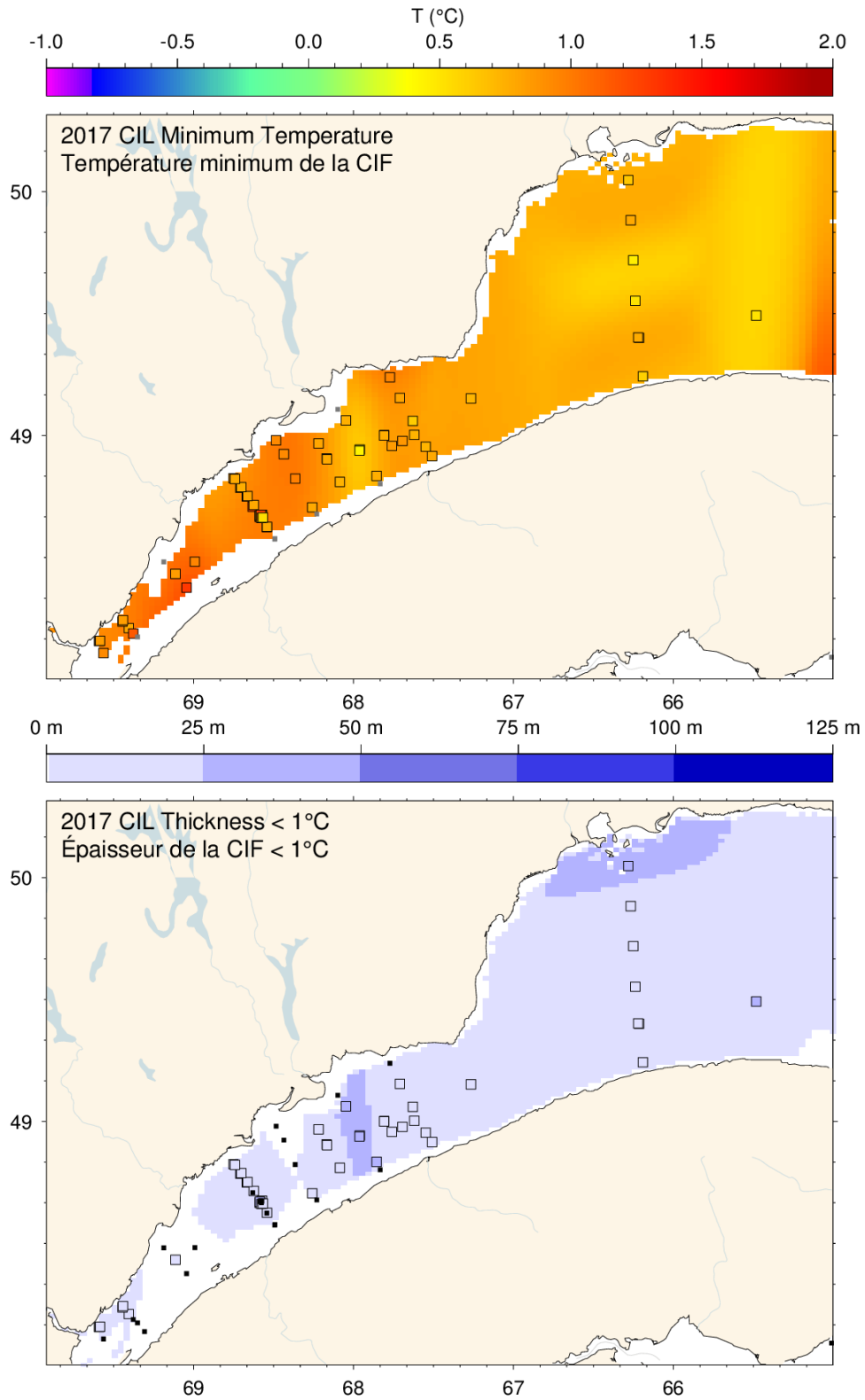


Figure 37. Cold intermediate layer minimum temperature and thickness ($T < 1^\circ\text{C}$) in November 2017 in the St. Lawrence Estuary.

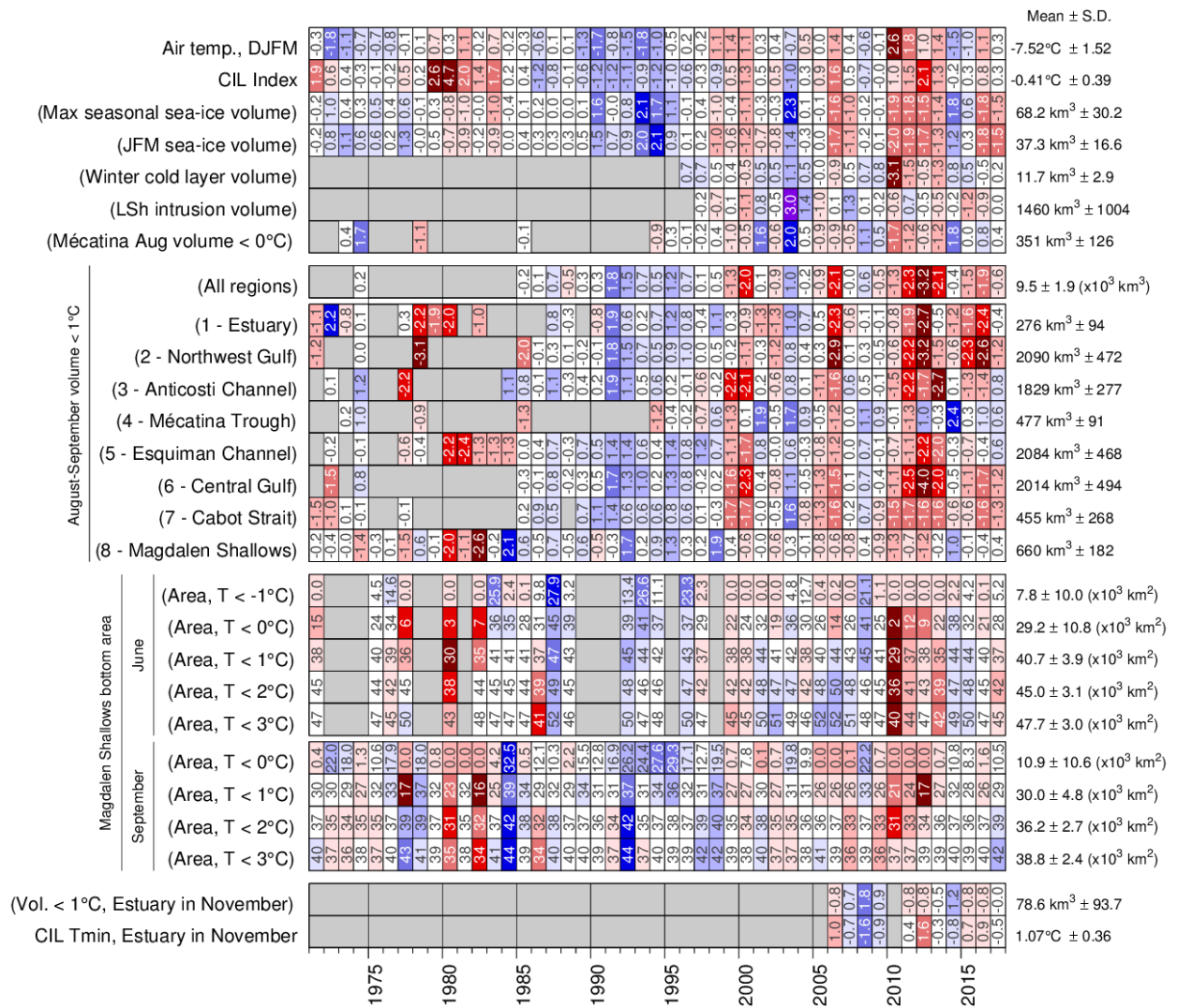


Figure 38. Winter and summertime CIL related properties. The top block shows the scorecard time series for Dec-Jan-Feb-March air temperature (Figure 5), the Gilbert and Pettigrew (1997) CIL index, yearly maximum sea-ice volume (Gulf + Scotian Shelf), Dec-Jan-Feb average sea-ice volume, winter (March) cold-layer (<-1°C) volume, volume of Labrador Shelf Water intrusion into the Gulf observed in March, and the August–September volume of cold water (<0°C) observed in the Mécatina Trough. Labels in parentheses have their colour coding reversed (blue for high values). The second block shows scorecard time series for August–September CIL volumes (<1°C) for all eight regions and for the entire Gulf when available. The third block shows the scorecard time series for the bottom areas of the Magdalen Shallows covered by waters colder than 0, 1, 2, and 3°C during the June and September survey. The last block shows the November survey CIL volume (<1°C) and average CIL minimum temperature in the Estuary. Numbers in cells express anomalies in units of standard deviation, except for bottom areas which are expressed in units of area (x10³ km²) (because of the occurrence of zeros).

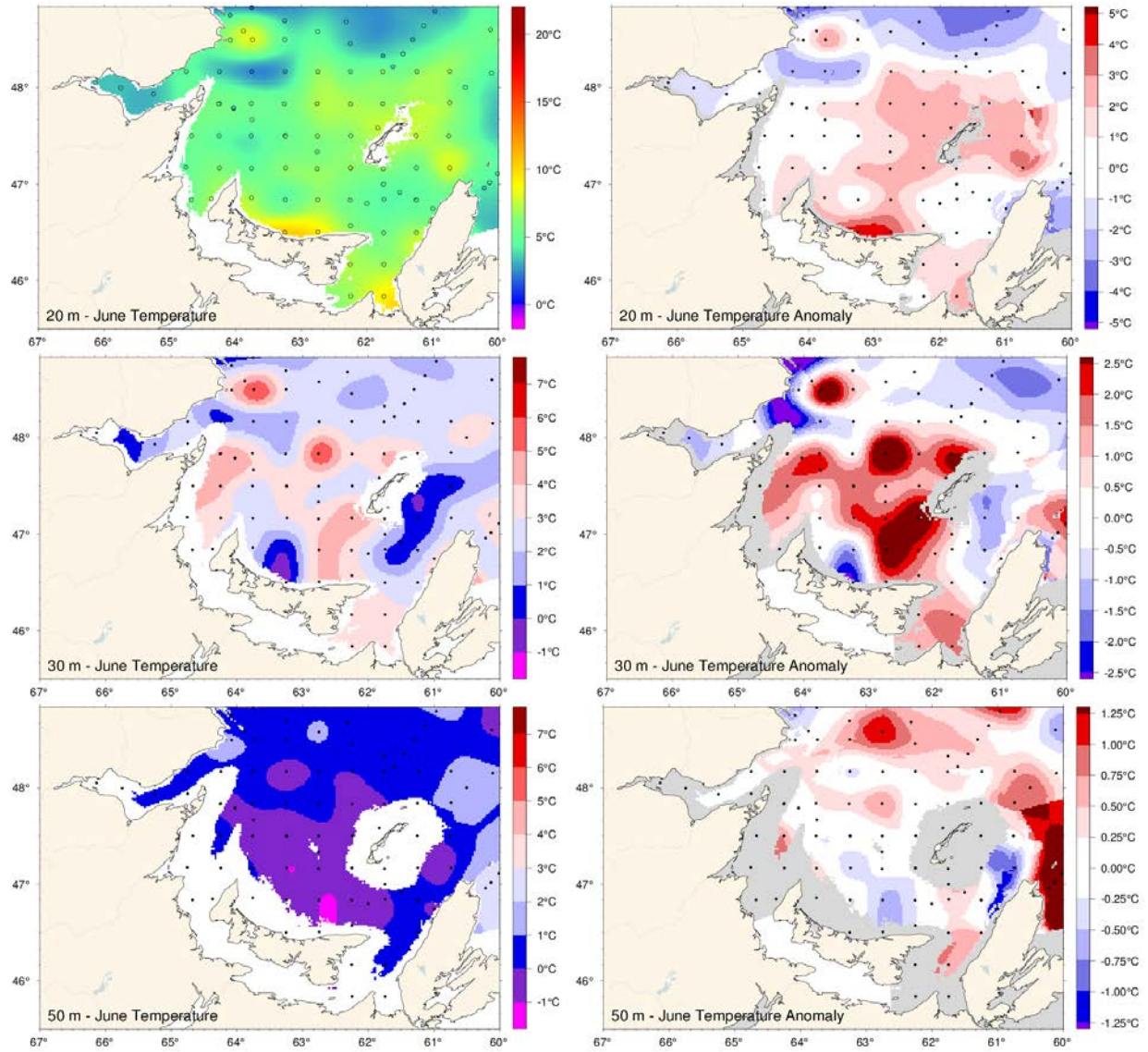


Figure 39. June depth-layer temperature and anomaly fields on the Magdalen Shallows at 10, 20 and 50 m. Anomalies are based on 1971-2010 climatologies for all available years (appearing on Figure 40).

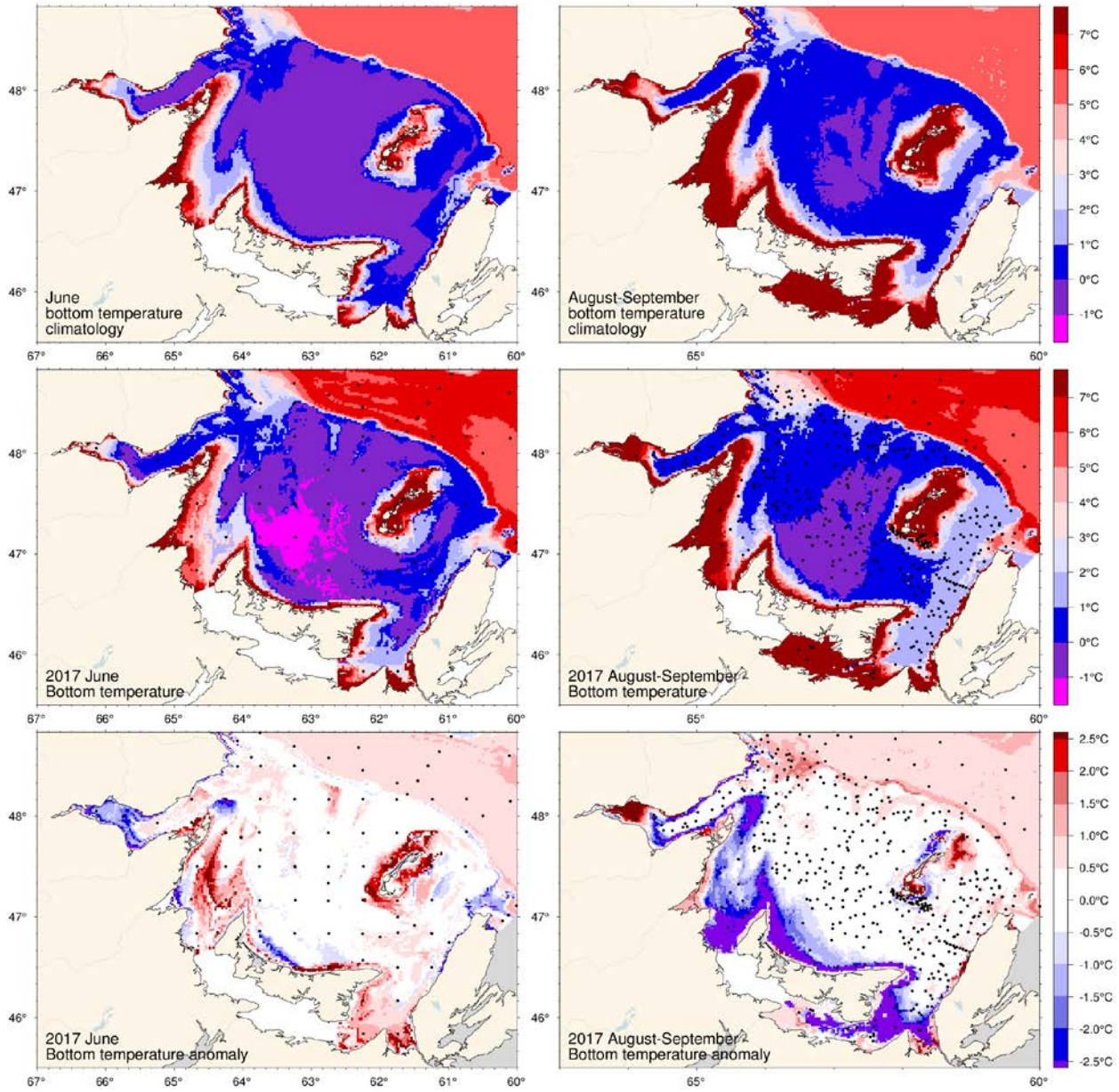


Figure 41. June (left) and August-September (right) bottom temperature climatology (top), 2017 observations (middle) and anomaly (bottom).

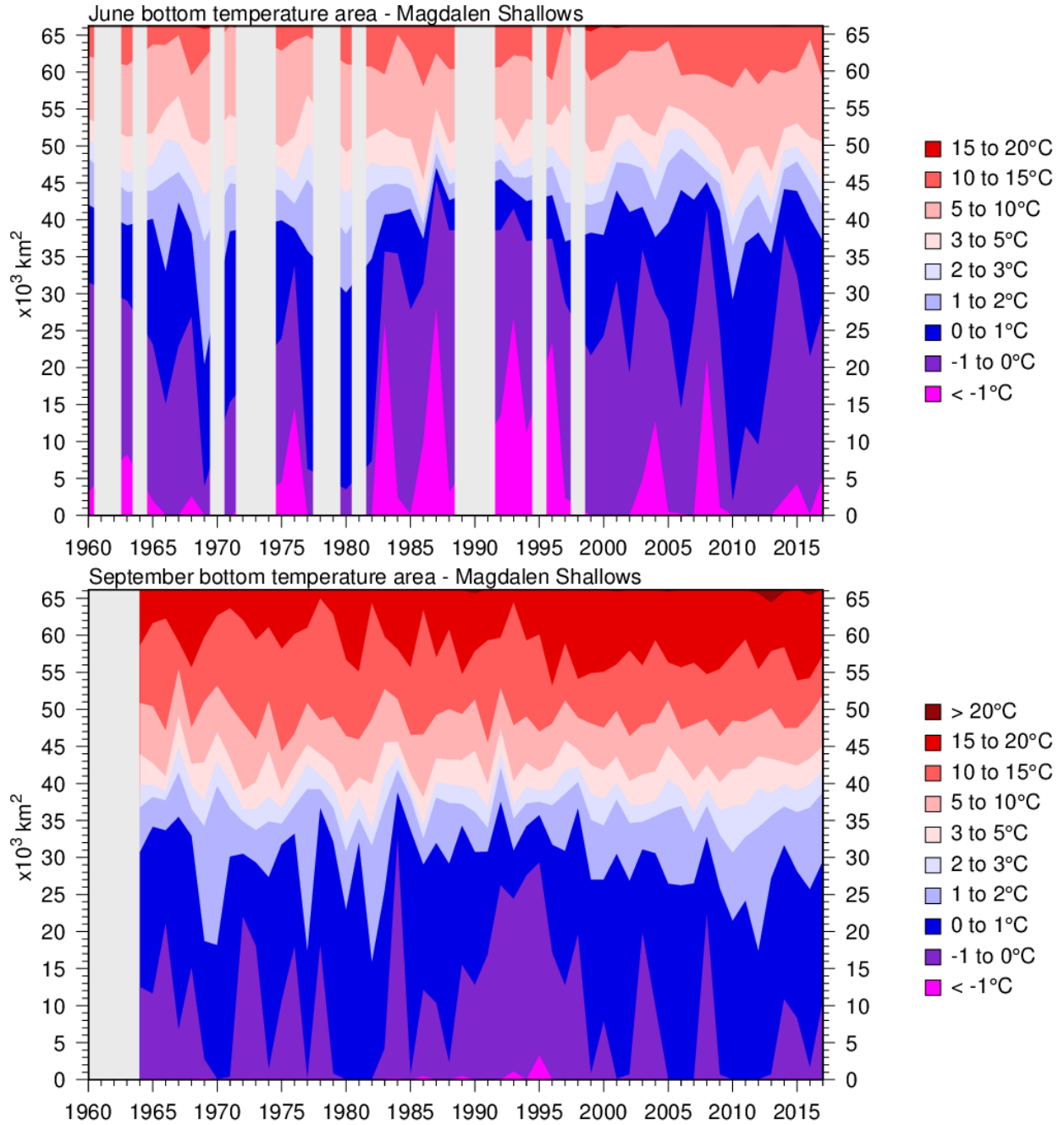


Figure 42. Time series of the bottom areas covered by different temperature bins in June (top) and August-September (bottom) for the Magdalen Shallows (region 8). Data are mostly from September for the bottom panel.

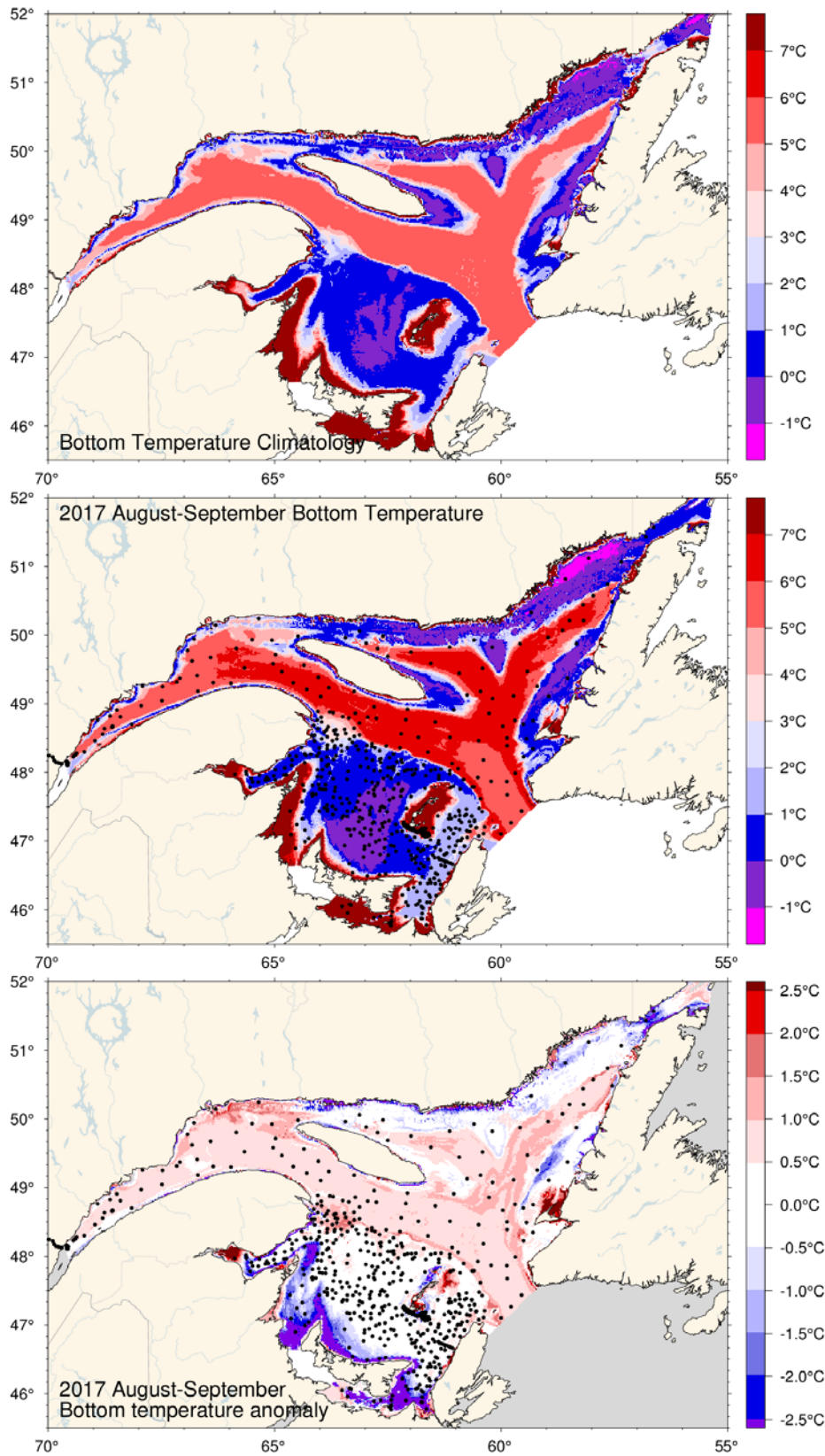


Figure 43. August-September bottom temperature climatology (top), 2017 observations (middle) and anomaly (bottom).

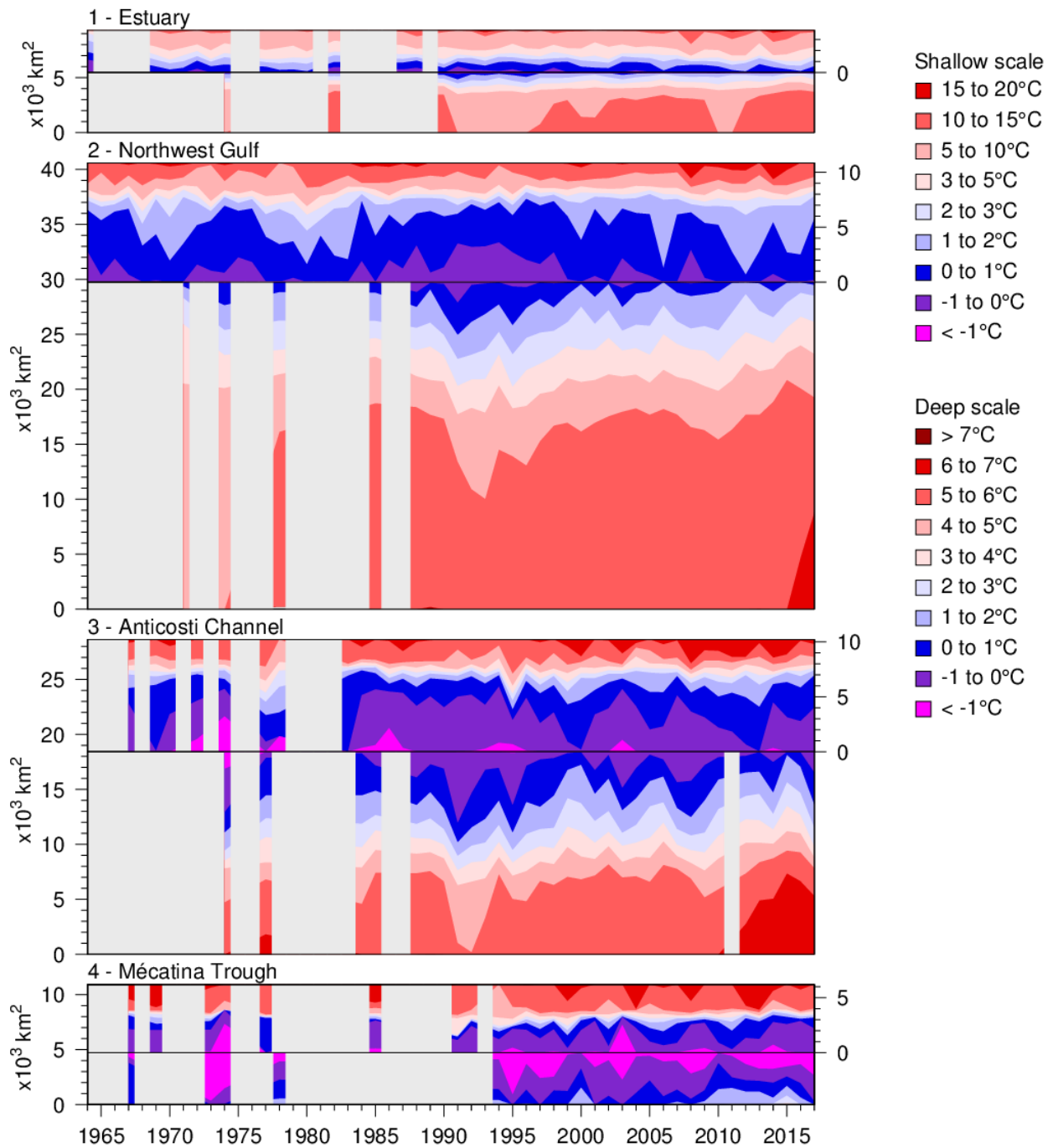


Figure 44. Time series of the bottom areas covered by different temperature bins in August and September for regions 1 to 4. The panels are separated by a black horizontal line into shallow (<100m) and deep (>100 m) areas to distinguish between warmer waters above and below the CIL. The shallow areas are shown on top using the area scale on the right-hand side and have warmer waters shown starting from the top end. The deep areas are shown below the horizontal line and have warmer waters starting at the bottom end. The CIL areas above and below 100 m meet near the horizontal line.

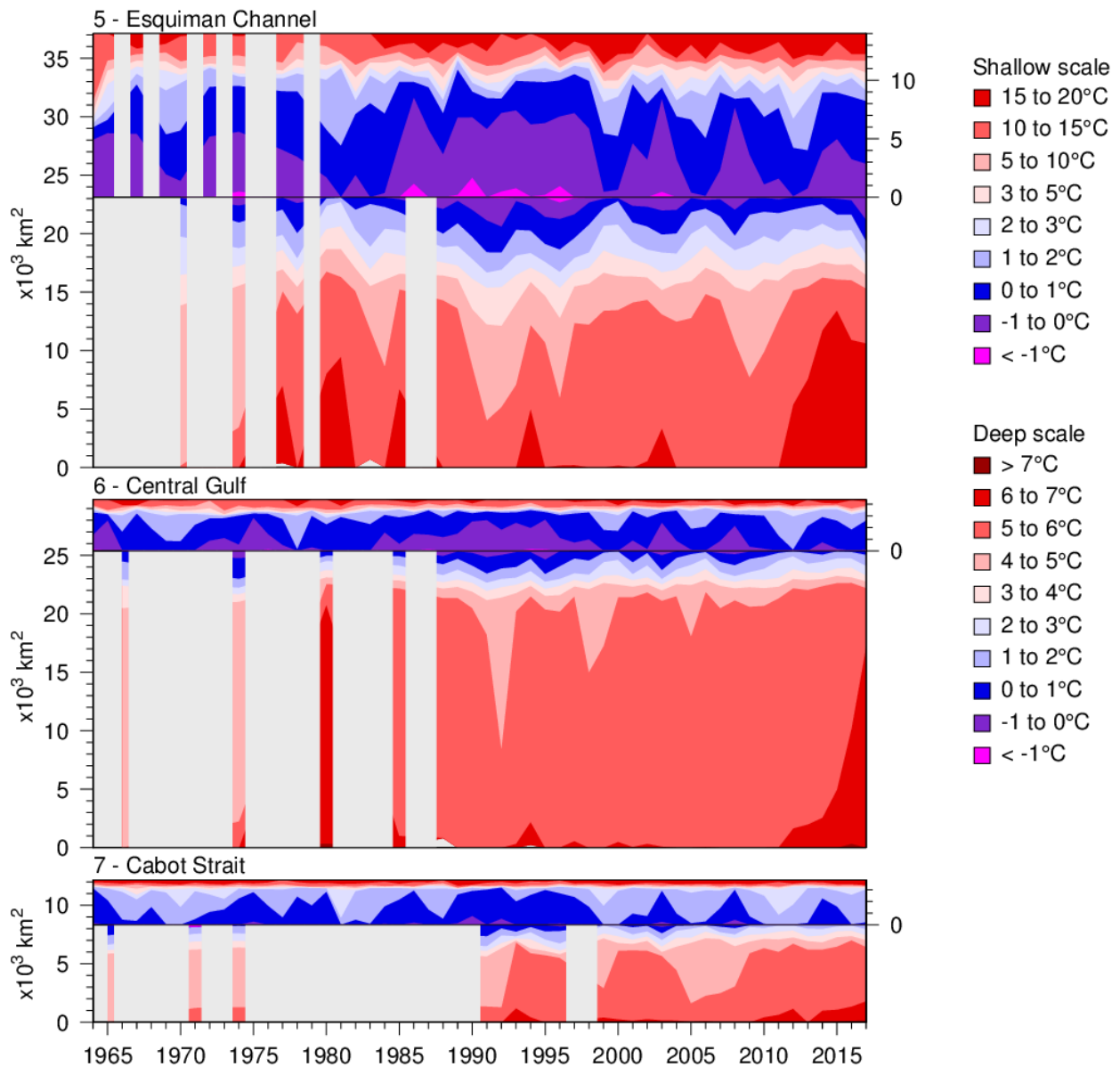


Figure 45. Time series of the bottom areas covered by different temperature bins in August and September for regions 5 to 7. The panels are separated into shallow (<100 m) and deep (>100 m) areas to distinguish between warmer waters above and below the CIL. See Figure 44 caption.

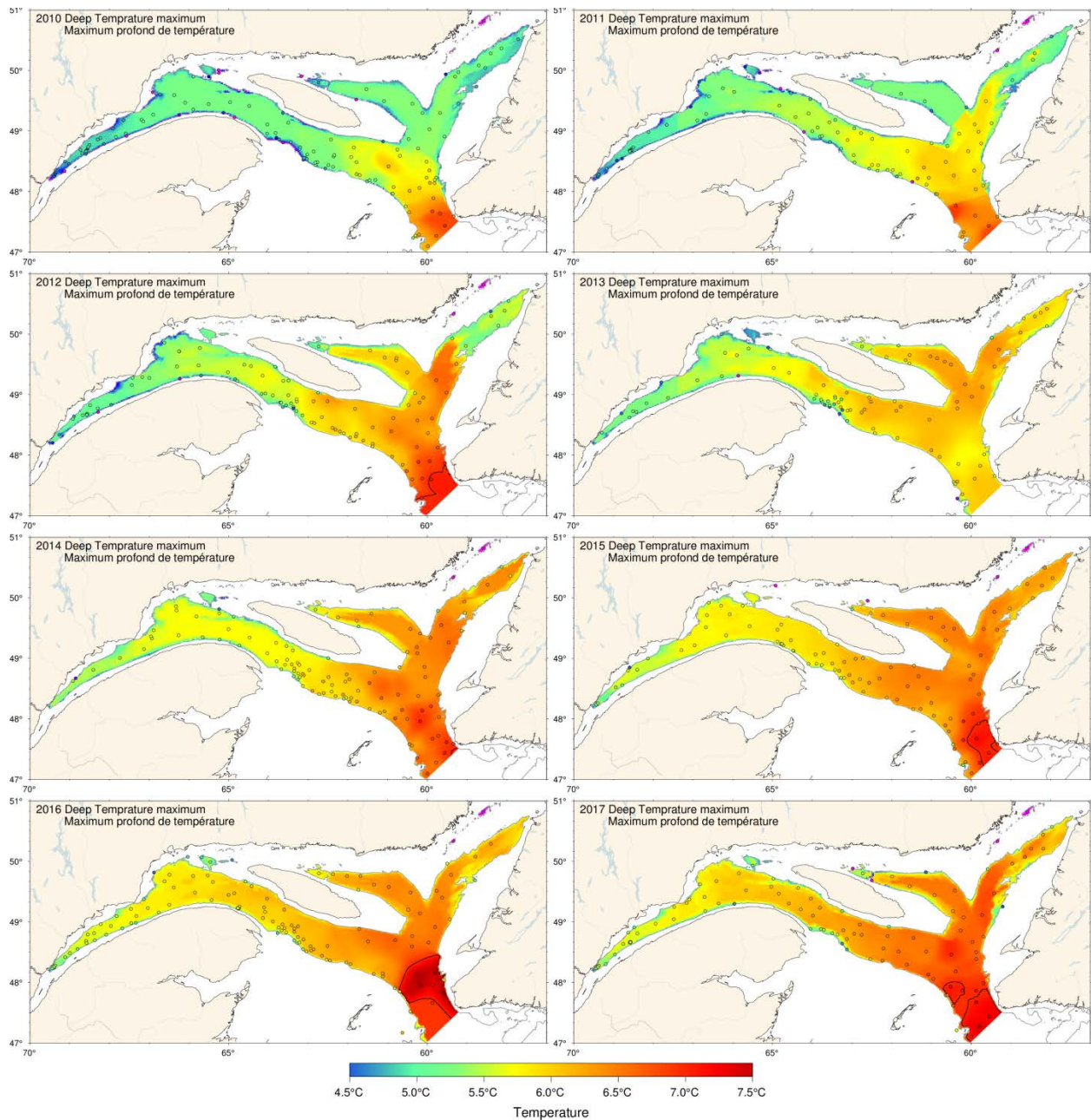


Figure 46. Map of the deep temperature maximum found typically between 200 and 300 m, 2010-2017. Maps are interpolated from August-September data available for each year. For 2012, 2013 and 2017, casts made in Cabot Strait during the fall survey were used to fill August sampling gaps.

	Gulf Avg T												Mean ± S.D.	
	150 m	200 m	250 m	Deep T max	300 m	Estuary	Northwest Gulf	Anticosti Channel	Esquiman Channel	Central Gulf	Cabot Strait	Laurentian Hermitage		Laurentian Mouth
	4.82	4.73	4.24	4.92	4.82	5.93	5.324	4.884	3.564	3.334	2.234	0.003	3.63	2.49°C ± 0.48
	4.91	4.89	4.23	2.62	4.91	7.56	6.334	4.864	4.994	6.244	0.234	8.22	4.22	4.42°C ± 0.44
	5.05	4.86	4.14	2.39	5.05	4.90	5.14	5.64	4.14	0.24	1.81	3.03	5.5	5.32°C ± 0.27
	5.01	4.97	4.97	4.28	5.01	7.33	5.944	8.844	3.334	3.13	8.94	4.30	3.66	5.45°C ± 0.16
	5.10	4.78	3.56	1.83	5.10	6.38	5.10	3.88	3.07	3.92	3.84	3.83	3.37	3.87°C ± 0.36
	5.06	4.80	4.12	2.65	5.06	6.99	6.404	8.94	4.014	4.88	3.35	3.91	3.55	4.31°C ± 0.38
	5.36	5.68	4.99	2.94	5.36	8.24	7.64	5.81	5.14	5.21	4.50	2.79	4.23	4.53°C ± 0.58
	5.44	5.06	4.23	2.77	5.44	6.79	5.84	4.61	4.44	4.44	4.44	4.44	4.23	4.89°C ± 0.58
	5.73	5.60	5.17	3.81	5.73	7.44	5.87	6.08	5.79	4.61	5.30	4.74	4.39	5.76°C ± 0.65
	6.00	5.93	5.18	3.25	6.00	6.58	6.18	5.76	5.38	5.66	4.87	4.81	3.97	6.31°C ± 0.91
	5.66	5.67	5.01	3.24	5.66	6.29	6.36	3.94	5.34	4.50	4.65	4.83	4.70	4.95°C ± 0.26
	5.52	5.33	4.41	2.78	5.52	5.24	4.88	4.62	4.10	5.00	3.85	4.54	4.70	5.24°C ± 0.23
	5.38	5.16	4.25	2.49	5.38	6.26	5.15	4.55	4.02	4.53	3.35	4.57	5.27	5.30°C ± 0.35
	5.33	5.23	4.52	2.92	5.33	7.16	6.33	5.20	4.63	4.77	4.32	4.25	4.31	5.59°C ± 0.23
	5.67	5.63	4.96	2.72	5.67	6.62	5.94	5.47	5.11	5.29	4.47	4.66	4.93	5.88°C ± 0.41
	5.76	5.69	4.87	2.55	5.76	6.94	6.48	5.34	5.21	5.00	4.47	4.92	4.93	4.97°C ± 0.23
	5.63	5.65	4.84	2.42	5.63	6.35	5.98	5.24	4.99	4.50	4.48	4.84	4.83	5.38°C ± 0.35
	5.63	5.61	4.82	2.52	5.63	6.34	5.63	5.59	4.71	5.04	4.66	4.74	4.29	5.59°C ± 0.23
	5.53	5.46	4.79	2.95	5.53	4.45	5.35	4.96	4.77	5.16	4.81	4.64	4.07	5.88°C ± 0.41
	5.37	5.11	4.18	2.22	5.37	5.95	5.13	4.13	2.94	3.14	4.40	3.95	3.83	5.93°C ± 0.34
	5.17	4.72	3.39	1.48	5.17	6.83	4.12	3.23	3.29	3.02	2.95	3.53	4.43	6.83°C ± 0.25
	5.11	4.70	3.33	1.38	5.11	4.74	5.21	4.09	3.29	3.00	2.95	3.53	4.43	5.93°C ± 0.34
	5.32	5.05	4.92	1.93	5.32	7.54	6.44	5.07	4.18	6.93	4.36	8.73	3.26	6.19°C ± 0.17
	5.67	5.62	5.48	4.43	5.67	5.12	6.05	4.99	4.60	4.83	4.49	3.73	3.50	5.56°C ± 0.19
	5.45	5.28	5.11	3.86	5.45	6.24	5.34	4.13	3.89	4.03	3.86	3.83	3.50	5.65°C ± 0.25
	5.78	5.73	4.83	3.93	5.78	5.78	5.64	4.18	3.63	3.56	3.54	3.81	3.33	5.82°C ± 0.36
	5.37	5.55	5.42	3.54	5.37	7.23	6.70	5.38	4.84	4.74	4.30	4.23	3.83	5.93°C ± 0.34
	5.35	5.35	5.25	4.28	5.35	6.41	5.68	4.67	4.39	4.51	3.80	4.16	3.84	6.03°C ± 0.36
	5.44	5.40	5.37	4.73	5.44	6.75	6.43	5.64	4.83	4.79	4.49	4.62	4.02	6.19°C ± 0.17
	5.53	5.52	5.42	4.61	5.53	6.25	5.85	5.16	4.77	4.69	4.14	4.52	4.03	6.31°C ± 0.91
	5.47	5.46	5.34	4.62	5.47	7.83	6.52	5.56	5.06	4.27	4.80	4.69	4.02	6.83°C ± 0.25
	5.59	5.59	5.57	4.76	5.59	5.49	5.03	4.85	4.68	4.94	4.27	4.44	4.07	6.83°C ± 0.25
	5.65	5.60	5.55	4.68	5.65	5.46	5.46	4.82	4.46	4.39	3.29	4.41	3.80	6.83°C ± 0.25
	5.64	5.60	5.47	4.30	5.64	5.46	5.46	4.82	4.46	4.39	3.29	4.41	3.80	6.83°C ± 0.25
	5.50	5.50	5.33	4.39	5.50	5.88	6.03	5.36	4.44	4.43	3.85	4.04	4.03	6.83°C ± 0.25
	5.30	5.56	5.48	4.91	5.30	5.84	5.92	4.75	0.75	0.74	4.64	4.64	4.28	6.83°C ± 0.25
	5.50	5.55	5.46	4.69	5.50	5.62	5.40	4.73	4.34	4.24	3.60	4.03	3.98	6.83°C ± 0.25
	5.41	5.33	5.24	4.25	5.41	8.01	6.49	4.96	4.30	4.11	3.65	4.03	3.86	6.83°C ± 0.25
	5.31	5.32	5.03	4.18	5.31	7.28	5.83	5.44	4.64	4.23	3.94	3.43	3.56	6.83°C ± 0.25
	5.54	5.51	5.39	4.52	5.54	8.13	6.26	5.81	4.72	4.54	4.27	4.10	3.88	6.83°C ± 0.25
	5.75	5.84	5.50	4.31	5.75	8.45	7.18	6.36	5.41	5.00	4.52	4.64	4.14	6.83°C ± 0.25
	5.75	5.84	5.50	4.31	5.75	8.22	5.89	5.43	4.23	3.94	3.57	4.49	4.04	6.83°C ± 0.25
	5.87	6.06	5.88	5.34	5.87	8.52	7.68	6.25	5.76	5.67	5.61	5.22	4.70	6.83°C ± 0.25
	6.02	6.19	6.06	5.60	6.02	8.68	7.61	6.15	5.77	5.87	5.61	5.22	4.70	6.83°C ± 0.25
	6.18	6.16	6.11	5.83	6.18	9.18	7.04	6.06	5.51	5.48	4.83	5.15	4.60	6.83°C ± 0.25
	6.27	6.28	6.04	5.02	6.27	8.69	7.29	5.84	5.31	5.10	4.14	4.32	4.56	6.83°C ± 0.25

Figure 47. Deep layer temperature. Gulf averages for temperature are shown for 150, 200, 250, 300 m, as well as for the deep temperature maximum usually found between 200 and 300 m. Regional averages are shown for 200 and 300m, and deep temperature maximum. The numbers on the right are the 1981–2010 climatological means and standard deviations. The numbers in the boxes are average temperatures. The colour-coding is according to the temperature anomaly relative to the 1981–2010 climatology of each region and depth.

		Mean ± S.D.													
Gulf Avg S	150 m	1.3	0.6	0.6	1.1	0.1	0.8	0.4	1.1	-0.8	1.5	1.6	0.8	0.8	33.45 ± 0.14
	200 m	-2.3	-1.7	-0.4	1.1	0.4	-1.2	-1.7	0.4	-2.3	0.6	-2.5	-0.1	-1.7	34.09 ± 0.11
	250 m	-1.7	-2.3	-1.4	-0.6	-0.8	-2.0	-0.5	-0.2	-2.2	0.7	0.8	2.1	1.0	34.48 ± 0.08
	300 m	0.6	0.9	0.6	0.7	0.7	0.8	2.1	1.0	-0.4	1.3	0.1	0.8	-0.8	34.65 ± 0.05
	Estuary	-3.0	-2.1	-2.5	-0.5	0.1	-0.6	0.8	-1.6	1.6	1.4	0.6	0.9	-0.5	
200-m Yearly Salinity	Northwest Gulf	0.9	-0.8	0.2	0.9	1.4	0.6	0.9	-0.5	2.1	1.4	0.6	0.9	-0.4	33.99 ± 0.16
	Anticosti Channel	-0.9	-0.1	0.4	0.9	1.0	1.6	-1.8	1.2	1.7	1.5	-0.2	0.0	-2.7	34.11 ± 0.11
	Mécatina Trough	-2.0	0.5	0.7	0.7	1.5	-0.2	1.4	0.0	2.7	1.7	1.4	0.0	1.4	33.95 ± 0.14
	Esquiman Channel	0.7	1.4	0.7	1.4	0.4	1.8	2.7	1.5	1.8	1.7	1.4	1.1	1.1	32.74 ± 0.18
	Central Gulf	0.4	1.5	1.9	1.8	0.4	0.5	-1.9	1.8	1.8	1.7	1.4	1.1	1.1	34.10 ± 0.15
	Cabot Strait	0.1	0.3	0.4	1.4	0.1	0.3	0.4	1.4	0.6	0.7	-0.1	2.1	1.9	34.10 ± 0.13
	Laurentian Hermitage	-0.1	0.1	0.3	0.1	0.7	-0.3	-0.4	0.2	0.5	0.5	1.8	0.5	1.2	34.17 ± 0.14
	Laurentian Mouth	0.7	-0.3	-0.4	0.2	1.5	0.1	0.4	0.4	0.6	0.6	-0.9	-0.2	-0.1	34.32 ± 0.15
	Estuary	-1.8	-1.7	1.8	0.5	-1.8	-1.7	1.8	0.5	0.2	1.4	0.7	1.7	1.7	34.42 ± 0.25
	Laurentian Mouth	-1.0	1.3	1.0	1.2	-0.1	1.6	0.5	2.2	2.2	1.2	0.7	0.6	1.2	
300-m Yearly Salinity	Estuary	0.1	-0.4	1.3	1.3	0.1	-0.4	1.3	1.3	1.3	0.1	-0.4	1.3	1.3	34.44 ± 0.09
	Northwest Gulf	-1.5	-1.4	-0.2	0.4	-1.5	-1.4	-0.2	0.4	-0.1	-0.4	-1.8	-0.4	-0.1	34.61 ± 0.06
	Central Gulf	-0.8	-2.1	-2.9	-2.0	-0.8	-2.1	-2.9	-2.0	-1.2	-0.2	-0.8	-0.9	-1.5	34.68 ± 0.06
	Cabot Strait	-0.2	-0.8	-0.9	-1.5	-0.2	-0.8	-0.9	-1.5	-1.3	0.5	0.7	-0.6	0.2	34.70 ± 0.06
	Laurentian Hermitage	0.1	-0.4	0.4	0.4	0.5	0.7	-0.6	0.2	0.1	0.1	-0.4	0.4	0.7	34.73 ± 0.06
	Laurentian Mouth	-0.5	0.4	0.4	0.4	-0.5	0.4	0.4	0.4	0.7	0.3	-0.3	-0.3	0.3	34.72 ± 0.08
	Estuary	0.1	-0.2	-0.6	-1.9	0.1	-0.2	-0.6	-1.9	-0.3	0.8	-1.5	-1.2	-1.2	
	Northwest Gulf	0.7	-2.1	-1.9	-2.3	0.7	-2.1	-1.9	-2.3	-2.1	-2.8	-1.7	-1.3	-3.2	
	Central Gulf	0.8	1.1	0.1	-0.1	0.8	1.1	0.1	-0.1	0.2	-0.9	-0.8	-0.4	-0.1	
	Cabot Strait	0.5	-0.1	-0.4	-0.3	0.5	-0.1	-0.4	-0.3	-0.1	0.2	-0.9	-0.8	-0.4	
Laurentian Hermitage	0.8	1.1	0.9	0.3	0.8	1.1	0.9	0.3	0.8	0.6	1.2	0.4	0.4		
Laurentian Mouth	0.9	0.2	-0.2	-0.1	0.9	0.2	-0.2	-0.1	0.2	0.8	0.1	-0.1	-0.1		
Estuary	0.4	0.8	-0.1	-0.2	0.4	0.8	-0.1	-0.2	-0.6	-0.6	-0.8	0.2	-0.2		
Northwest Gulf	1.1	0.2	0.9	0.8	1.1	0.2	0.9	0.8	0.6	1.1	0.8	0.1	0.4		
Central Gulf	-0.0	-0.4	0.0	0.3	-0.0	-0.4	0.0	0.3	0.6	-0.1	0.1	1.2	0.4		
Cabot Strait	0.0	0.5	-0.4	-0.4	0.0	0.5	-0.4	-0.4	-0.5	-0.9	-1.8	0.0	-0.2		
Laurentian Hermitage	0.7	0.7	0.6	-0.1	0.7	0.7	0.6	-0.1	-0.2	-0.5	-0.5	0.0	0.3		
Laurentian Mouth	1.0	1.4	1.3	1.5	1.0	1.4	1.3	1.5	1.0	0.5	1.9	1.3	0.3		
Estuary	-0.1	0.6	-0.1	0.8	-0.1	0.6	-0.1	0.8	-0.4	0.9	0.9	0.9	0.9		
Northwest Gulf	-0.7	-0.4	0.0	-0.5	-0.7	-0.4	0.0	-0.5	-0.7	0.2	-0.8	0.2	0.1		
Central Gulf	1.2	-0.3	0.3	-0.3	1.2	-0.3	0.3	-0.3	-0.4	-0.1	-0.1	-0.1	-0.1		
Cabot Strait	0.7	-1.2	0.5	-1.3	0.7	-1.2	0.5	-1.3	0.0	-0.1	-1.0	-0.8	-0.8		
Laurentian Hermitage	1.7	1.0	1.4	0.1	1.7	1.0	1.4	0.1	-0.7	0.5	-0.5	-0.2	0.2		
Laurentian Mouth	2.0	1.9	1.9	1.1	2.0	1.9	1.9	1.1	0.2	1.0	0.4	0.7	0.2		
Estuary	1.2	-0.4	0.2	0.6	1.2	-0.4	0.2	0.6	-0.1	-0.6	-0.1	-0.8	-0.5		
Northwest Gulf	1.4	1.8	1.0	1.3	1.4	1.8	1.0	1.3	0.7	1.2	0.4	-0.1	-0.2		
Central Gulf	1.6	2.0	1.4	1.7	1.6	2.0	1.4	1.7	1.5	1.4	2.1	1.4	0.9		
Cabot Strait	2.0	1.4	0.8	0.6	2.0	1.4	0.8	0.6	0.3	0.2	0.2	0.6	0.3		
Laurentian Hermitage	1.8	1.8	0.1	-0.1	1.8	1.8	0.1	-0.1	-0.6	-0.2	-1.4	-0.6	0.0		
Laurentian Mouth	3.1	3.5	1.8	1.2	3.1	3.5	1.8	1.2	0.2	-0.1	-0.1	-0.5	-1.2		

Figure 48. Deep layer salinity. Gulf averages for salinity are shown for 150, 200, 250, and 300 m. Regional averages are shown for 200 and 300m. The numbers on the right are the 1981–2010 climatological means and standard deviations. The numbers in the boxes are normalized anomalies.

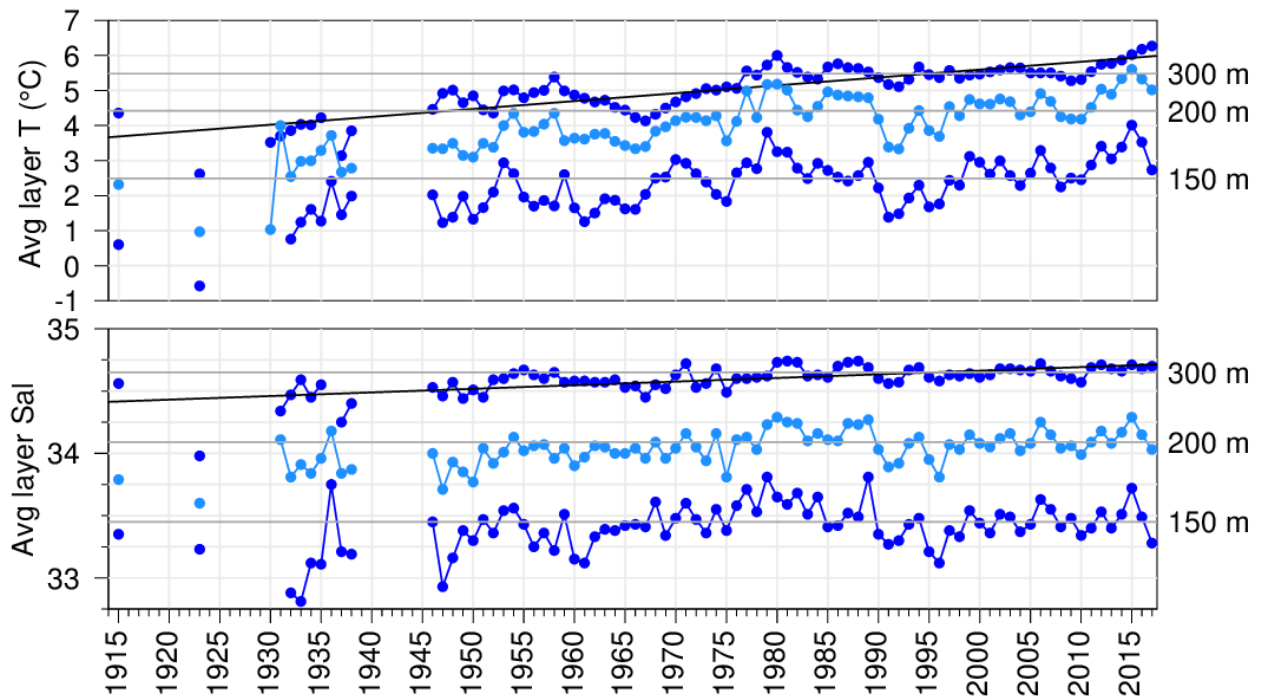


Figure 49. Layer-averaged temperature and salinity time series for the Gulf of St. Lawrence. The temperature and salinity panels show the 150 m, 200 m, and 300 m annual averages and the horizontal lines are 1981–2010 means. Sloped lines show linear regressions for temperature and salinity at 300 m of respectively 2.2°C and 0.3 per century.

March/mars 2017

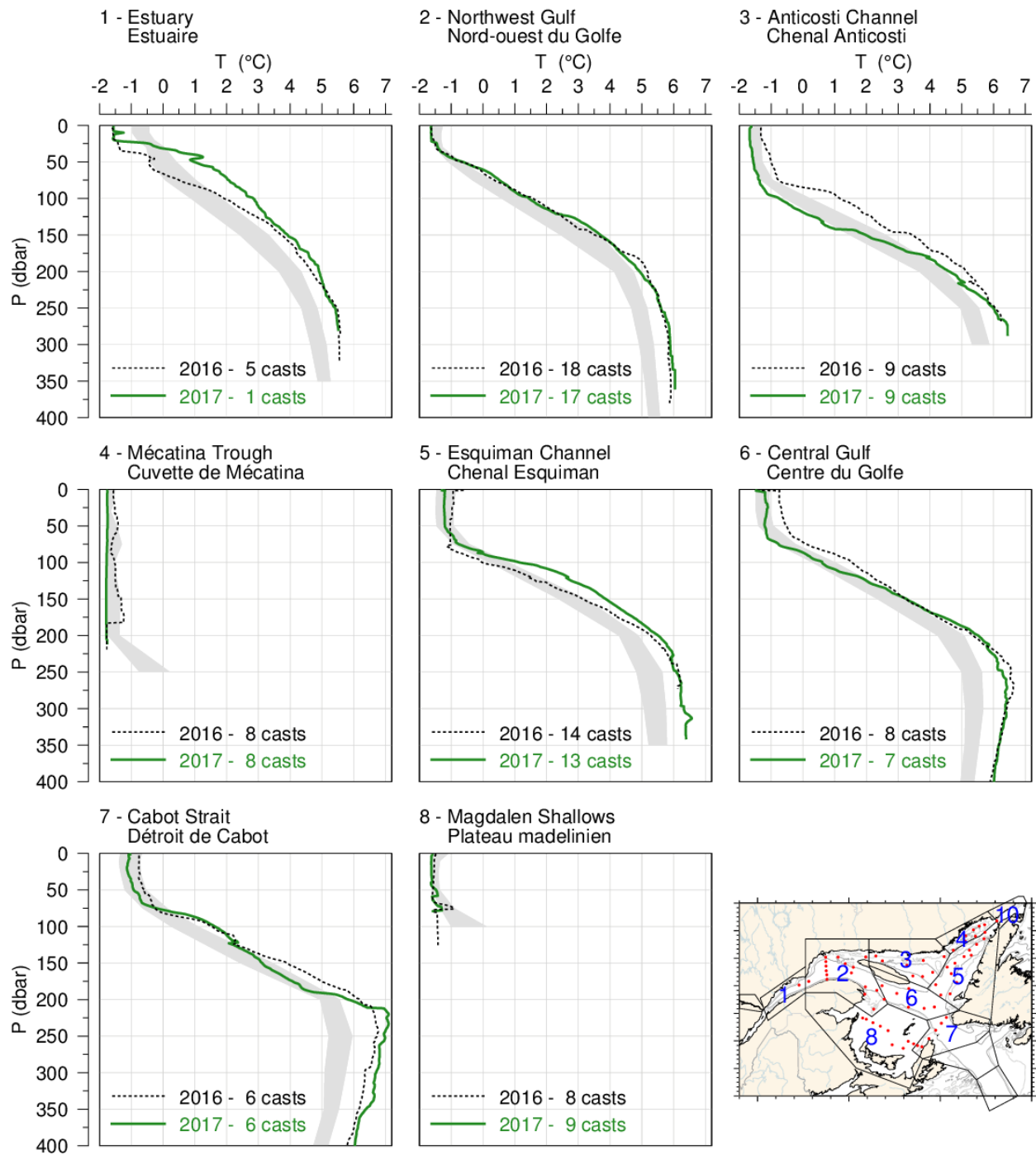


Figure 50. Mean temperature profiles observed in each region of the Gulf during the March 2017 survey. The shaded area represents the 1981–2010 (but mostly 1996–2010) climatological monthly mean \pm 0.5 SD. Mean profiles for 2016 are also shown for comparison.

June/juin 2017

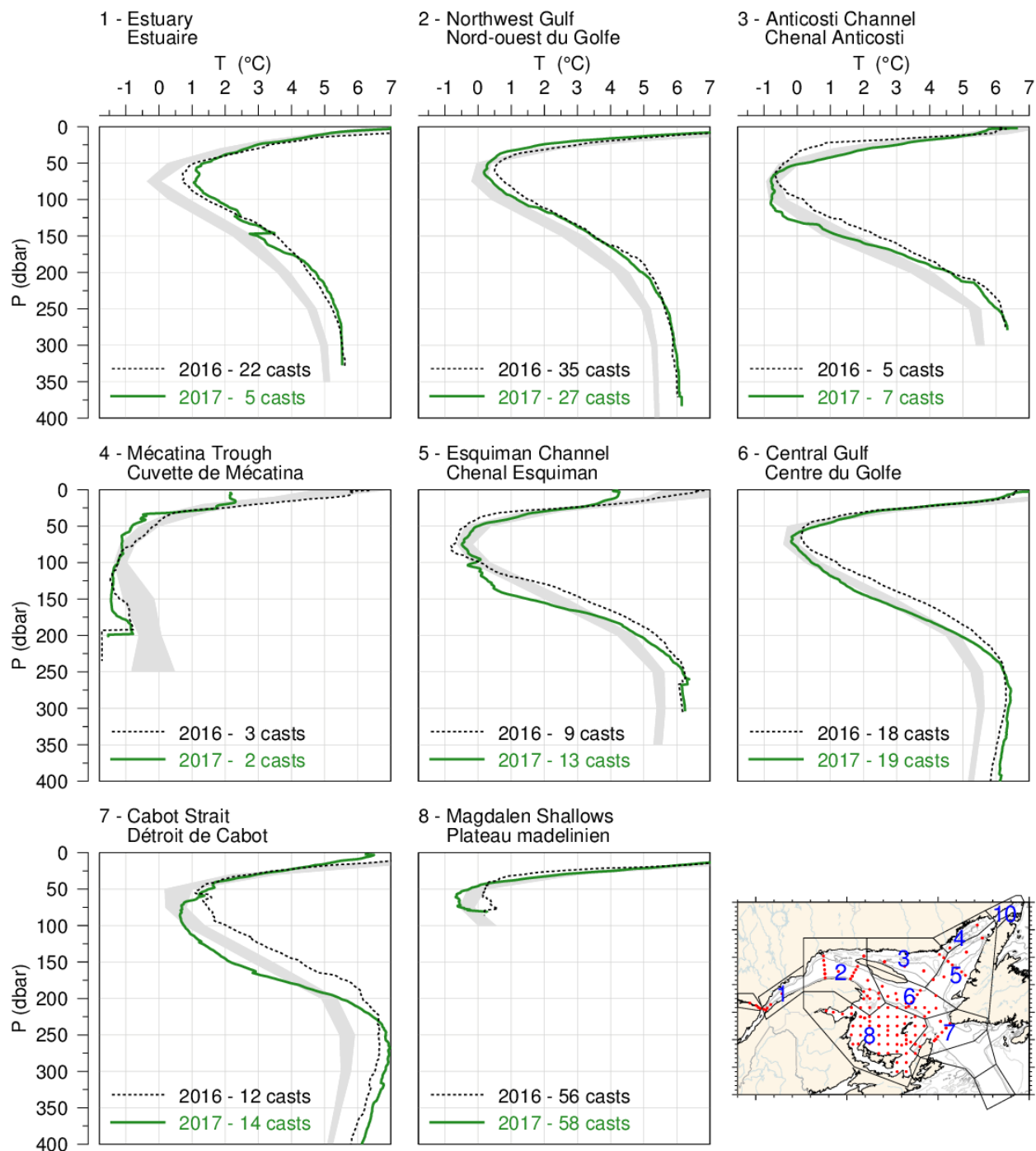


Figure 51. Mean temperature profiles observed in each region of the Gulf during June 2017. The shaded area represents the 1981–2010 climatological monthly mean ± 0.5 SD. Mean profiles for 2016 are also shown for comparison.

August-September 2017

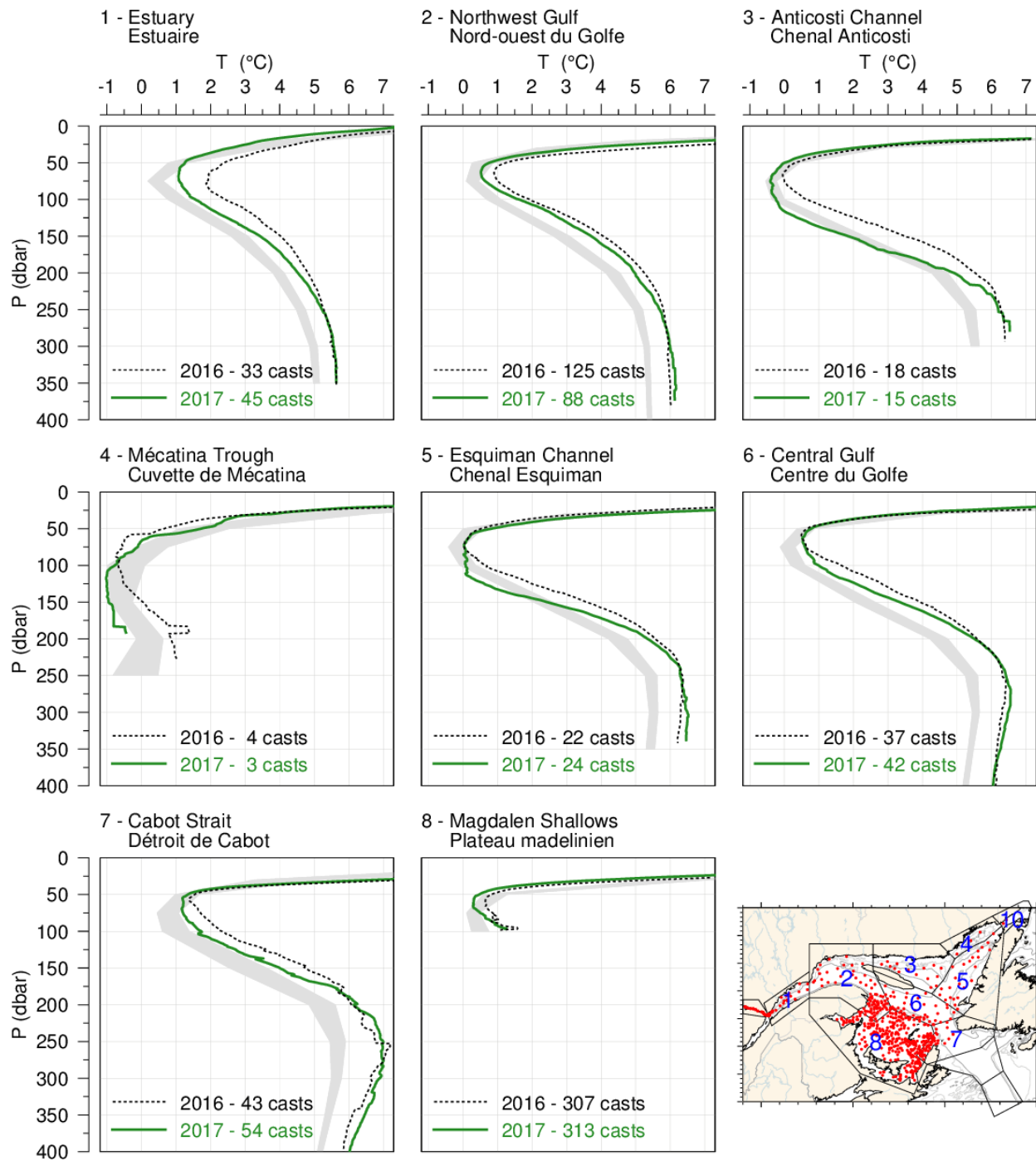


Figure 52. Mean temperature profiles observed in each region of the Gulf during August and September 2017. The shaded area represents the 1981–2010 climatological monthly mean \pm 0.5 SD for August for regions 1 through 7 and for September for region 8. Mean profiles for 2016 are also shown for comparison.

November 2017

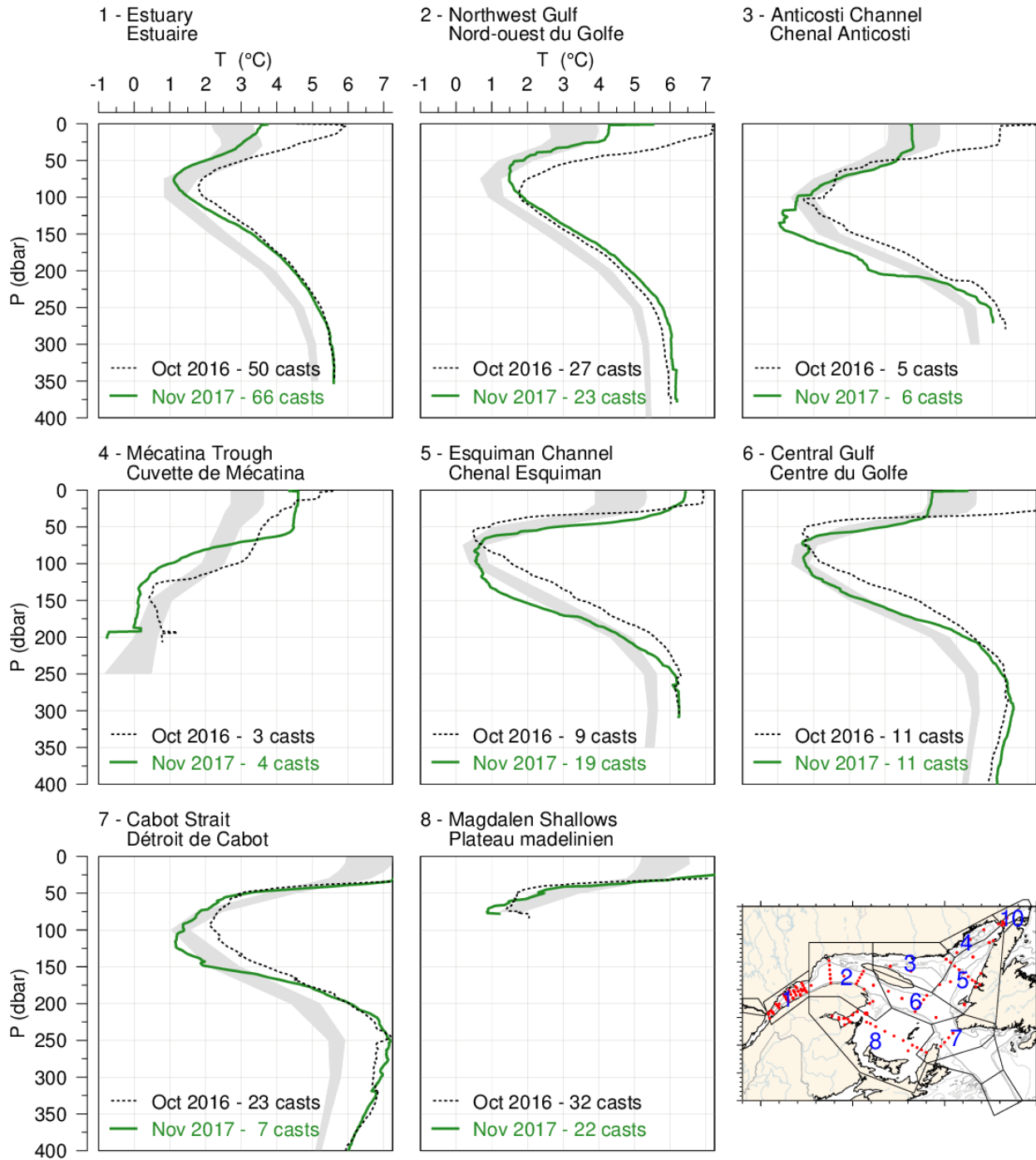


Figure 53. Mean temperature profiles observed in each region of the Gulf during the November 2017 AZMP survey. The shaded area represents the 1981–2010 climatological monthly mean ± 0.5 SD. Mean profiles for 2016 are also shown for comparison.

Figure 55. Depth-layer monthly average stratification and salinity summary for months during which the eight Gulf-wide oceanographic surveys took place in 2016 and 2017. Stratification is defined as the density difference between 50 m and the surface and its colour-coding is reversed (blue for positive anomaly).

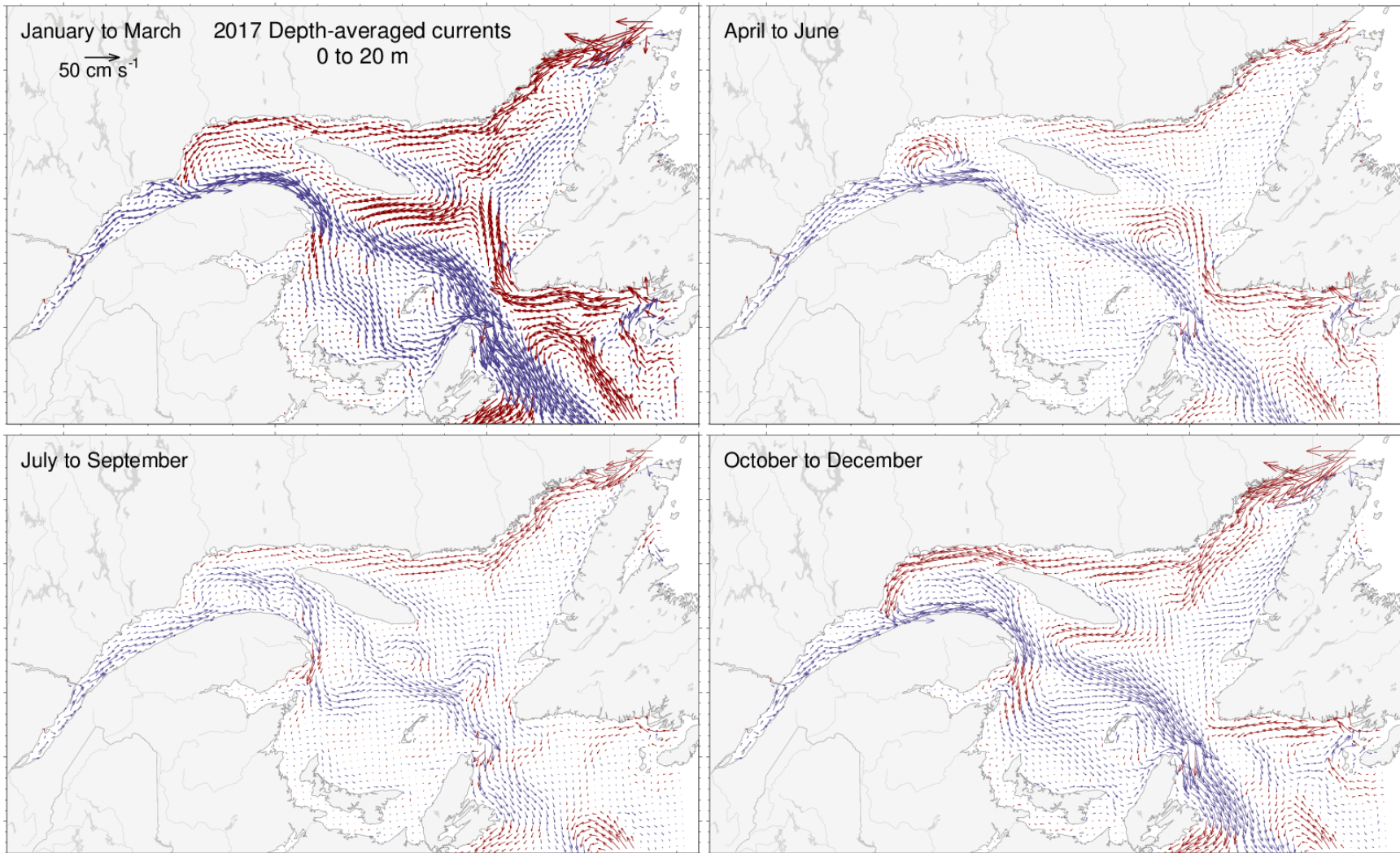


Figure 56. Depth-averaged currents from 0 to 20 m for each three-month period of 2017. Vectors drawn in blue are towards the East and those drawn in red are towards the West.

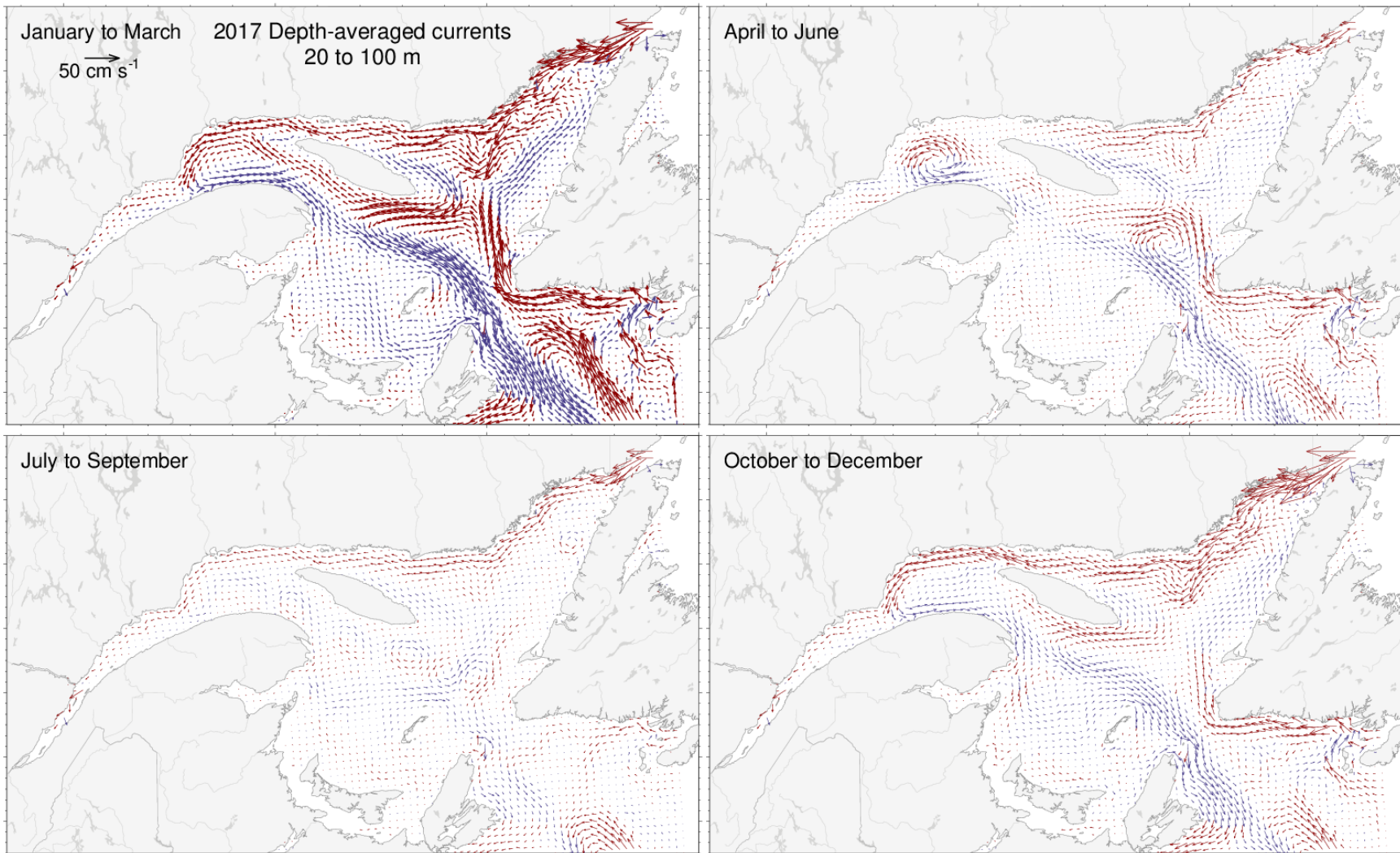


Figure 57. Depth-averaged currents from 20 to 100 m for each three-month period of 2017. Vectors drawn in blue are towards the East and those drawn in red are towards the West.

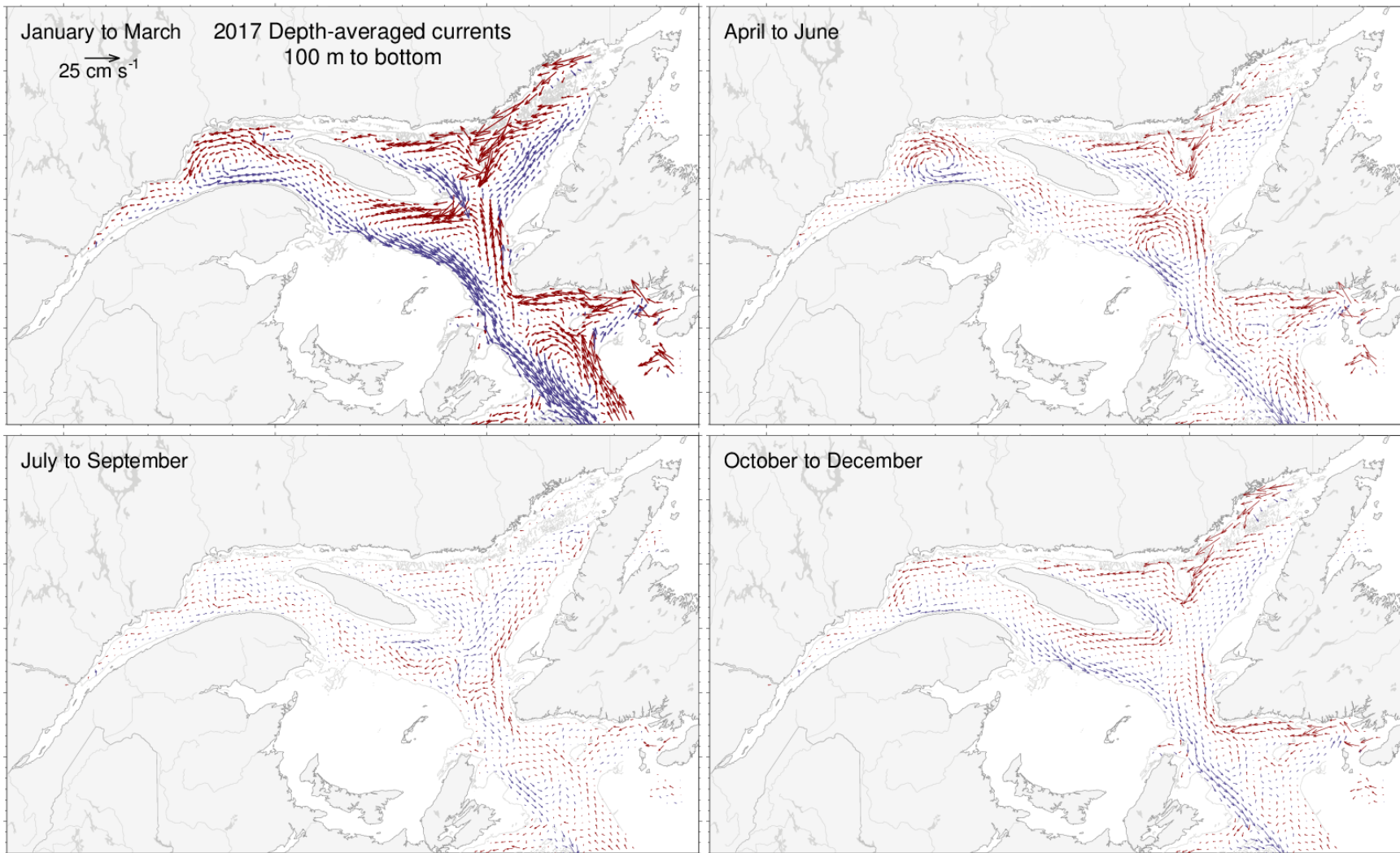


Figure 58. Depth-averaged currents from 100 m to the bottom for each three-month period of 2017. Vectors drawn in blue are towards the East and those drawn in red are towards the West.

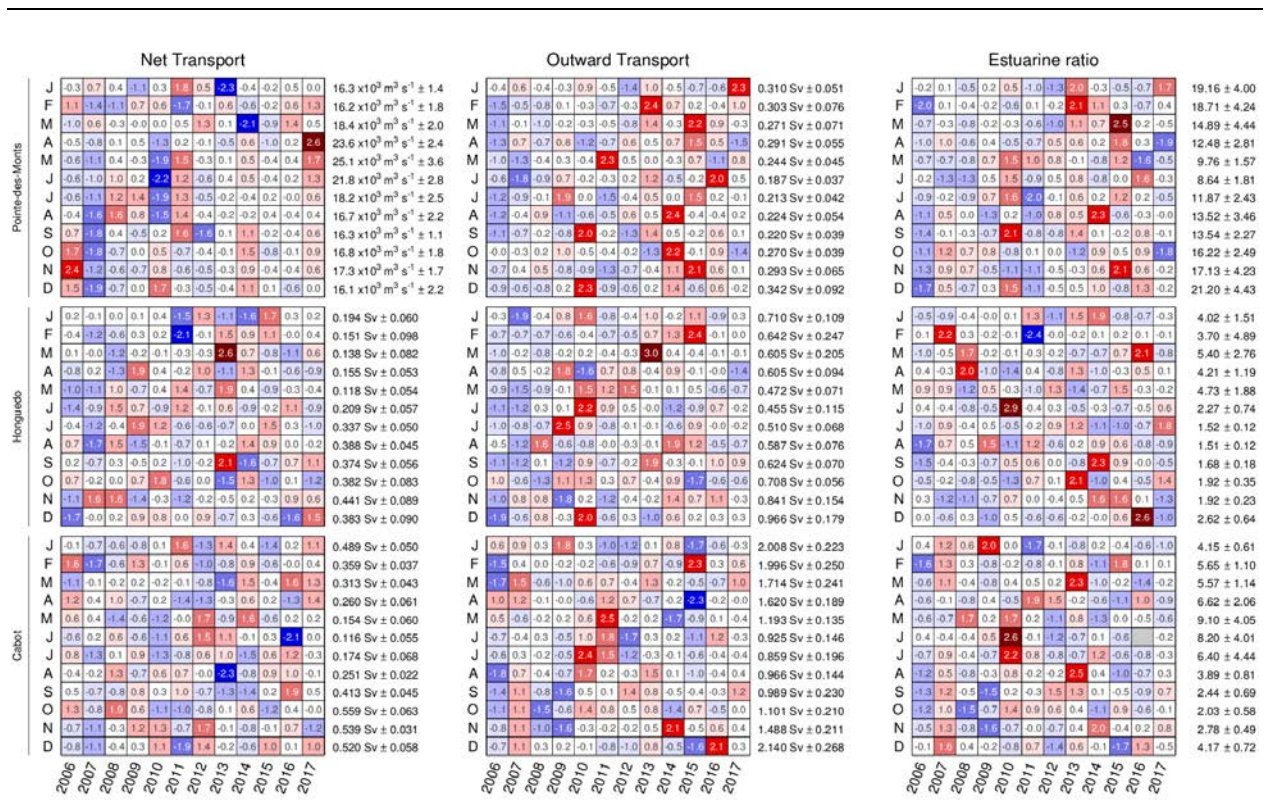


Figure 59. Monthly averaged modelled transports and estuarine ratio across sections of the Gulf of St. Lawrence since 2006. The numbers on the right are the 2006–2017 means and standard deviations. The numbers in the boxes are normalized anomalies. Colours indicate the magnitude of the anomaly. Sv (Sverdrup) are units of transport equal to $10^6 \text{ m}^3 \text{ s}^{-1}$.

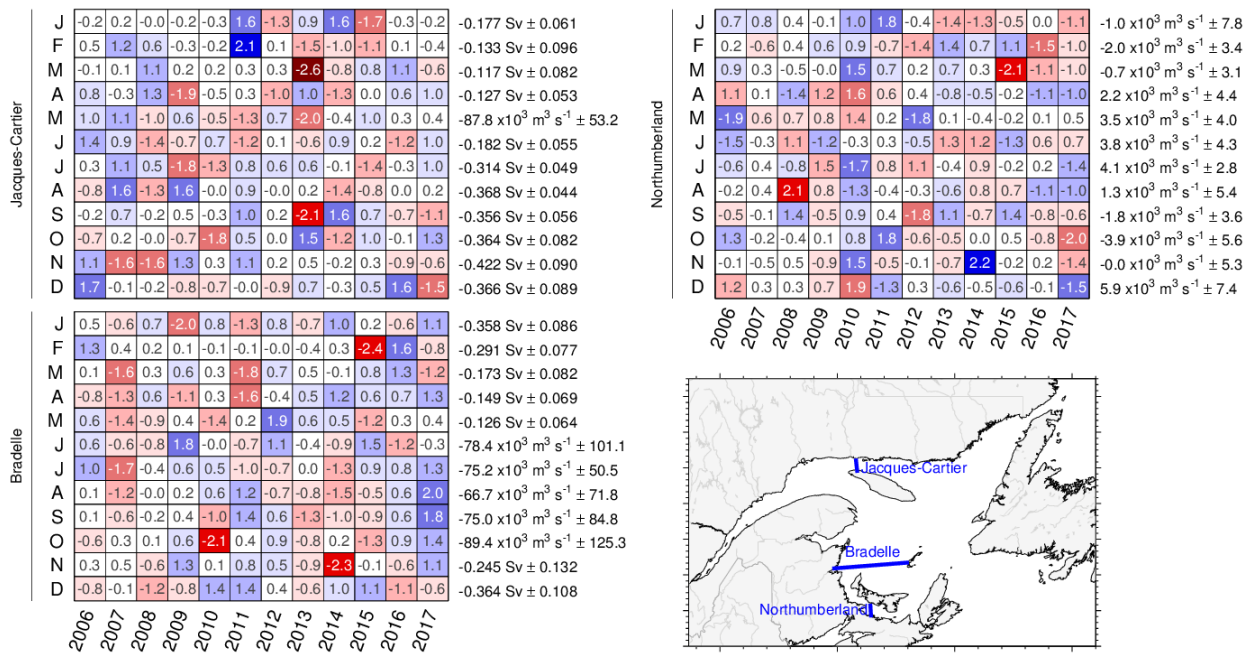


Figure 60. Monthly averaged modelled transports across sections of the Gulf of St. Lawrence since 2006. The numbers on the right are the 2006–2017 means and standard deviations, with positive values toward east and north. The numbers in the boxes are normalized anomalies. Colours indicate the magnitude of the anomaly (e.g., negative anomalies are still shown in red when the mean transport is negative across the section).

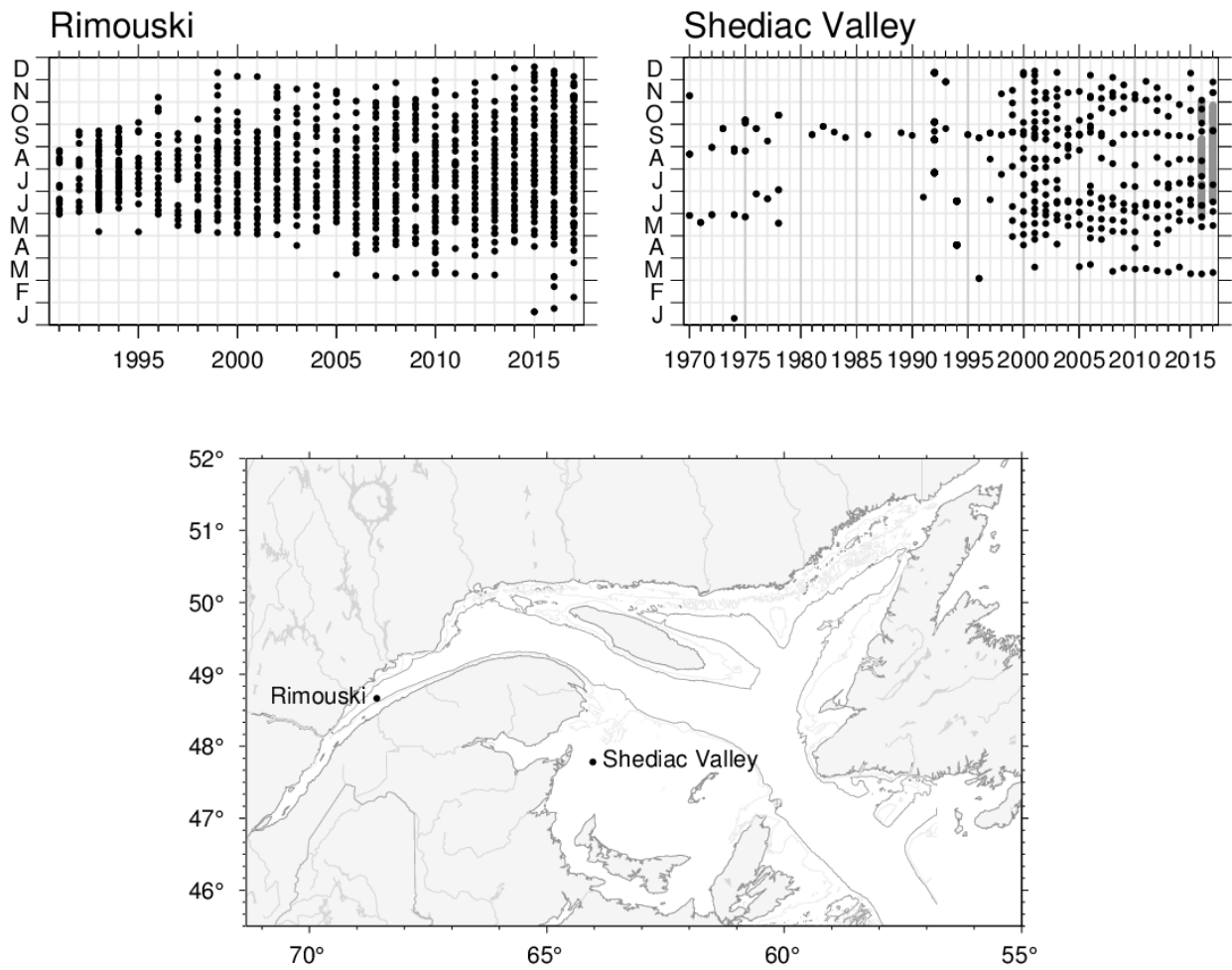


Figure 61. Sampling frequency and positions of the AZMP stations Rimouski and Shediac Valley. Gray overlay in 2017 at Shediac Valley shows span of 866 temperature and salinity profiles made by an automatic oceanographic buoy.

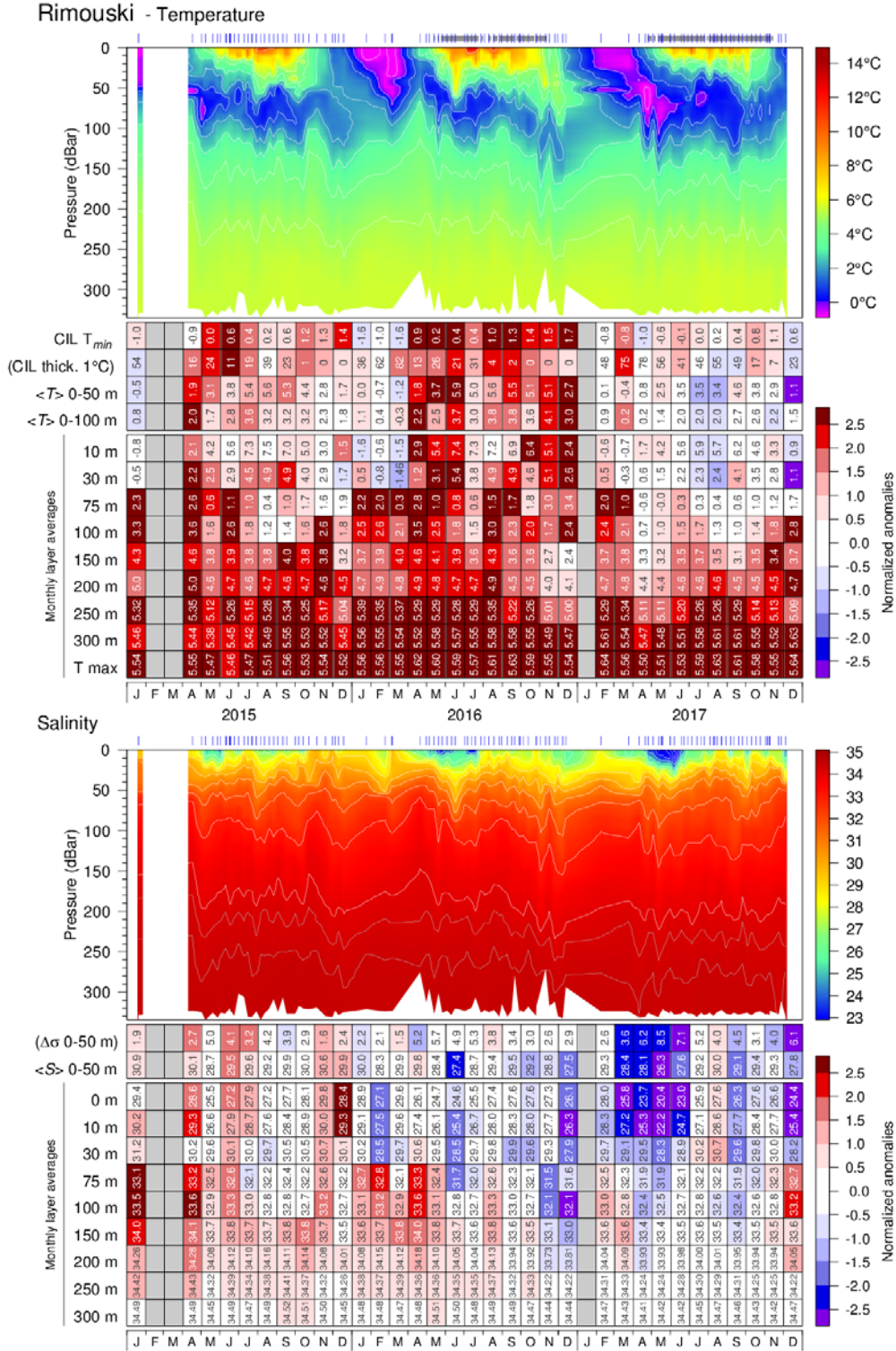
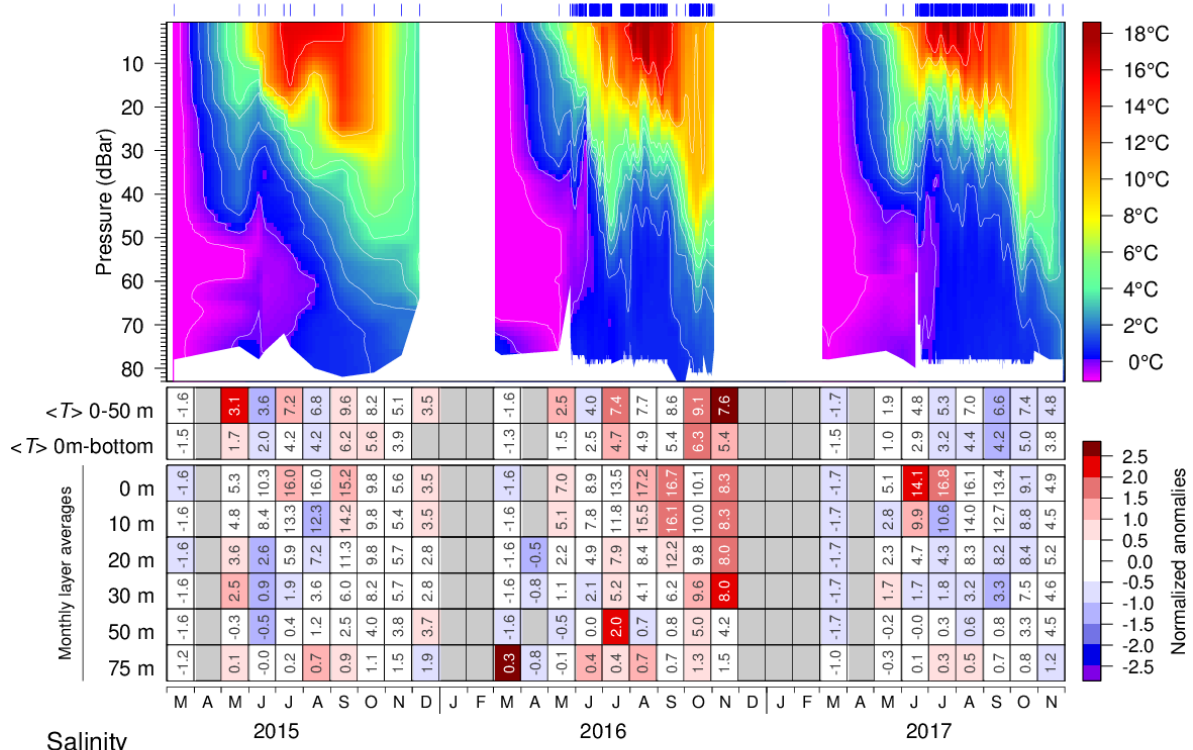


Figure 62. Isotherm (top) and isohaline (bottom) time series at the Rimouski station; tick marks above indicate sample dates and shaded area indicates casts made by a Viking automatic buoy. The scorecard tables are monthly layer averages colour-coded according to the anomaly relative to the 1991–2010 monthly climatology for the station (yearly climatology for 250 m and deeper). Thickness of the CIL and stratification have reversed colour codes where red indicates thinner CIL (warmer water) and less stratification (higher surface salinity).

Shediac Valley - Temperature



Salinity

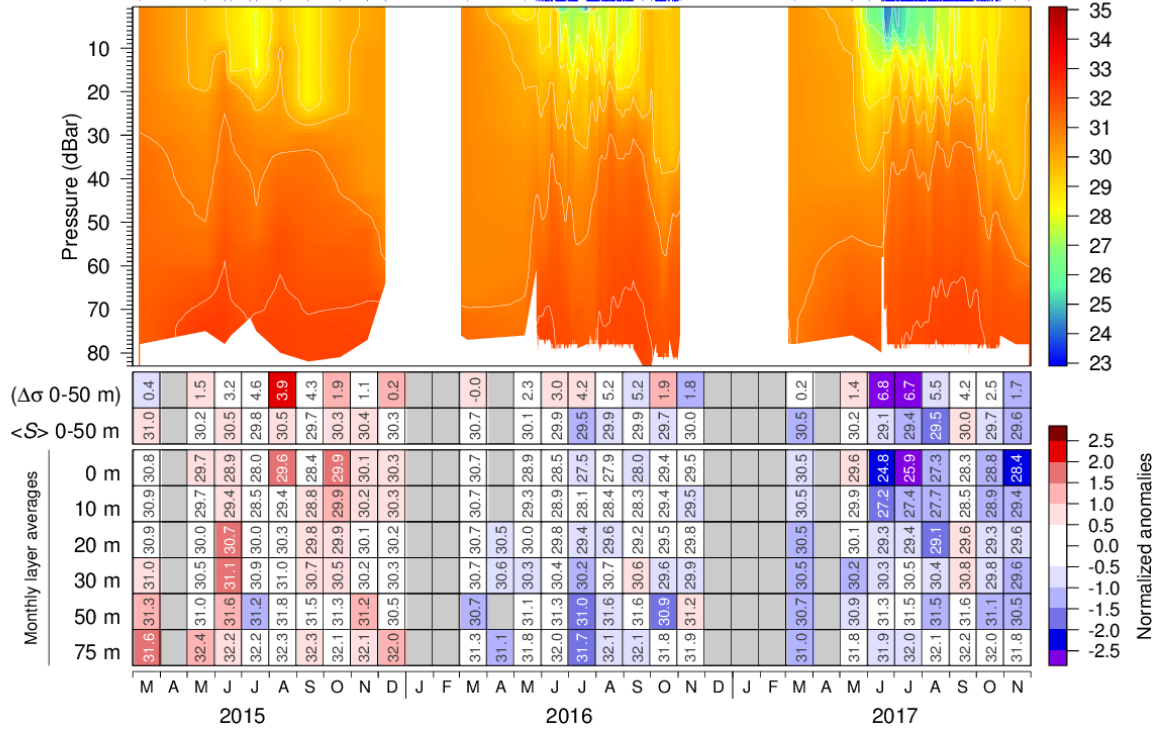


Figure 63. Isotherm (top) and isohaline (bottom) time series at the Shediac Valley station; tick marks above indicate sample dates (including from automatic buoy starting in 2016). Scorecard tables are monthly layer averages colour-coded according to the anomaly relative to the 1981–2017 monthly climatology for the station (input to climatology is sparse prior to 1999). The 10, 20, 30 and 75 m monthly layer averages for June–September 2015 are from mooring data. Internal tide oscillations are smoothed out.

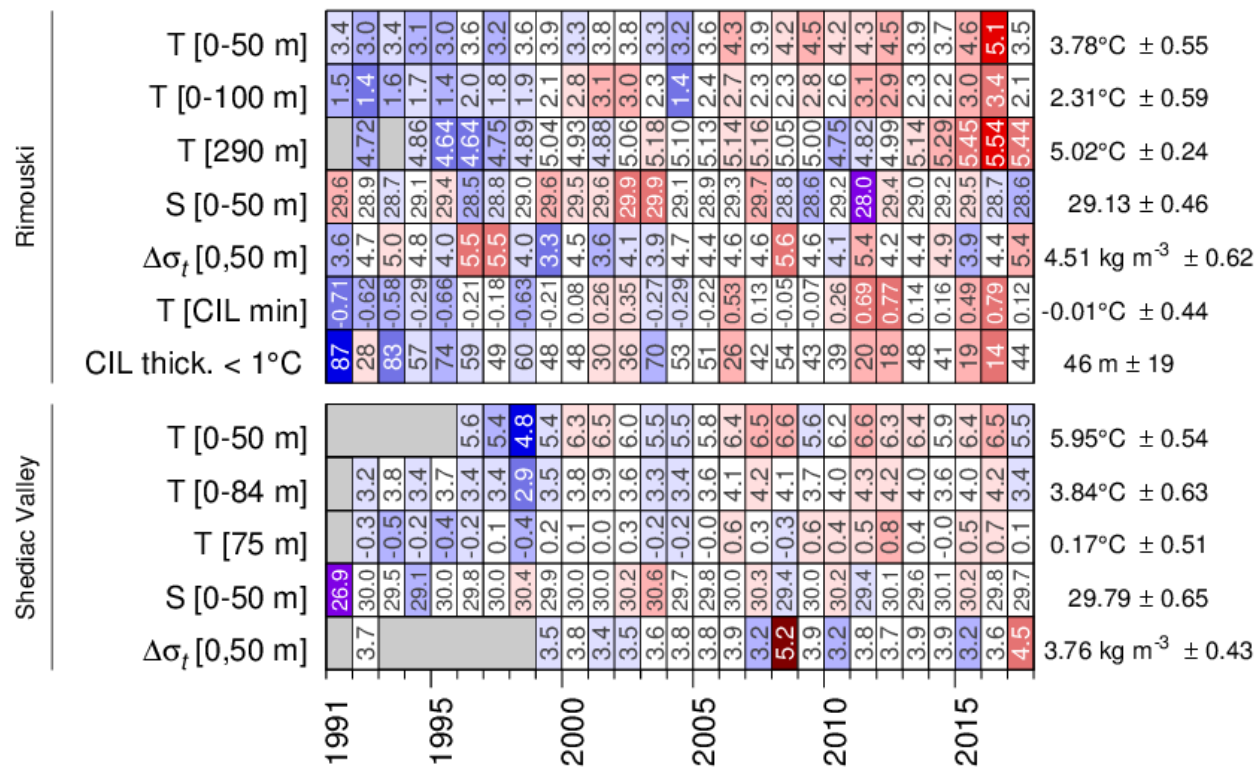


Figure 64. May to October temperature and salinity layer averages, stratification (expressed as the density difference between 0 and 50 m), and CIL temperature minimum and thickness ($T < 1^\circ\text{C}$) for high frequency monitoring stations. Numbers in panels are monthly average values colour-coded according to the anomaly relative to the 1991–2017 timeseries. Three months of anomaly data, between May and October, are required to show an average anomaly for any given year, except for deep water temperature at Rimouski station. Temperatures at 290 m and 75 m at Rimouski station and Shediac Valley station are considered to represent near-bottom temperatures.

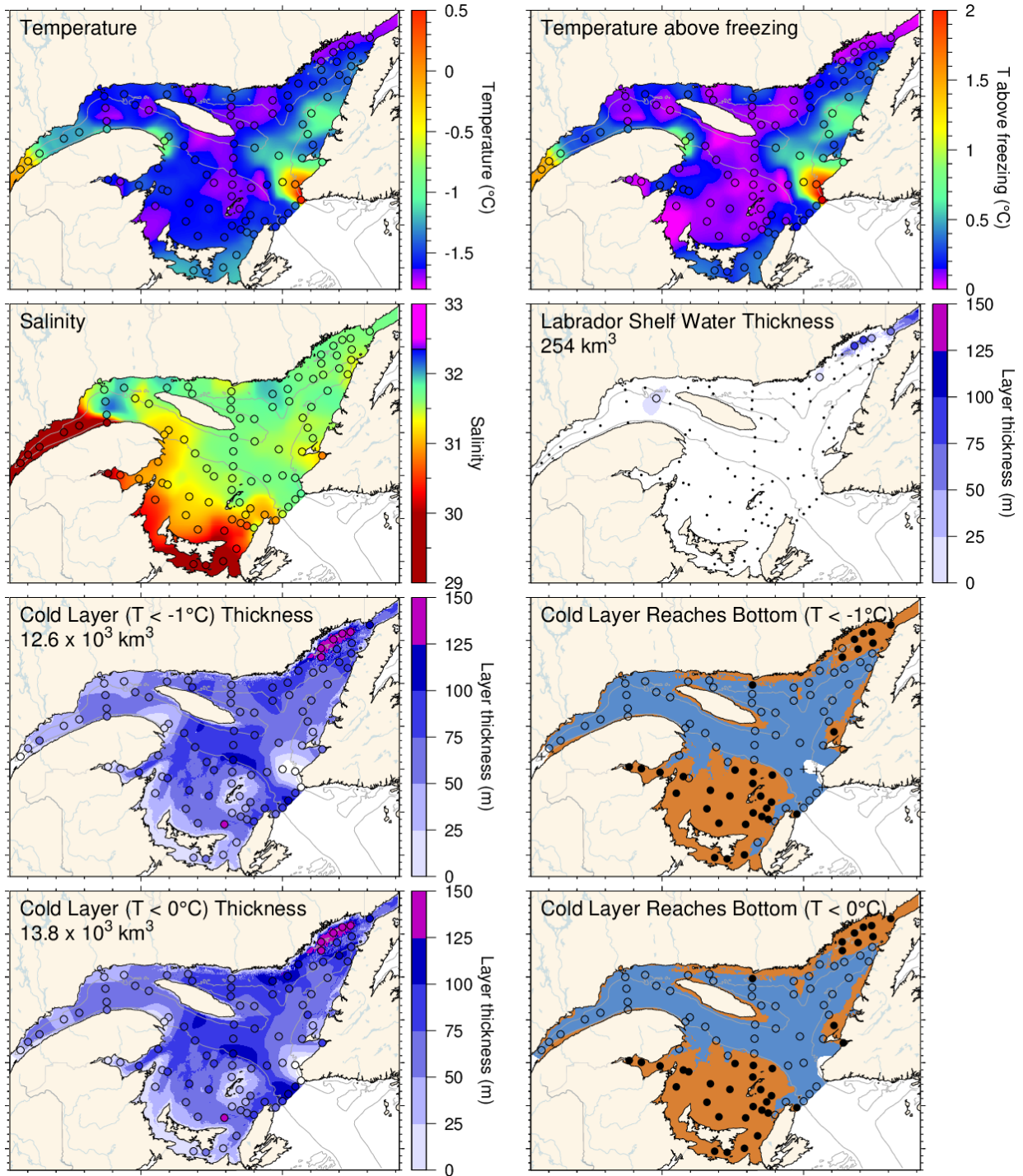


Figure 65. March 2018 surface cold layer characteristics: surface water temperature (upper left), temperature difference with the freezing point (upper right), salinity (second row left), estimate of the thickness of the Labrador Shelf water intrusion (second row right), and cold layer ($T < -1^{\circ}\text{C}$ and $< 0^{\circ}\text{C}$) thicknesses and where they reach bottom. The symbols are coloured according to the value observed at the station, using the same colour palette as the interpolated image. A good match is seen between the interpolation and the station observations where the station colours blend into the background.

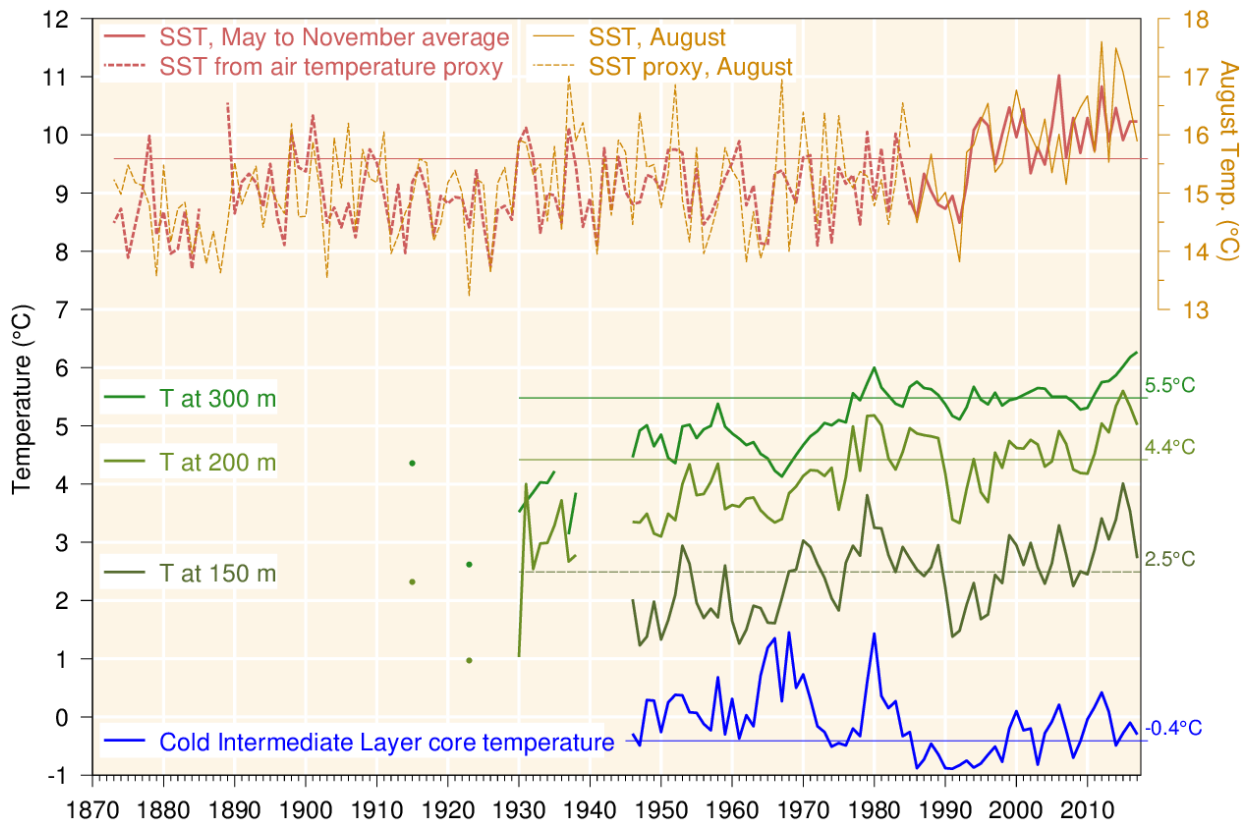


Figure 66. Water temperatures in the Gulf of St. Lawrence. May–November SST averaged over the Gulf excluding the Estuary (1985–2017, red line), completed by a proxy based on April–November air temperature (1873–1984, red dashed line; average of all AHCCD stations in Figure 4 but excluding Estuary stations at Baie Comeau and Mont-Joli). August SST is shown using temperature scale offset by 6°C; its proxy is based on the average air temperature in July and August. Layer-averaged temperature for the Gulf of St. Lawrence at 150, 200 and 300 m (green lines). Cold intermediate layer minimum temperature index in the Gulf of St. Lawrence (blueline). SST air temperature proxy is similar to that of Galbraith et al. (2012). Climatological averages based on the 1981-2010 period are indicated by thin lines labeled on the right side. Figure adapted from Benoit et al. (2012).

	1971	1975	1980	1985	1990	1995	2000	2005	2010	2015	Mean ± S.D.	
Surface												
SST, GSL August average	-0.7	-1.0	0.0	1.9	-0.1	-0.3	-4.8	-0.6	0.4	-2.3	-1.5	15.61°C ± 0.75
SST, GSL May-Nov average	0.9	-0.6	-1.0	-0.5	1.0	-5.1	-0.8	0.8	-2.2	-1.3	-1.3	9.61°C ± 0.66
(SST, Spring timing)	1.6	0.0	-0.9	-0.3	1.0	-1.2	-0.2	-0.0	-0.7	-0.4	-2.5	27.2 w ± 1.2
SST, fall timing	3.8	-1.8	-0.0	-1.7	-0.3	-3.8	-1.8	-0.4	-0.2	-0.1	-0.4	37.9 w ± 1.2
Sum of standardized anomalies	1.0	-1.0	0.0	1.9	-0.1	-0.3	-4.8	-0.6	0.4	-2.3	-1.5	
Intermediate												
(Ice, max volume)	1.0	-1.0	0.0	1.9	-0.1	-0.3	-4.8	-0.6	0.4	-2.3	-1.5	62.3 km ³ ± 25.5
GSL, summer CIL Index	0.8	0.6	-0.1	0.4	0.4	-0.9	-0.2	0.1	0.6	1.3	-0.9	-0.41°C ± 0.39
(sGSL, Sep. T<1°C Btm Area)	-0.1	-0.7	-0.6	-0.3	-0.3	0.5	1.4	0.4	-0.1	0.5	-1.3	30.0 ± 4.8 (x10 ³ km ²)
Bottom temp., Magdalen Shallows, Sep.	1.3	-0.1	0.7	-0.2	0.4	-2.2	-0.5	-2.7	0.5	0.6	2.2	5.10°C ± 0.49
Sum of standardized anomalies	2.7	-1.6	1.4	0.2	-0.1	-2.7	1.6	1.0	1.7	2.8	-1.3	
Deep indicators												
150 m GSL avg temp.	5.8	-4.1	-2.2	-0.4	0.9	-5.3	3.6	1.6	-0.4	0.3	-0.9	2.49°C ± 0.48
200 m GSL avg temp.	-5.2	2.7	-1.7	-0.6	0.2	-5.2	2.7	-1.7	-0.6	0.2	-5.2	4.42°C ± 0.44
250 m GSL avg temp.	-5.6	2.9	-1.3	-0.3	0.9	-5.6	2.9	-1.3	-0.3	0.9	-5.6	5.32°C ± 0.27
300 m GSL avg temp.	-5.0	-2.6	-2.1	-0.7	0.3	-4.1	0.5	1.3	1.3	0.9	-1.0	5.48°C ± 0.16
Sum of standardized anomalies	7.4	1.6	1.0	1.7	2.8	-7.4	1.6	1.0	1.7	2.8	-7.4	

Figure 67. Surface, intermediate (and sea-ice) and deep indicators used in the composite climate index (Figure 68).

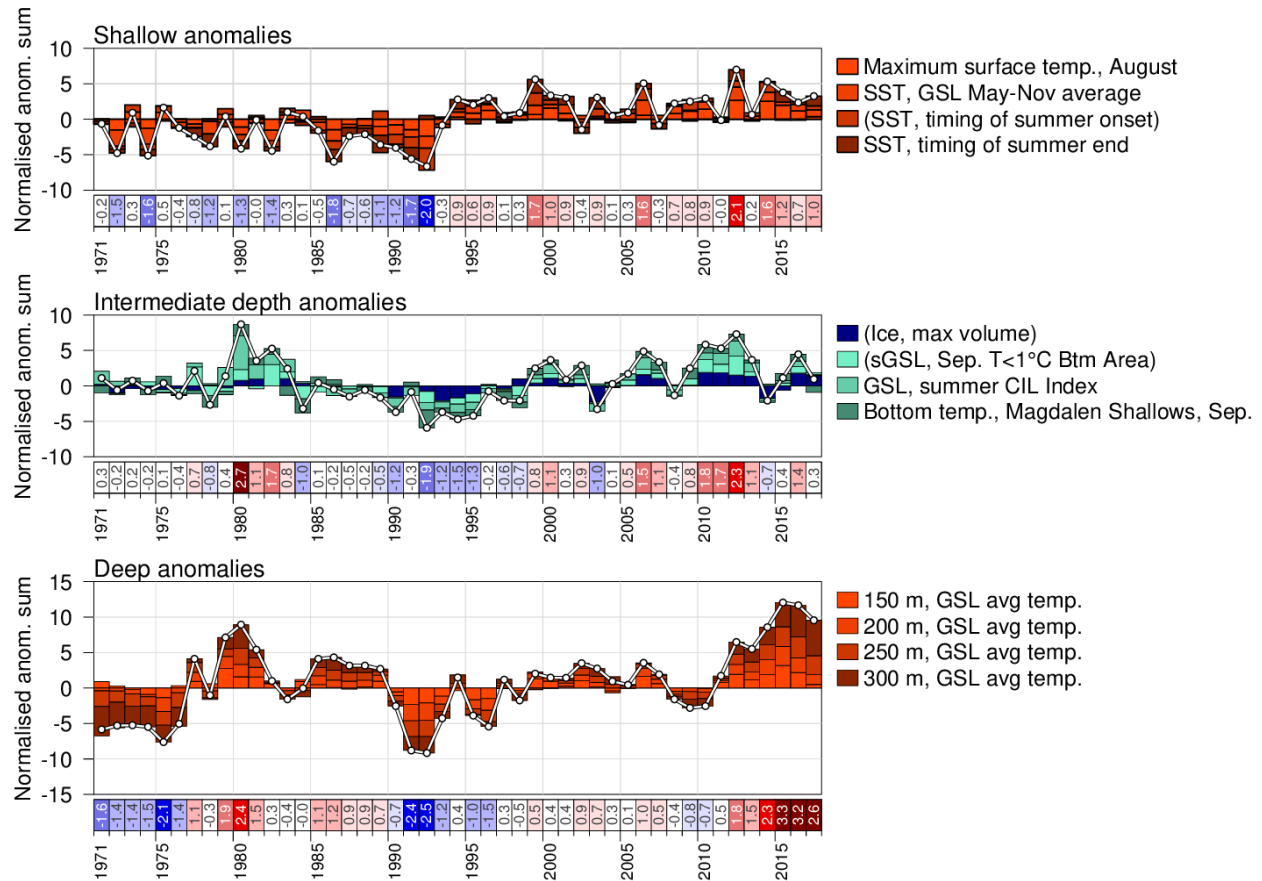


Figure 68. Composite climate indices (white lines and dots) derived by summing various normalized anomalies from different parts of the environment (colored boxes stacked above the abscissa are positive anomalies, and below are negative). Top panel sums anomalies representing shallow temperature anomalies, middle panel sums intermediate depth temperature anomalies and sea-ice (all related to winter formation), and bottom panel sums deep temperature anomalies.